MCR-71-58  Copy No.  9

# PASSIVE RETENTION/EXPULSION METHODS
# FOR SUBCRITICAL STORAGE OF CRYOGENS

## FINAL REPORT

## JULY 1971

Prepared for
National Aeronautics and Space Administration
Manned Spacecraft Center
Under Contract NAS9-10480

**MARTIN MARIETTA**
DENVER DIVISION

RECEIVED
OCT 1971
NASA STI FACILITY
INPUT BRANCH

MCR-71-58

*CR 115149*

Contract NAS9-10480

PASSIVE RETENTION/EXPULSION METHODS

FOR

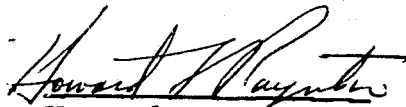SUBCRITICAL STORAGE OF CRYOGENS

Final Report

July 1971

Prepared for

NASA Manned Spacecraft Center
Houston, Texas

by

Richard P. Warren
Ralph N. Eberhardt
K. C. Lunden
James R. Tegart
T. Richard Barksdale
Dale A. Fester
G. Robert Page

Approved by

Howard L. Paynter
Program Manager

MARTIN MARIETTA CORPORATION
Denver, Colorado 80201

## FOREWORD

This report is submitted in accordance with Exhibit C of Contract NAS9-10480, dated 19 February 1970. It documents and summarizes the results of the entire contract, including recommendations and conclusions based on the experience and results obtained. The document includes tables, graphs, diagrams, curves, sketches, photographs, and drawings in sufficient detail to comprehensively explain the results achieved.

The work was performed in the Fluid Mechanics Section, Thermodynamics and Fluid Mechanics Department, of the Martin Marietta Corporation, Denver, Colorado. The NASA Technical Monitor was Mr. Jerry C. Smithson of the Power and Propulsion Division, Manned Spacecraft Center, Houston, Texas. Martin Marietta personnel who made technical contributions to the program include: Richard P. Warren, Ralph N. Eberhardt, James R. Tegart, and K. C. Lunden, who worked the parametric study (including development of the passive retention/expulsion device computer model); and Dale A. Fester, T. Richard Barksdale, Dennis E. Gilmore and Robert Wilson, who designed the subscale model delivered to the NASA. Dr. Ralph E. Hise was responsible for the test plan to evaluate the passive model under one- and low-g (drop tower and aircraft) using nitrogen as the test fluid. Mr. G. Robert Page led the Shuttle Orbiter point design effort.

# CONTENTS

# ABSTRACT

The objective of the program was to achieve a thermal performance increase for the subcritical storage of cryogens during low g by using passive retention/expulsion systems. Several different passive concepts are described along with the basic design studied, the so-called "dual-screen-liner." The latter positions and stabilizes the liquid and gas for expulsion and venting, respectively, by the proper positioning of foraminous material within the storage tank. The desired fluid separation and control are achieved by ullage and surface tension forces acting at the surface of the foraminous material. The system is, therefore, completely passive (no moving parts) and requires no additional energy source.

The dual-screen-liner was modified, as required, to satisfy a wide range of subcritical storage applications for oxygen, hydrogen, methane, and nitrogen. The parametric results are presented for both spherical and cylindrical tankage (L/D≤5 for volumes to 500 cu ft and L/D≤10 for volumes of 1000 cu ft and greater) and for liquid outflow rates as low as 3 $lb_m$/hr to as high as 100 $lb_m$/sec. A constant heat leak of 0.25 Btu/hr-ft$^2$ was assumed. A point design was made for the low-crossrange Shuttle orbiter (50,000-$lb_m$ payload) and the recommended passive design for the $LO_2$ and $LH_2$ storage is presented.

No testing was conducted; however, a detailed test plan was formulated to verify the dual-screen-liner design and demonstrate its venting and expulsion performance using a subscale model with liquid nitrogen as the test medium. The proposed testing, including bench (1-g) and drop tower and KC-135 aircraft (low-g) tests, is described with the model design. The latter was fabricated, assembled, and checked out at Martin Marietta prior to delivery to the NASA-MSC.

# NOMENCLATURE

Symbols | | | Subscripts | |
---|---|---|---|---
A | Area, $ft^2$ | | o | Initial condition
a | Acceleration, $ft/sec^2$ | | a | Entrance loss
Bo | Bond number, dimensionless | | c | Capillary
C | Heat capacity, $Btu/lb_m$ °R | | Cr | Critical
D | Diameter, ft, in. | | e | Exit condition
f | Friction factor, dimensionless | | f | Viscous loss
$g_c$ | Conversion factor, 32.174 $lb_m$ $ft/lb_f$ $sec^2$ | | g | Gas
 | | | h | Hydraulic
h | Enthalpy, $Btu/lb_m$ | | l | Liquid
K | Ratio of Vent Rate-to-Evaporation Rate | | m | Mixture
 | | | max | Maximum
k | Thermal conductivity, $Btu/hr$ $ft$ °R | | p | Process at constant pressure
L | Characteristic dimension, ft | | s | Surface
M,m | Mass, $lb_m$ | | sv | Saturated vapor
 | | | T | Total
P | Pressure, $lb_f/in.^2$ | | v | Process at constant volume
Q | Heat rate, Btu/hr | | vh | Velocity head
q | Heat flux, $Btu/hr$ $ft^2$ | | |
R | Gas constant, $ft$ $lb_f/lb_m$ °R | | |
$R_1$ | Inner-screen radius, in. | | |
$R_2$ | Outer-screen radius, in. | | |
r | Radial coordinate | | |
T | Temperature, °R | | |
U | Internal energy, $Btu/lb_m$ | | |
u | Radial velocity, ft/sec | | |
V | Volume, $ft^3$ | | |
v | Specific Volume, $ft^3/lb_m$ | | |
We | Weber number, dimensionless | | |

## Symbols

$\alpha$      Cryogen-to-tank volume fraction

$\beta$      Kinematic surface tension, $ft^3/sec^2$

$\Delta h$      Enthalpy difference, $Btu/lb_m$

$\Delta P$      Pressure difference, $lb_f/in.^2$

$\Delta R$      Vapor annulus gap, in.

$\gamma$      Ratio of specific heat, dimensionless

$\xi$      Liquid/gas density function, dimensionless

$\theta$      Time, hr, sec

$\lambda$      Latent heat of vaporization, $Btu/lb_m$

$\rho$      Mass density, $lb_m/ft^3$

# I. INTRODUCTION

As shown in a number of recent studies, including Ref I-1 and I-2, the most attractive method to provide low-g propellant orientation and control uses ullage and surface tension forces only. Foraminous material, screen and perforated plate, is configured within the storage tank so that the ullage and capillary forces acting at the surface of the material properly position and stabilize the liquid, as described in Ref I-3. These passive control systems have been used successfully in a number of vehicles using noncryogen propellants, such as Agena, Transtage, and the Apollo CSM (Ref I-4).

During the initial phase of this 14-month program, various passive concepts proposed and/or being developed for cryogenic storage (Ref I-5 thru I-9) were briefly reviewed along with the Martin Marietta dual-screen-liner (DSL). Except for the latter, none of the others are designed to provide (by themselves) all three of the following:

1) Gas-free liquid expulsion on demand;

2) Tank pressure relief, as required;

3) Near-continuous bulk propellant control.

The other capillary concepts are designed to provide liquid only. Additional subsystems are required to satisfy the other requirements. For example, thermodynamic vent systems are incorporated to relieve tank pressure with, or without, propellant mixer devices. Conversely, the DSL (by itself) separates and stabilizes liquid and vapor to afford direct venting of vapor, as well as liquid expulsion. It also positions and maintains the bulk propellant away from the tank wall by providing a thin layer of vapor between the two. The DSL configuration is an efficient device for controlling and stabilizing the bulk propellant (Ref I-10 and 11). By holding the bulk propellant away from the tank wall, it tends to minimize any stratification problems. For these reasons, the DSL was selected as the baseline passive retention/expulsion concept for this program. It was modified, as required, to satisfy the wide range of potential storage applications studied.

The program, as shown in Fig. I-1, was divided into five separate tasks:

I - Design a passive retention/expulsion system;

II - Conduct a parametric study to indicate range of applicability;

```
                          ┌─────────────────────┐
                          │  Contract Go-Ahead  │
                          ├─────────────────────┤
                          │  Orientation Meeting│
                          │    at NASA-MSC      │
                          └─────────────────────┘
                          ┌─────────────────────┐
                          │    Program Plan     │
                          └─────────────────────┘
```

| Task I - Design a Passive Retention/Expulsion System | Task II - Conduct a Parametric Study to Indicate Range of Applicability |
|---|---|
| Review Passive Control Concepts | Review Applications and Requirements |
| Select DSL Concept as Baseline | Develop DSL Analytical Model / Conduct Tradeoff |
|  | Conduct Shuttle Orbiter Point Design |
| DSL Design Analysis | |
| Preliminary Design of DSL Subscale Model | Parametric Study Results |
| NASA-MSC Review and Approval | |
| Detailed Subscale Design | Task III - Formulate a Test Plan |
| Submit Design Drawings to NASA-MSC | Develop Test Requirements -Bench Tests -Drop Tower Tests -KC-135 Aircraft Tests |
| Task IV - Fabricate the Subscale Passive Device | Identify Test Procedures, Instrumentation, etc |
| Procurement | Task V - Reporting |
| Fabrication and Assembly | Monthly Progress Reports |
| Subscale Model Checkout | Test Plan, MCR-71-38 |
| Deliver to NASA-MSC | Contract Summary Report, MCR-71-37 |
| | Contract Final Report, MCR-71-58 |

Figure I-1  Program Work Plan

III - Formulate a test plan;

IV - Fabricate the subscale passive device;

V - Reporting.

The baseline DSL concept was compared to other control and venting methods during Task I. The subscale DSL model, to be used for the tests described during Task III, was also designed during the initial task.

The parametric study (Task II) dealt with storage of hydrogen, oxygen, methane, and nitrogen using the DSL in spherical and cylindrical tankage from 5 cu ft to 10,000 cu ft. A constant heat leak of 0.25 $Btu/hr-ft^2$ was assumed for all fluids. The tank pressure range was 14.7 to 150 psia. An acceleration environment ranging up to 7 g (during boost) and 0.02 g (in orbit) was considered. The propulsion duty cycle included up to 20 restarts with the burn duration ranging from 1 sec to depletion. Liquid expulsion was as low as 3 $lb_m/hr$ and as high as 100 $lb_m/sec$.

A point design was included as part of the Task II effort along with development of an analytical model for the DSL. The point design was for a low-crossrange Shuttle orbiter (50,000-$lb_m$ payload). The parametric analysis and point design did not include feedline and associated chilldown problems, nor were pump requirements (NPSP) handled directly.

Although no testing was conducted during the study, a detailed test plan was formulated during Task III to obtain operational information and data on the DSL. These tests are essential for verifying the DSL concept and assessing its practicability for cryogenic storage during low g. The plan, detailed in Ref I-12, includes bench tests (one g), drop tower tests and KC-135 aircraft tests (low-g) using the subscale DSL model with liquid nitrogen as the test fluid. The DSL model was fabricated, assembled and checked out at Martin Marietta (Task IV) prior to delivery to the NASA-MSC at the close of the program.

The results of this program are presented here and in the following reports (Task V);

1) Summary Report, MCR-71-37, Martin Marietta Corporation, Denver, Colorado, July, 1971;

2) Test Plan - Sub-Scale Dual Screen Liner Retention/Expulsion System, MCR-71-38, Martin Marietta Corporation, Denver, Colorado, July, 1971.

## II. SYSTEM SELECTION

The DSL was selected as the baseline passive retention/expulsion concept
for this study. As mentioned in the Introduction, it can provide liquid
expulsion, tank pressure control, and a near-continuous propellant control.
A number of propellant control concepts are briefly discussed in Section A
with the DSL described separately in Section B. Vapor venting, as provided
by the passive DSL, is compared to other venting techniques in Section C.

### A. CAPILLARY SYSTEMS

Capillary systems pose design problems with regard to stability and
control of the fluid to assure single-phase fluid withdrawal. Additionally,
tank loading is a concern, as are material/propellant compatibility, and the
fabrication, cleaning, handling, inspection and maintenance of the passive
device. The latter, so-called "hardware" considerations, are particularly
important to the reusable Shuttle orbiter.

Stability criteria are available for selecting pore size of the foraminous
material used in the capillary device configurations, as discussed in Chapter
IV. Whether the capillary system is a small trap or a near-complete liner,
screen breakdown* under vehicle maneuvers during the entire mission is a prime
design consideration. The high-g boost phase, for example, tends to dictate
a small trap device over the liquid drain which is submerged in the propellant
during boost. This may eliminate the breakdown question, at least during
boost; however, the trap device must be refillable†with liquid expulsions or
become unattractively large in size.

In addition to reducing the size of the passive device to afford greater
stability, the designer may use finer foraminous material of micronic pore
size. If this material is still not adequate to provide the desired control,
the material may be calendered or additional layers may be used. The calendering
process (Ref II-1) will yield an increase in the pressure retention on the
order of only 15%, or so, whereas stability may be increased in a near-linear
fashion with the addition of foraminous layers (Ref II-2). However, if ten
layers of screen are used in a passive design, up to nine may break down.

---

*The term, screen breakdown, is used to represent the condition where the
liquid/vapor interface at the surface of the foraminous material becomes
unstable, i.e., vapor displaces liquid, and vice versa, through the pores
of the material. Bubble point, a direct measure of interface stability for
a given foraminous material, is discussed in Section E.2 of Chapter IV.

†Refillability is when the design allows for ullage to be purged from the trap
by liquid displacement during expulsions. If the ullage cannot be purged, the
trap volume must be increased to contain sufficient propellant to meet the
expulsion requirements.

Gas is then between each of the screen sandwiches to the tenth screen.  This poses a critical problem as to whether there is direct communication between the bulk propellant and the liquid stabilized by the tenth screen, or whether the gas pockets have interrupted the desired communication.  The layered foraminous design also tends to present more stringent quality control, fabrication, and handling requirements than do single-layer devices.

Vaporization of liquid within the controlled propellant region due to heat leak into the cryogen through support structure, tank walls, feedlines (engine heat soakback), and from warm pressurization gas, for example, is another major design consideration.  It is critical to the so-called "zero heat leak" designs where no vaporization is allowable in the controlled region. It tends to be less critical with the DSL where a controlled region is provided for vaporization to occur during storage.

Weight, complexity and reliability are also key considerations, particularly for large, integrated, reusable cryogenic storage systems such as for the Shuttle orbiter.  The primary attractiveness of the capillary devices is that they are completely passive, i.e., they have no moving parts within the storage tank.  The use of a single valve in the trap system to assure refill-ability, as in the device described in Ref II-3, tends to reduce this attractiveness.

Capillary systems are invariably designed to function over a limited range of operating conditions that are highly mission dependent.  Additionally, to minimize residuals, the capillary design is a function of the tank geometry. System designs to supply the relatively small flow rates required for attitude control motors or restart requirements for the main thrusters may not necessarily satisfy the requirements for the supply or receiver tank for an orbital transfer. When propellant tanks are to supply propellant for $\Delta V$ maneuvers, the drain is located so that the thrust produced will tend to position the propellant over the drain area.  The capillary device for this type of application must supply propellant only for engine start and until the bulk propellant has been settled. When propellant is supplied for ACS maneuvers that do not necessarily produce settling of the liquid, the sump (or trap) can be refilled via capillary feeder ducts that provide communication between the trap and remote locations within the tank.  These feeder ducts will not generally have sufficient cross section to provide the flow rates required for an efficient low-orbital transfer.  To provide sufficient flow capacity for orbital transfer under the condition of zero or small accelerations, a total orientation device such as the DSL is required.

For cryogenic applications, venting of the storage tank to control pressure must be considered.  At least three methods exist to accomplish the vent function: (1) the capillary device may exclude liquid from an overboard gas vent; (2) the vehicle may be accelerated during a vent cycle to ensure a dry vent inlet; and (3) the capillary device may provide liquid (preferably gas-free) to an open-loop refrigeration system that will absorb the heat load on the vessel.  The first method can probably only be accomplished with the DSL.  The second is undesirable since it affects the flight path.  The third method is one which has been employed in specific system designs (Ref II-3 thru II-9).

In addition to acting as a liquid acquisition device, the capillary system must filter entrained gas bubbles from the outflowing liquid. This is generally accomplished by screen filters located near the tank outlet and positioned normal to the flow. The flow streamlines in the vicinity of the exit are shaped so that bulk ingestion of gas into the outlet is precluded when the outflow rate is high and liquid level is low. The Advanced Maneuvering Propulsion System (AMPS) design, for example, tends to accomplish this flow streamline shaping by locating the spherical helium tank adjacent to the exit (Ref II-3). The outflow from the DSL occurs from the liquid annulus, thus the streamlines are similar in shape to those in the AMPS configuration.

A capillary design for a cryogen tends to be more complicated (relative to designs for space storables) in that the liquid containment device must be thermally isolated from the environment. Otherwise, vapor will be generated within the device. The DSL accomplishes the required isolation by creating a vapor layer adjacent to the tank wall; vaporization thus occurs from the outer surface of the liquid annulus. A start tank design may accomplish this by immersing the tank in the bulk fluid. Vapor generation within the liquid containment device in the AMPS design, as proposed by Lockheed Missiles & Space Division and General Dynamics/Convair (Ref II-10 and II-11), is precluded by refrigeration of the sump region by a liquid vent heat exchanger.

### B. DUAL-SCREEN-LINER CAPILLARY CONCEPT

The DSL is unique when compared to other capillary concepts because it passively controls the bulk propellant during low-g. This is accomplished by a complete screen device within the storage tank that is capable of encasing all of the bulk propellant. This complete liner isolates the propellant from the tank wall during the low-g storage period. The region between the liner and tank wall is, therefore, devoid of liquid and provides a controlled volume from which vapor can be vented to control tank pressure. This volume is limited by the ullage gas volume since, as mentioned, the liner encloses the bulk propellant.

Vaporization of liquid at the surface of the foraminous liner tends to thermally isolate the bulk propellant by intercepting heat. The vaporization process, however, tends to raise the pressure in the vapor region. The pressure buildup may be relieved by venting gas overboard. If the pressure is allowed to increase (no venting), gas will break through the screen and enter the bulk propellant region. Breakthrough will result when the difference between the pressure in the vapor region and that of the bulk liquid exceeds the bubble point of the screen.

Single-phase liquid may be expelled from the tank by providing another capillary device within the liner to provide a preferential path for gas-free liquid to flow to the tank outlet, on demand. This second passive device may be another foraminous liner (from which the DSL term was coined) or it may assume other geometries, as dictated by system/mission requirements. Several different DSL configurations, are shown and discussed in this section and in

Chapter V, Space Shuttle Orbiter Capillary System Design. There is no single DSL design best for all applications. For example, the best DSL for a 5-cu-ft LO$_2$ tank may not necessarily be preferred if scaled upwards to a 500-cu-ft tank application. It may be less efficient, too heavy, etc. Each application must be reviewed to yield the best DSL system design. On the other hand, the design for the Shuttle orbiter (Chapter V) is flexible and can be used efficiently for a range of orbiter missions.

The DSL concept serves as a baseline for this discussion. It is composed of two concentric annular regions, as illustrated in Fig II-1. The outer-annulus adjacent to the tank wall becomes filled with vapor under low-g conditions. The inner-annulus is filled with liquid during tank loading. This liquid annulus is stabilized and maintained during boost and low g. The central region contains bulk liquid and an ullage region. Liquid is expelled from the tank from the liquid annulus, which is supplied with liquid from the central region.

Stability of the liquid annulus is assured when the maximum hydrostatic head for the configuration is less than the pressure retention (bubble point) for the screens forming the annulus. However, the maximum head may exist for brief periods (1 or 2 sec), such as during an ACS maneuver. Centrifuge tests results (Ref II-12), have shown that the amount of liquid lost during such short periods may be negligible. A design alternative is, therefore, to design the passive system to support hydrostatic heads that exist for sufficiently long durations and the amount of gas ingested into the liquid annulus would be great enough to pose a serious degradation on the DSL performance.

To support liquid within the central region, the pressure in the outer annulus must exceed the ullage pressure within the central region by the amount $\rho ah$. On the high side, the pressure difference between the gas annulus and bulk regions must not exceed the bubble point of the screen forming the outer-surface of the liquid annulus. If this bubble point is exceeded, gas is ingested into the liquid annulus. To ensure that this does not occur, either gas must be vented overboard or communication ports may be provided between the two regions, as shown. A screen with a lower bubble point than that forming the liquid annulus is located in the communication port and is wetted by liquid from the liquid annulus. The wetted screen condition is required for support of the bulk propellant.

Vapor venting to control tank pressure occurs from the outer-annular region. A fine pressure control (less than 0.5 psi, or so) is needed if the bulk liquid is to be continually supported, i.e., kept out of the outer annulus. This pressure support was discussed in the previous paragraph. Venting may be intermittent or continuous, as desired, with continuous support of the bulk propellant. A different venting scheme may be used when the acceleration vector acting on the vehicle is known. For this type of venting, the fine pressure control requirement is not needed. As an example, during Earth orbit, the direction of the steady-state drag vector acting on the Shuttle orbiter is known. As a result, the probable bulk propellant location in the
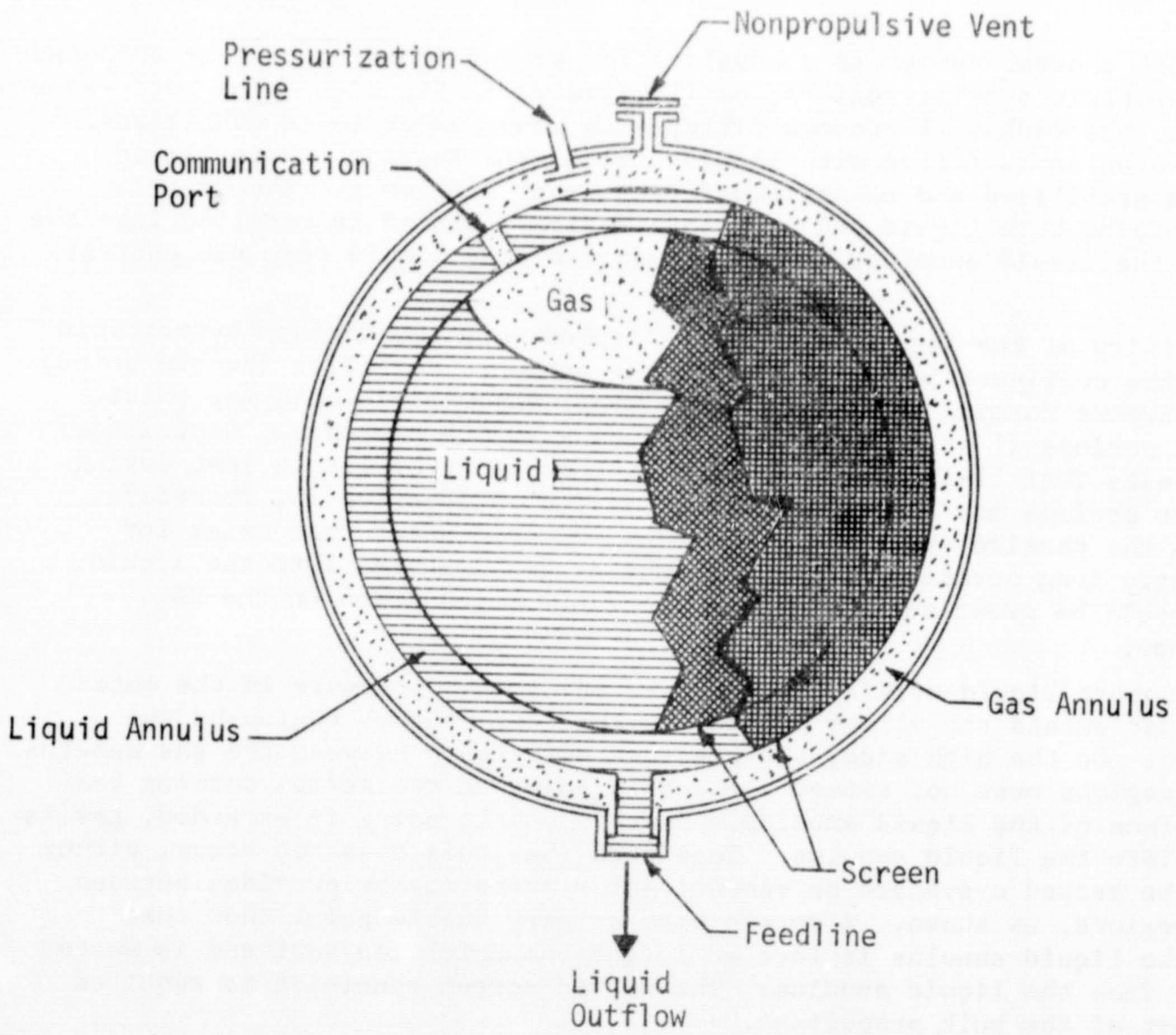
Fig. II-1  Baseline DSL Concept

tank under this vector is known. If a sudden and dramatic reduction in tank pressure were desired, vapor could be rapidly vented from the outer annulus through the nonpropulsive vent. If the vented mass rate is large, the communication screen will break down, possibly even dry out. The sudden reduction in gas pressure in the outer annulus may result in loss of the bulk propellant pressure support. Bulk liquid may, therefore, enter the vapor annulus. To preclude liquid being ingested with vapor, the vent should be positioned on the tank wall opposite where the drag vector tends to position liquid. This type of pressure relief, whereby the tank pressure is reduced significantly, tends to produce: (1) ullage in the bulk region entering the gas annulus through the communication screen and being vented overboard; and (2) liquid vaporization at the liquid/ullage interfaces in the tank, including the liquid annulus region which is not necessarily lost during this rapid pressure sequence. (As noted earlier, the screen material for the liquid annulus is selected to provide stability under the low-g accelerations.) The first condition is desired, i.e., gas, rather than liquid is vented. The undesired liquid vaporization is not unique to this drastic tank pressure relief (greater than the 0.5 psi restriction posed by screen bubble point limitations). During the fine pressure relief, vaporization of liquid in the liquid annulus is also a design concern. As discussed earlier, vaporization at the outer screen tends to thermally isolate the bulk propellant from its environment. The liquid being vaporized is at the saturation temperature dictated by the vapor pressure in the gas annulus. When the gas pressure is reduced during venting, the liquid will tend to vaporize. Based on earlier Martin Marietta bench test results of a DSL configuration (200 x 1400 mesh screen) using pentane as the test liquid, this vaporization phenomenon did not produce formation of vapor in the liquid annulus during venting (Ref II-13). More quantitative data are needed to support these qualitative results.

Pressurization gas may be introduced into either the bulk or outer annular regions. With the latter, pressurant flows from the outer annulus, through the communication screens, and into the central region displacing the bulk liquid during expulsions.

The DSL will have little effect on separating and controlling the liquid and gas phases before and during launch, because the small capillary forces will not be dominant. When the low-g condition is reached, vaporization will cause pressure to rise in the outer annulus and force any liquid there into the lower-pressure bulk region. If desired, this process may be hurried by pressurizing the outer region. Once the outer annulus is devoid of liquid, vaporization occurs at the outer surface of the screen forming the liquid annulus.

A variation to the baseline DSL is to configure eccentric regions between the two single-layer screens and the screen/tank wall. This variation is pictured in Figure II-2. The vapor annulus gap is greatest in the vicinity of the vent port. The liquid annulus is narrowest at the liquid drain. The possible effect of gas ingested into the liquid annulus during screen

10
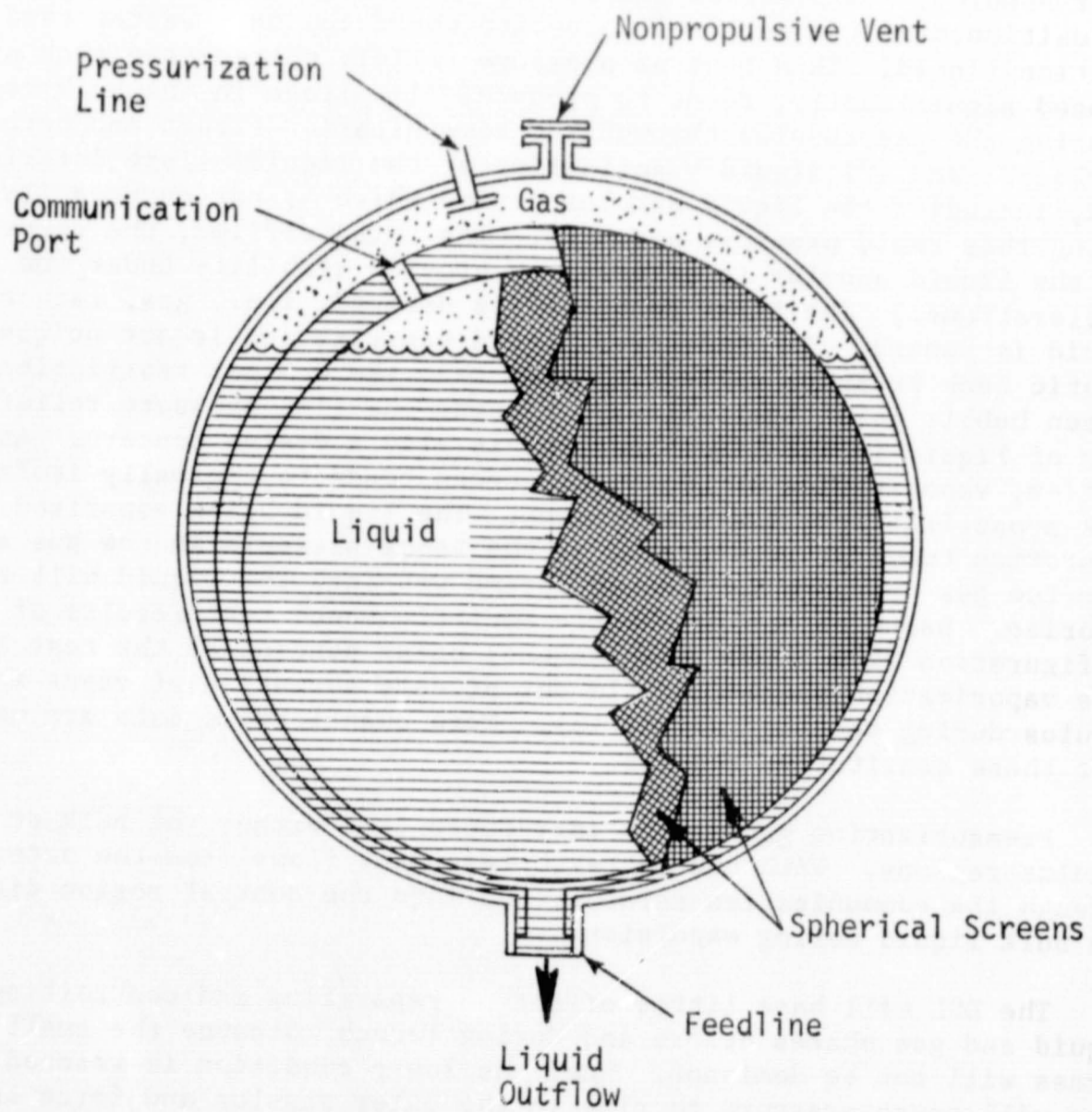


Figure II-2  DSL with Eccentric Screen Liners
(High-g Boost Condition Pictured)

breakdown during launch, for example,* may be lessened with this configuration, because the ullage bubble (neglecting temperature gradients and resultant thermocapillary effects, Ref II-14) will tend to remain away from the liquid drain during low g, as well. This is based on the principle of minimization of surface energy. Conversely, any liquid in the gas annulus will tend to be positioned away from the vent.

There is some possibility that capillary pumping during low g will tend to reduce the volume of ullage trapped in the liquid annulus; however, if Dutch twill metal cloth is used, the probability is remote (Ref II-2). If the ullage is propellant vapor, it may collapse completely during subsequent pressurization and tank pressure buildup. The screen trapping the bubble will intercept the heat leak provided it remains wetted. If it were to dry out, liquid would tend to refill the annulus during rewetting of the screen. In other words, the passive device can, by itself, correct certain undesired conditions.

Expulsion efficiency and system weight become more important as tank size increases and tend to dictate use of the DSL configuration, as shown in Fig. II-3 with separate liquid passageways joined together above the liquid drain port. The number of channels is dictated, in part, by the degree of communication desired within the complete screen liner. The screen channels present an acceptable method to reduce system mass (dry weight) in comparison to a complete inner liner. The cross-sectional flow area of the channels may be triangular, circular, etc, as dictated by fabrication considerations and flow area (including entrance from the bulk region) requirements, based on the expulsion flowrates. Expulsion efficiency for the DSL is discussed in Section C of Chapter IV; system mass is documented in Section E.2 of Chapter IV.

## C. COMPARISON OF DSL TO OTHER VENTING TECHNIQUES

To maintain steady conditions within a vessel containing a cryogenic liquid, energy must be convected out of the system via the vent gas at a rate equal to the rate of heat transfer to the vessel. The vent rate, which will maintain steady conditions, will be minimized when the energy addition to the vent gas is maximized. In the venting process normally considered, the vent gas leaving the system is saturated at the tank pressure. With the dual-screen-liner there exists the potential for superheating the vent gas and thus reducing the vent rate. The liquid or thermodynamic vent system achieves an increased heat addition by causing the phase change to occur at a reduced pressure. For the Shuttle orbiter tank pressure range, the DSL and liquid vent systems compare favorably.

A heat balance on a cryogenic storage vessel which receives heat at rate Q, and which has outflow rates of liquid and gas of $\dot{m}_\ell$ and $\dot{m}_g$, yields

---

* As discussed earlier in Section A, additional screen layers may be used for greater stability, as well.

12



Pressurization Line

Nonpropulsive Vent

Liquid

(Gas)

A

A

Screen

Feedline

a.

b.
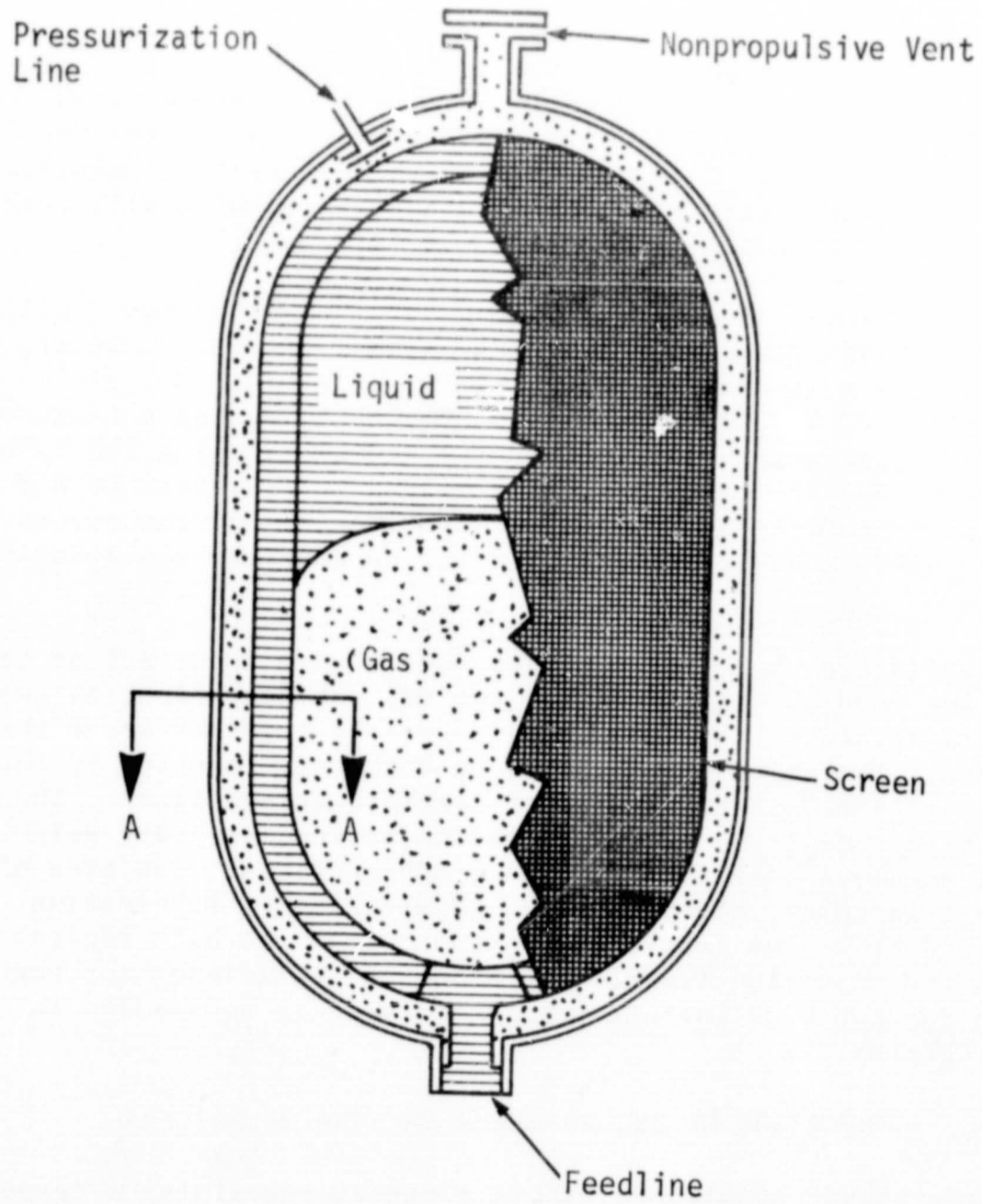
Example Configurations
Section A-A

Figure II-3    DSL with a Channel-Type Liquid Annulus
(Low-g Steady-State Condition Pictured)

$$Q d\theta - \dot{m}_\ell h_{\ell e} d\theta - \dot{m}_g h_{ge} d\theta = dU$$

$$= m_g dU_g + U_g dm_g + m_\ell \, dU_\ell + U_\ell \, dm_\ell \qquad \text{(II-1)}$$

The enthalpies, $h_{\ell e}$ and $h_{ge}$, are to be evaluated at the system boundary. The internal energy of the system is represented by U, time by $\theta$, and mass by m. The subscripts $\ell$ and g refer to liquid and gas. If the vent system comprises a liquid or thermodynamic vent with a heat exchanger, the system boundary is chosen to correspond to the exit plane of the heat exchanger. The continuity equation for the liquid and gas phases within the tank yields,

$$dV_g = -dV_\ell$$

or

$$\frac{dm_\ell}{\rho_\ell} = - \frac{dm_g}{\rho_g} \qquad \text{(II-2)}$$

where $\rho$ is the density. A mass balance equating the outflow quantities to the change in mass within the tank is written

$$- (\dot{m}_\ell + \dot{m}_g) \, d\theta = dm_\ell + dm_g \qquad \text{(II-3)}$$

where the minus signs result since $\dot{m}_\ell$ and $\dot{m}_g$ are positive for outflow. Replacing the internal energy terms in Eq (II-1) with $h - P/\rho$, and combining with Eq (II-1) and (II-2) yields

$$Q d\theta - \dot{m}_g d\theta \left\{ \Delta h_g + \lambda \left( \frac{\rho_\ell}{\rho_\ell - \rho_g} \right) \right\} - \dot{m}_\ell d\theta \left\{ \Delta h_\ell + \lambda \left( \frac{\rho_g}{\rho_\ell - \rho_g} \right) \right\} = m_g dU_g + m_\ell dU_\ell \quad \text{(II-4)}$$

where $\Delta h_\ell$ and $\Delta h_g$ are the enthalpy excesses of the vent fluids relative to the stored fluids.

### 1. Case I - Tank Conditions Steady, No Liquid Outflow

For this case

$$\dot{m}_\ell = 0$$
$$dU_g = 0$$
$$dU_\ell = 0, \text{ and}$$

Solving for $\dot{m}_g$ in Eq (II-4)

$$\dot{m}_g = \frac{Q}{\Delta h_g + \lambda \xi} \qquad \text{(II-5)}$$

14

where

$$\xi = \frac{\rho_\ell}{\rho_\ell - \rho_g} \quad .$$

Equation (II-5) is applicable to any vent process. With saturated vapor venting, $\Delta h_g = 0$. With the dual screen liner, $\Delta h_g$ may be finite, in which case the vent rate will be reduced from the previous case.

The function $\xi$ is plotted on Fig. II-4 for the four study fluids in the pressure range 15 to 150 psia. Note that with all the fluids except hydrogen, $\xi$ differs very little from 1.0. With hydrogen it is clear that in the higher pressure range it is important to account for the correct value of $\xi$.

## 2. Liquid Vent Process

The liquid vent process is best described with reference to pressure-enthalpy coordinates. Pressure-enthalpy diagrams for the four study fluids are plotted on Fig. II-5 thru II-8. Liquid vent processes are shown for tank pressures of 100 psia and heat exchanger pressure of 5 psia. Liquid is withdrawn from the tank at point A. A constant enthalpy expansion to point B occurs across a throttling orifice. The quality varies at point B from 25% for oxygen to 33% for hydrogen. The two-phase mixture is converted entirely to vapor, point C, in a heat exchanger which is in contact with the bulk liquid. From C to D the vapor is superheated to a temperature approaching that of the stored liquid. The total enthalpy added in the process is the difference between the enthalpy values at A and D. The latent heat of vaporization in the denominator of Eq (II-5) is the enthalpy difference between points A and E. The enthalpy difference $\Delta h_g$ appearing also in the denominator of Eq (II-5) is the enthalpy difference between points D and E.

Defining

$$\eta = \frac{\dot{m}}{\dot{m}_{sv}} \qquad (II-6)$$

where $\dot{m}_{sv}$ is given by Eq (II-5) with $\Delta h_g = 0$, leads to

$$\eta = \frac{1}{\dfrac{\Delta h_g}{\lambda \xi} + 1} \quad . \qquad (II-6a)$$

The fractional reduction in vent rate $(1 - \eta)$ for the liquid vent process relative to saturated vapor venting is plotted as a function of tank pressure on Fig. II-9 to II-12. Note that with the exception of hydrogen the vent rate reduction increases from about one percent at one atmosphere to about 10% at 10 atmospheres. With hydrogen the reduction is substantial; changing from 4% at one atmosphere to 35% at 10 atmospheres.
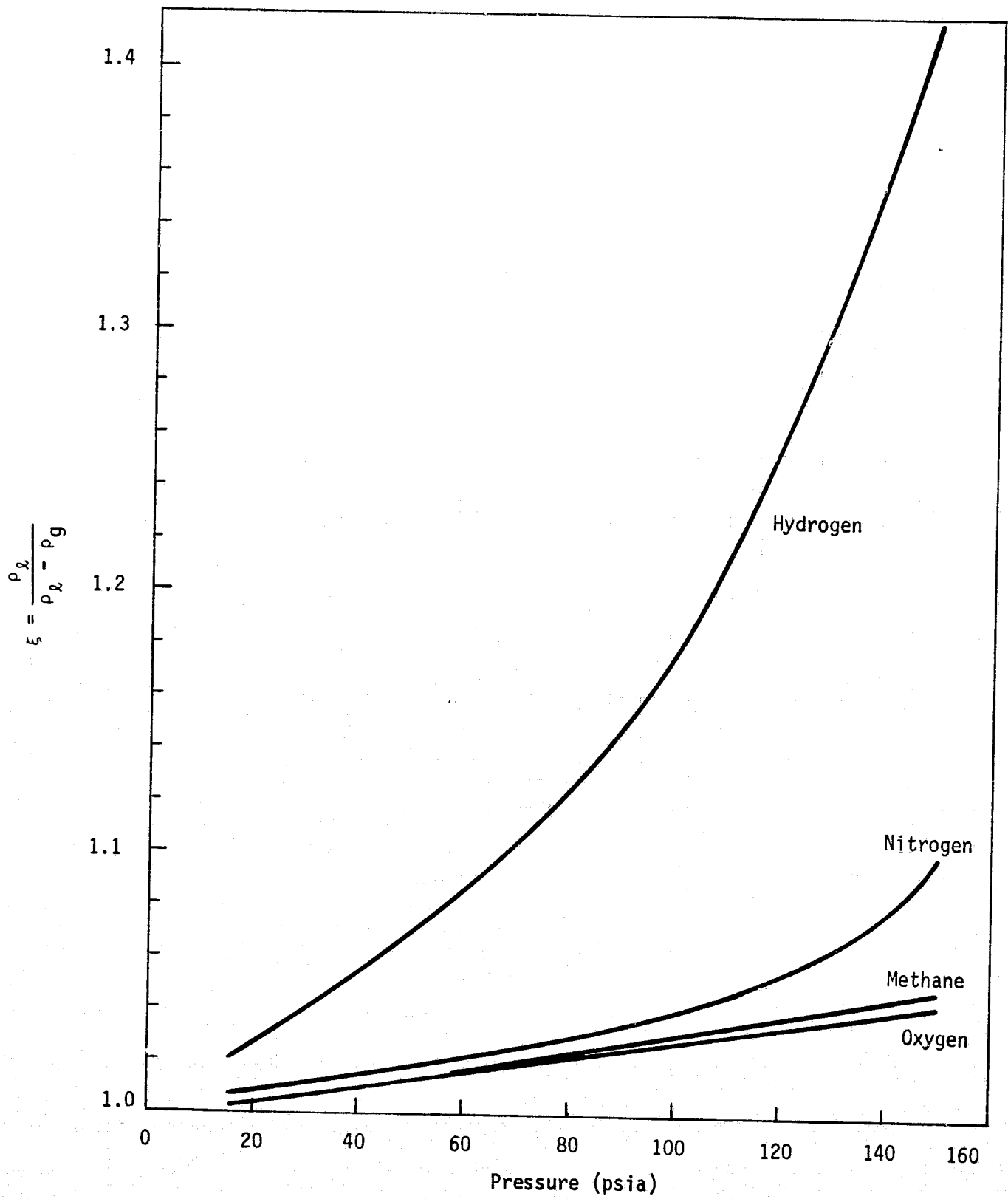
Figure II-4   Liquid/Gas Density Function
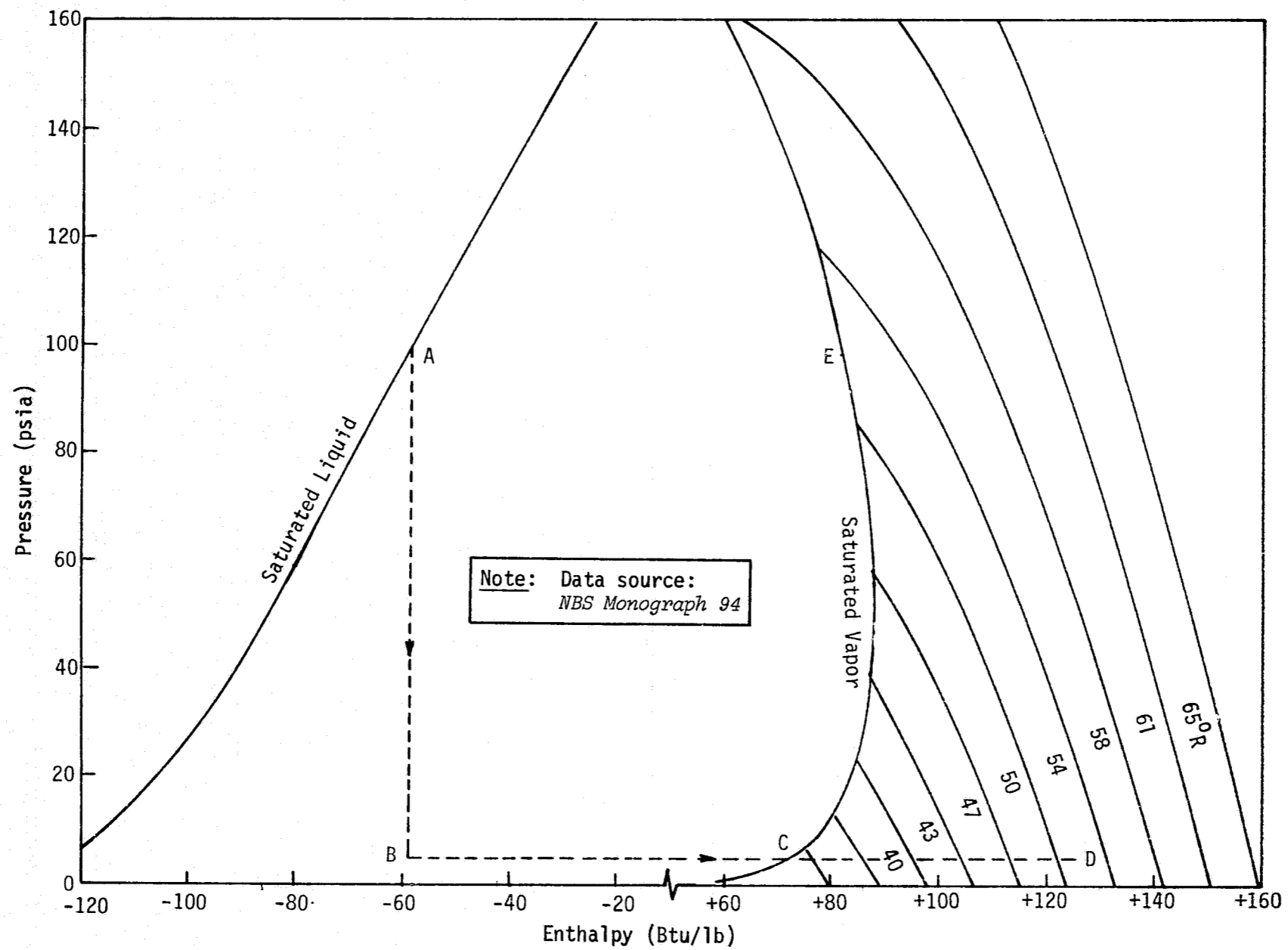
Figure II-5  Pressure/Enthalpy Diagram for Hydrogen
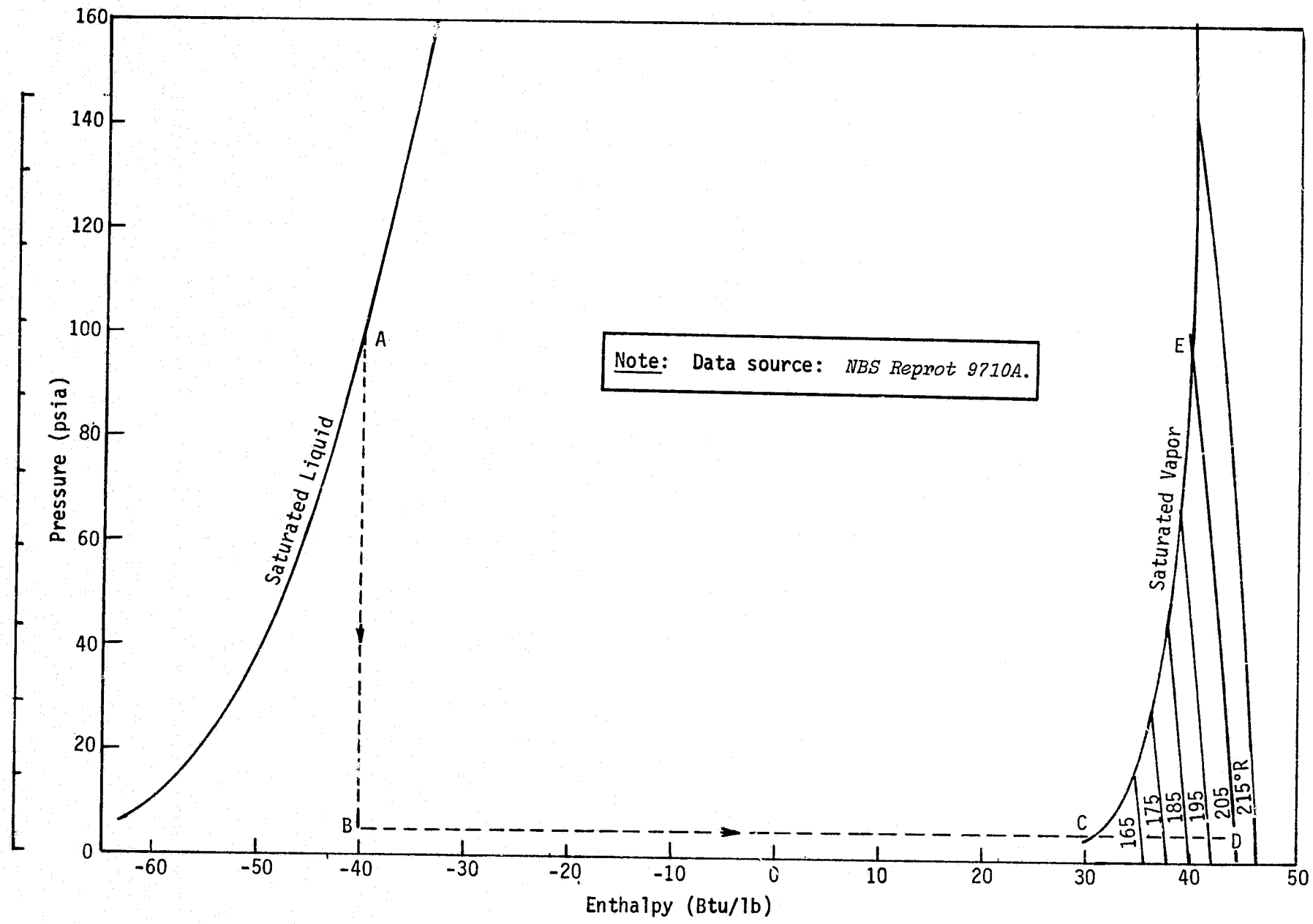
Figure II-6 Pressure/Enthalpy Diagram for Oxygen
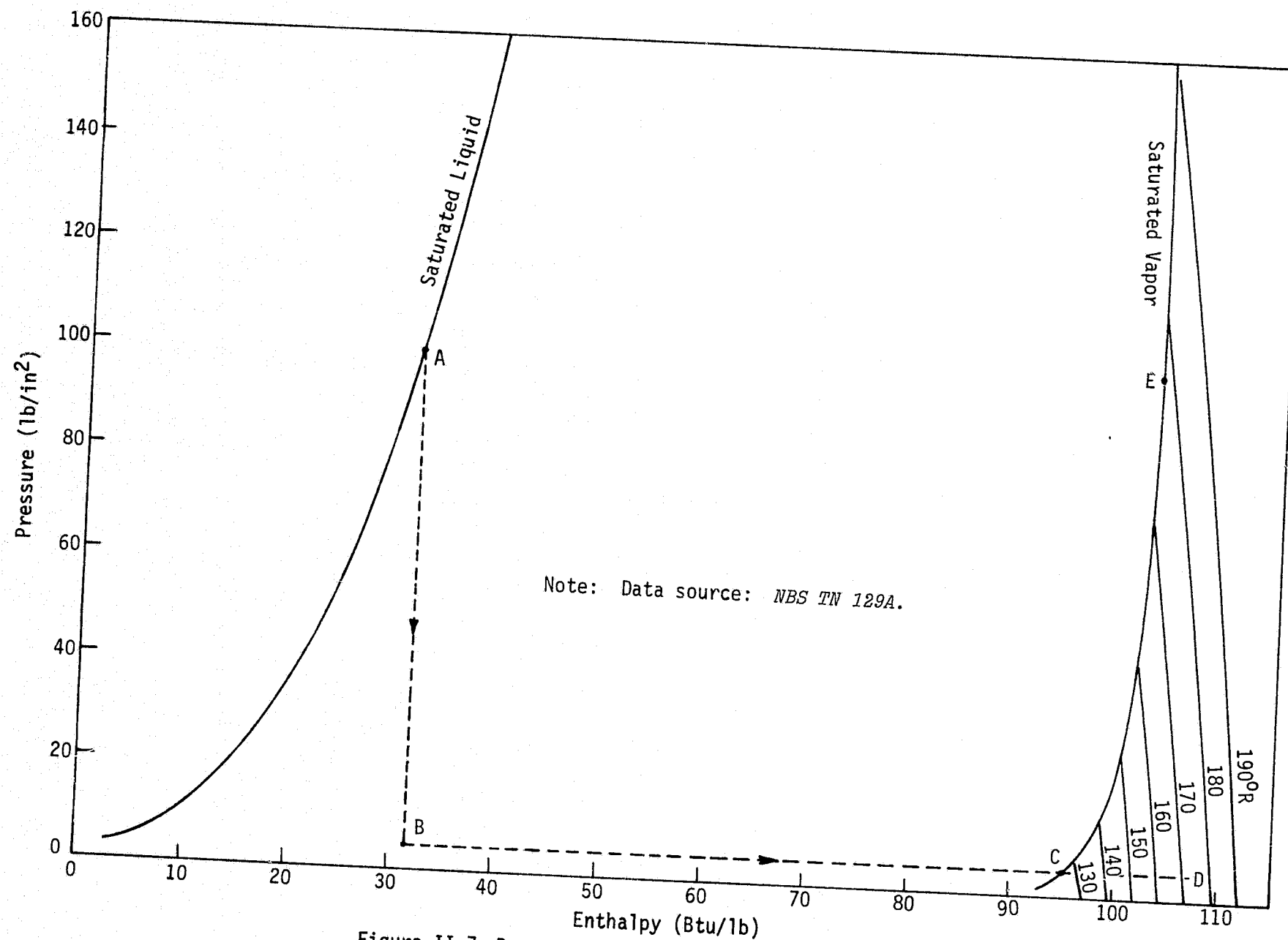
Figure II-7 Pressure/Enthalpy Diagram for Nitrogen

Note: Data source: *NBS TN 129A.*
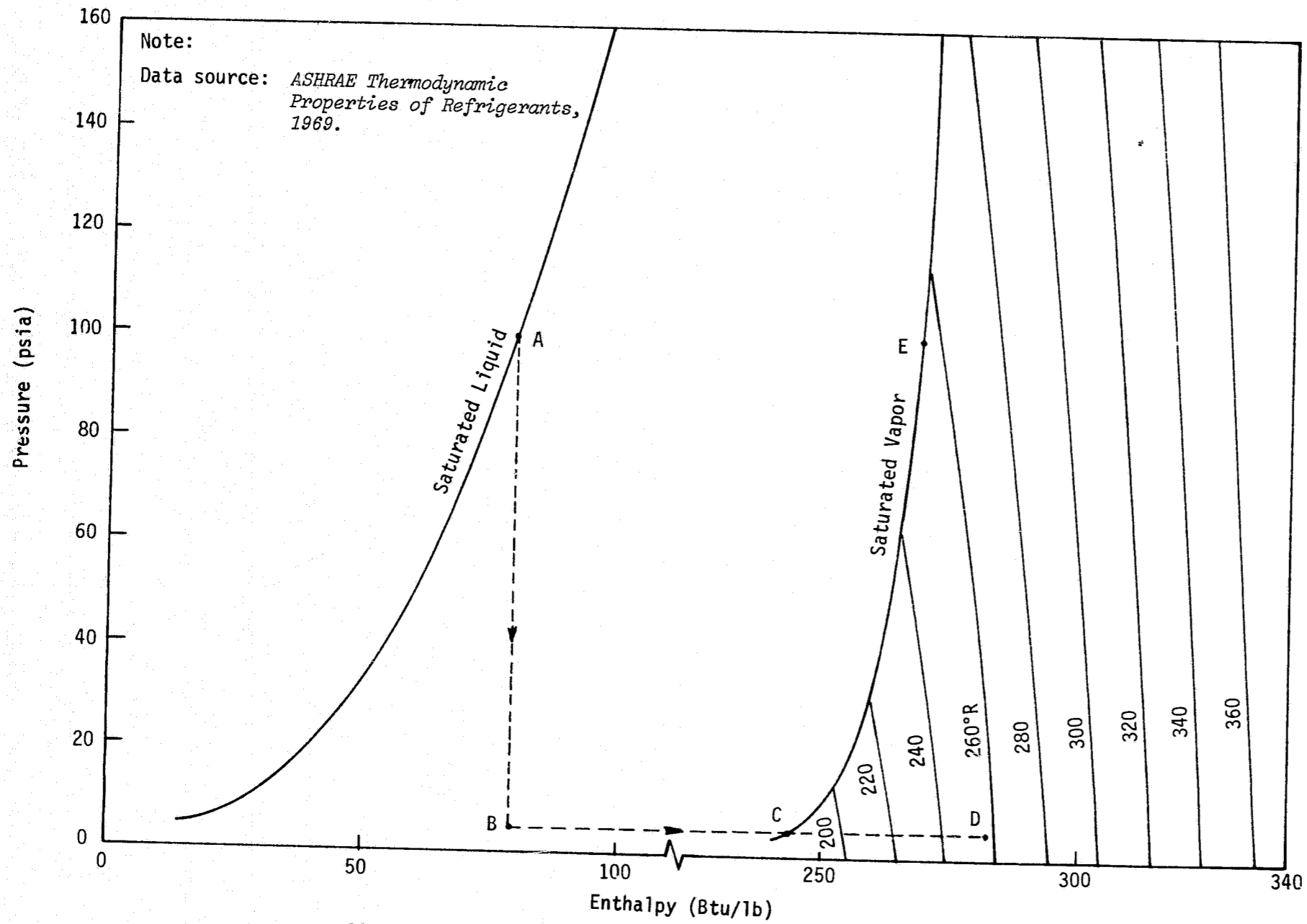
Figure II-8   Pressure/Enthalpy Diagram for Methane
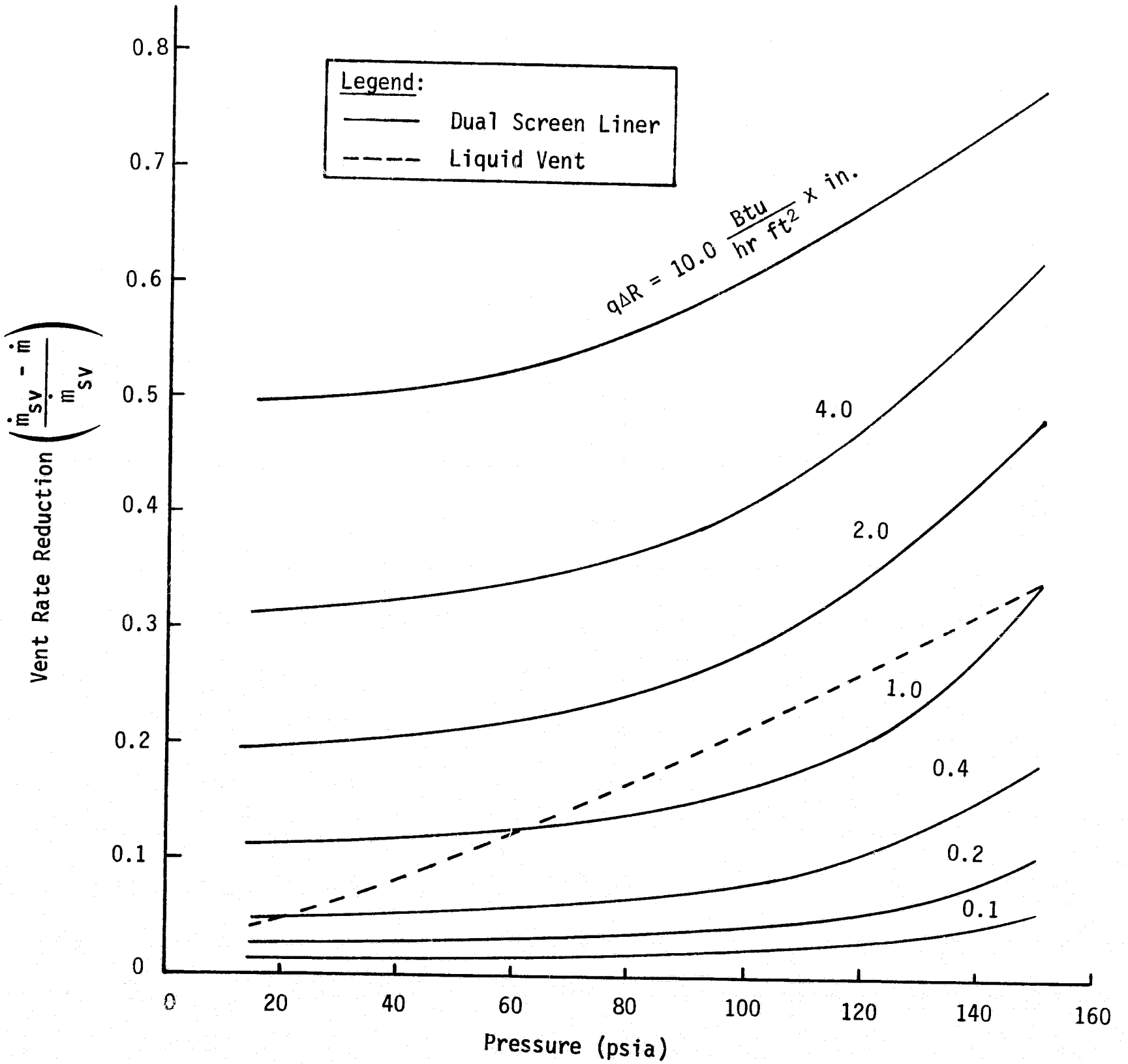
Figure II-9  Comparison of Hydrogen Vent Rate for the DSL and Liquid
(Thermodynamic) Vent System
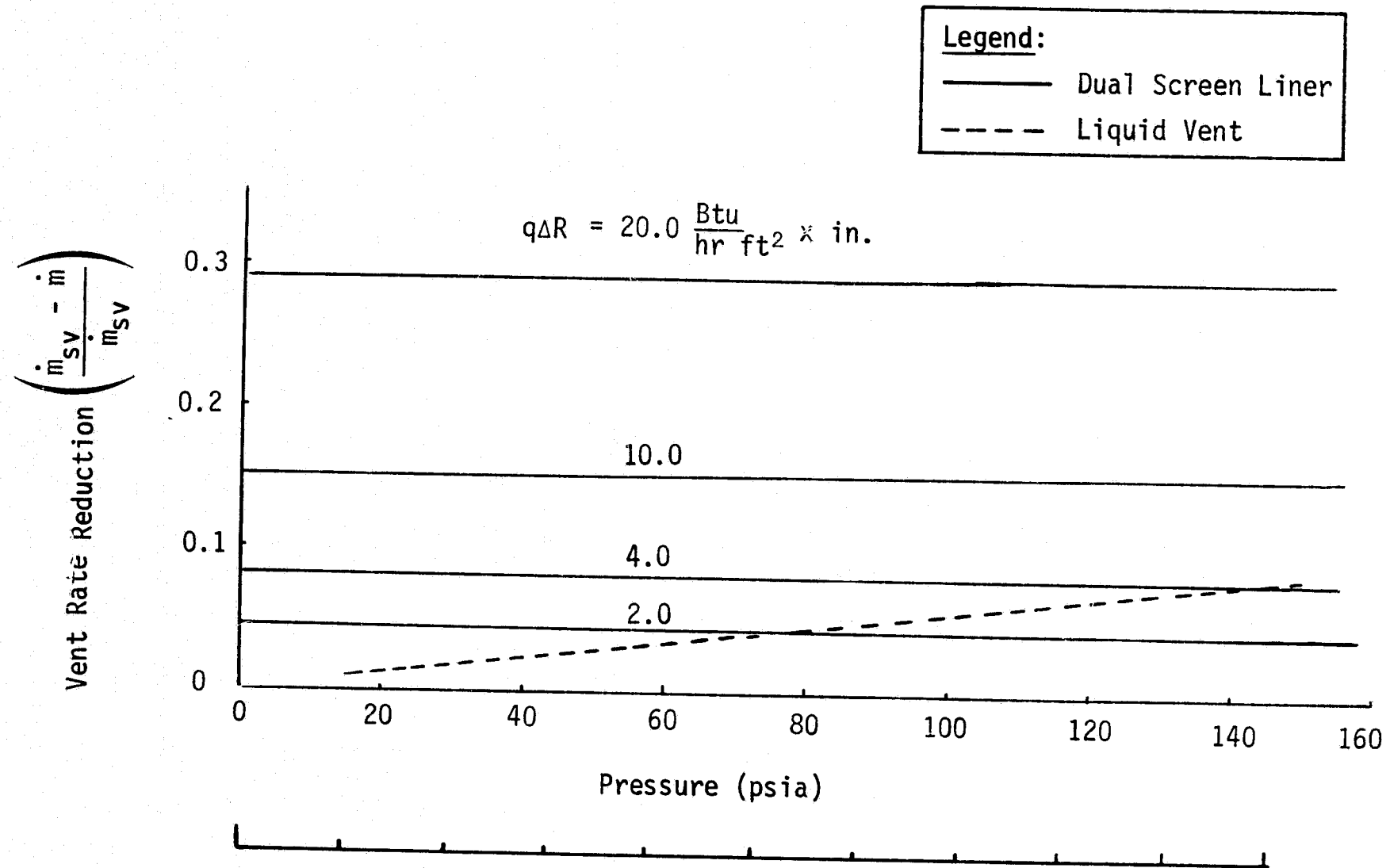
Figure II-10 Comparison of Hydrogen Vent Rate for the DSL
and Liquid (Thermodynamic) Vent System
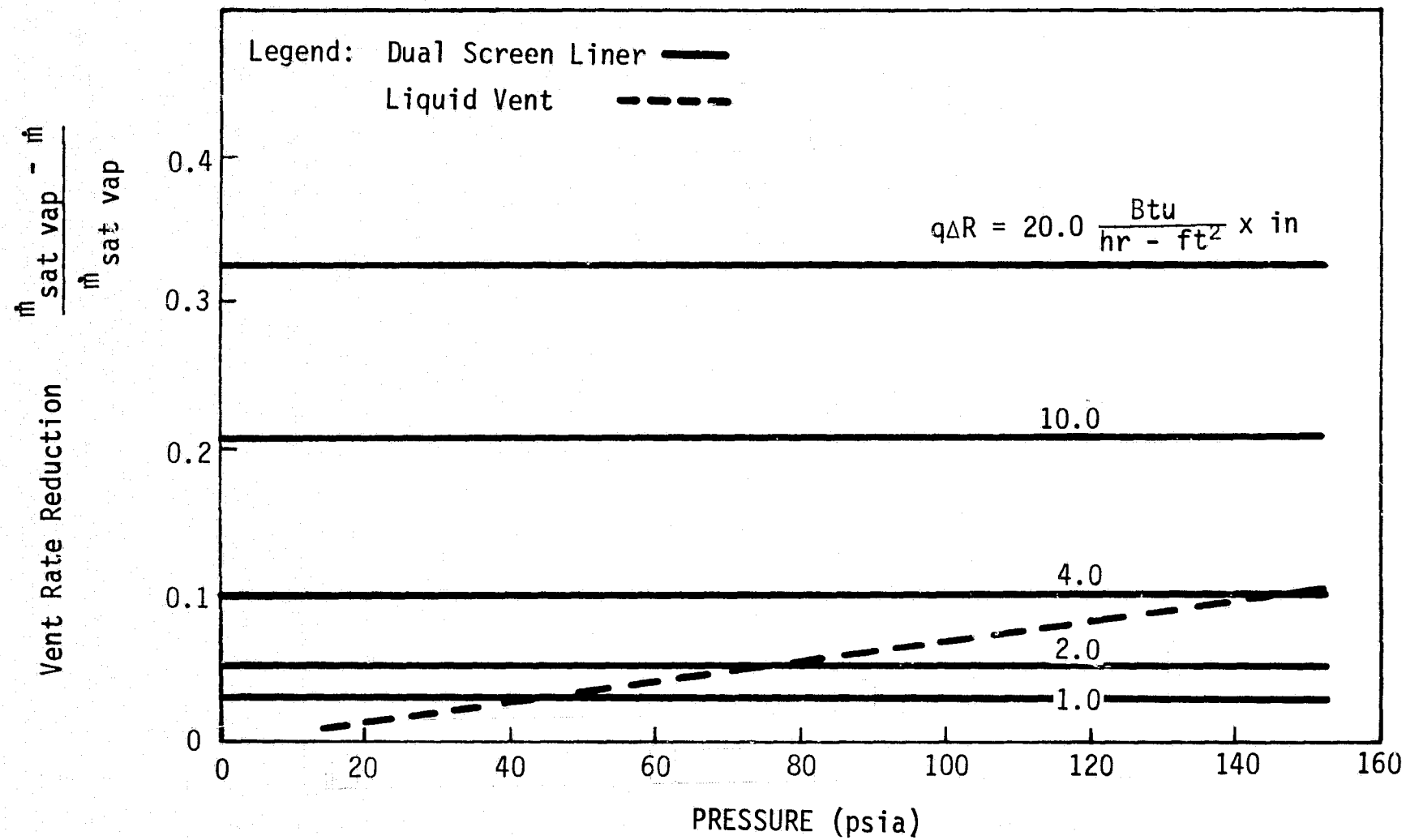
Fig. II-11  Comparison of the Nitrogen Vent Rate from the DSL
and Liquid (Thermodynamic) Vent System
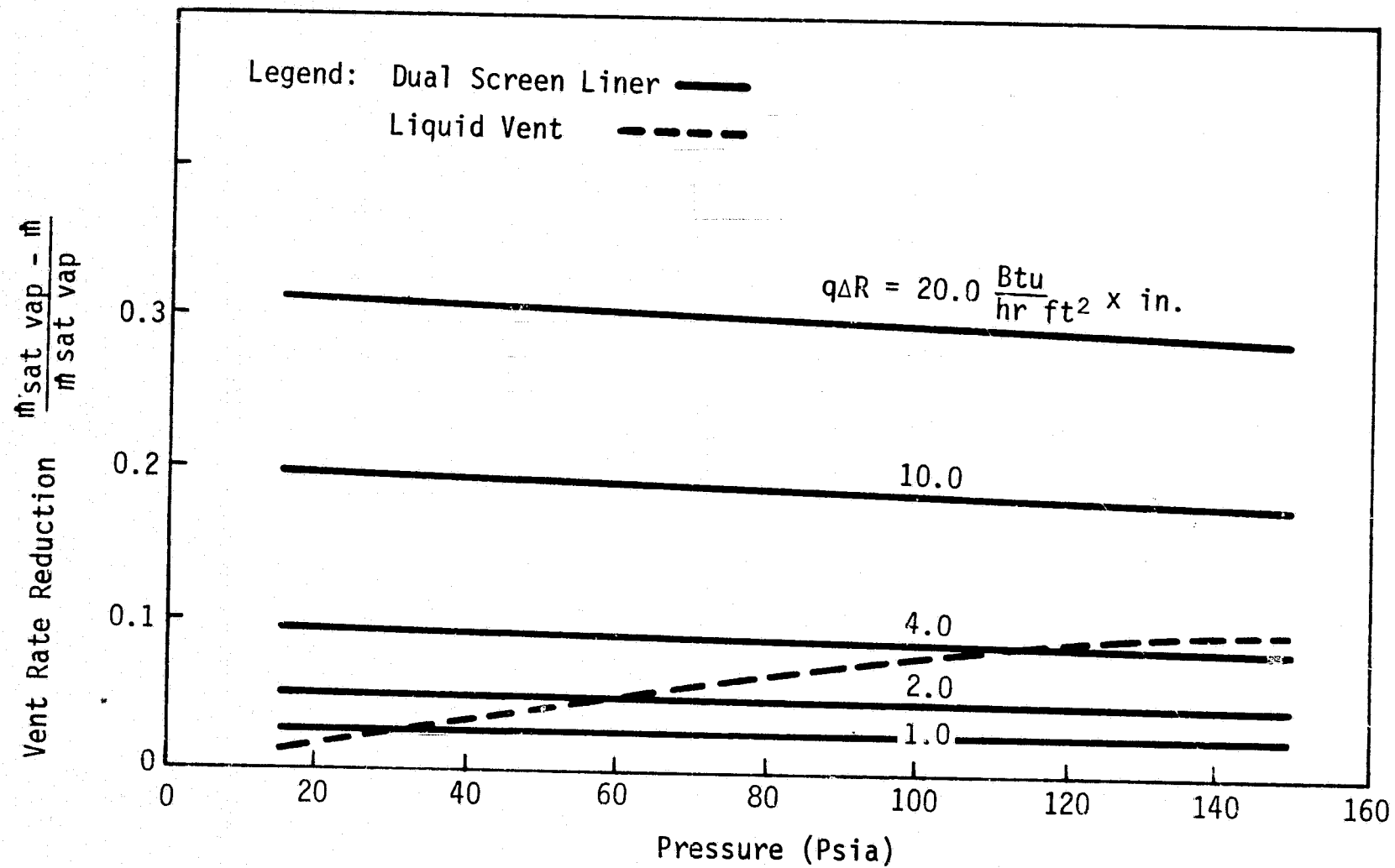
Figure II-12  Comparison of the Methane Vent Rate for the DSL
and Liquid (Thermodynamic) Vent System

24

### 3. Dual Screen Liner

The superheat term in Eq (II-5) must be computed from a heat flow equation. Consider a spherical gas layer in which we admit only steady radial flow. An energy balance on the layer results in

$$\frac{\partial}{\partial r} \left\{ u \rho C_p T r^2 - k r^2 \frac{\partial T}{\partial r} \right\} = 0 \qquad (II-7)$$

where u represents the radial velocity component. Assuming fluid properties to be constant, results in

$$\rho C_p T \frac{\partial}{\partial r} (u r^2) + \rho C_p u r^2 \frac{\partial T}{\partial r} - k \frac{\partial}{\partial r} \left( r^2 \frac{\partial T}{\partial r} \right) = 0. \qquad (II-7a)$$

Continuity requires that

$$\frac{\partial}{\partial r} (u r^2) = 0$$

so that the energy equation becomes

$$\left( \frac{\rho C_p}{k} \right) u \frac{\partial T}{\partial r} = \frac{1}{r^2} \frac{\partial}{\partial r} \left( r^2 \frac{\partial T}{\partial r} \right). \qquad (II-7b)$$

The boundary conditions to be satisfied are

$$\text{at } r = R_1, \qquad -k \frac{\partial T}{\partial r} = \frac{\dot{m} \lambda \xi}{A} \quad *$$

$$r = R_2, \qquad -k \frac{\partial T}{\partial r} = q$$

$$r = R_1, \qquad T = T_s .$$

Solution of Eq (II-6b), subject to the boundary conditions, results in

$$T - T_s = \frac{Q}{4 \pi k B} \left( e^{-B/r} - e^{-B/R_1} \right) \qquad (II-8)$$

---

\*This boundary condition results from the solution of Eq (II-1) and (II-2) together with an energy balance on the inner surface of the gas annulus.

where

$$B = \frac{\dot{m}C_p}{4\pi k}$$

the flow rate is defined by

$$\ln B + B \ln\left(\frac{e^{1/R_1}}{e^{1/R_2}}\right) = \ln\left(\frac{QC_p}{k4\pi\lambda\xi}\right) \tag{II-9}$$

making the approximation $R_2 - R_1 = \Delta R \ll R_1$ and using Eq (II-6) results in

$$\eta^{1/\eta} = \exp\left[-q \Delta R\left(\frac{C_p}{\lambda k \xi}\right)\right] . \tag{II-10}$$

The radial flow solution predicts the maximum superheat obtainable with the DSL. The vent rate predicted with Eq (III-10) will be somewhat less than is obtainable in practice because true radial flow will not be obtained. The fractional reduction in vent rate relative to saturated vapor venting $(1-\eta)$ computed from Eq (III-7), is plotted as a function of pressure on Fig. II-9 thru II-12 for the four study fluids.

Curves are plotted for constant values of the parameter $q \Delta R$, where $q$ is the heat flux and $\Delta R$ the width of the vapor annulus. Note that relatively large values of $q \Delta R$ are required to achieve a significant reduction in vent rate. However, even for $q = 0.25$ Btu/hr-ft$^2$, as specified for this study (see Table IV-1), and a gap width of 1 in., $q \Delta R$ is equal to $0.25$ (Btu/hr-ft$^2$) (in.), a vent reduction of 5% is possible at a system pressure of about 20 psia with hydrogen. This reduction is identical to that for the liquid vent at 20 psia. A vent reduction of 10% is possible with the same $q \Delta R$ value at 150 psia.

## 4. Case II - Tank Conditions Steady, Liquid Outflow

In the above discussion, gas venting was considered for pressure control. We will now consider the need for gas venting under the condition of liquid withdrawal. Solving Eq (II-4) for the liquid outflow rate with $\dot{m}_g$, $du$, and $du_g$ set to zero yields

$$\dot{m} = \frac{Q}{\lambda(\xi-1)} . \tag{II-11}$$

Consider now, a spherical tank of diameter D that is steadily depleted of liquid over a period of $\theta$ days. The liquid outflow rate is then

$$\dot{m} = \frac{\alpha \frac{4}{3} (\pi)\left[\frac{D}{2}\right]^3 \rho_\ell}{24\theta} \tag{II-12}$$

the heat rate Q can be expressed in terms of the flux q and tank area.

$$Q = q \pi D^2 .$$ (II-13)

Combining Eq (II-11), (II-12) and (II-13) leads to

$$\frac{D}{q\theta} = \frac{144(v_g - v_\ell)}{\alpha \lambda} .$$ (II-14)

Equation (II-14) is plotted as a function of pressure in Fig. II-13 for the four study fluids and $\alpha = 0.95$. For example, in the use of Fig. II-13 consider a pressure level of 30 psia. Then with oxygen, nitrogen, or methane, in the absence of gas venting, stable conditions will be maintained when $D/q\theta = 3.6$ ft/(Btu/hr-ft$^2$)(day). Therefore, if a 10-ft-diameter oxygen tank is heated at the rate of 0.25 Btu/hr-ft$^2$, a steady pressure of 30 psia will be maintained if the depletion time is $10/(0.25 \times 3.6) = 11$ days. With hydrogen, the corresponding figures for a 16-ft-diameter tank and 30 psia pressure are $D/q\theta = 5.3$, and $\theta = 12$ days. These times are independent of the time period required to reach this pressure. As a result of the liquid heat capacity, the time to reach 30 psia from one atmosphere saturation is 95 and 12 days for oxygen and hydrogen, respectively.

Equation (II-11) is also plotted in Fig. II-14 for the additional constraint of $q = 0.25$ Btu/hr-ft$^2$.
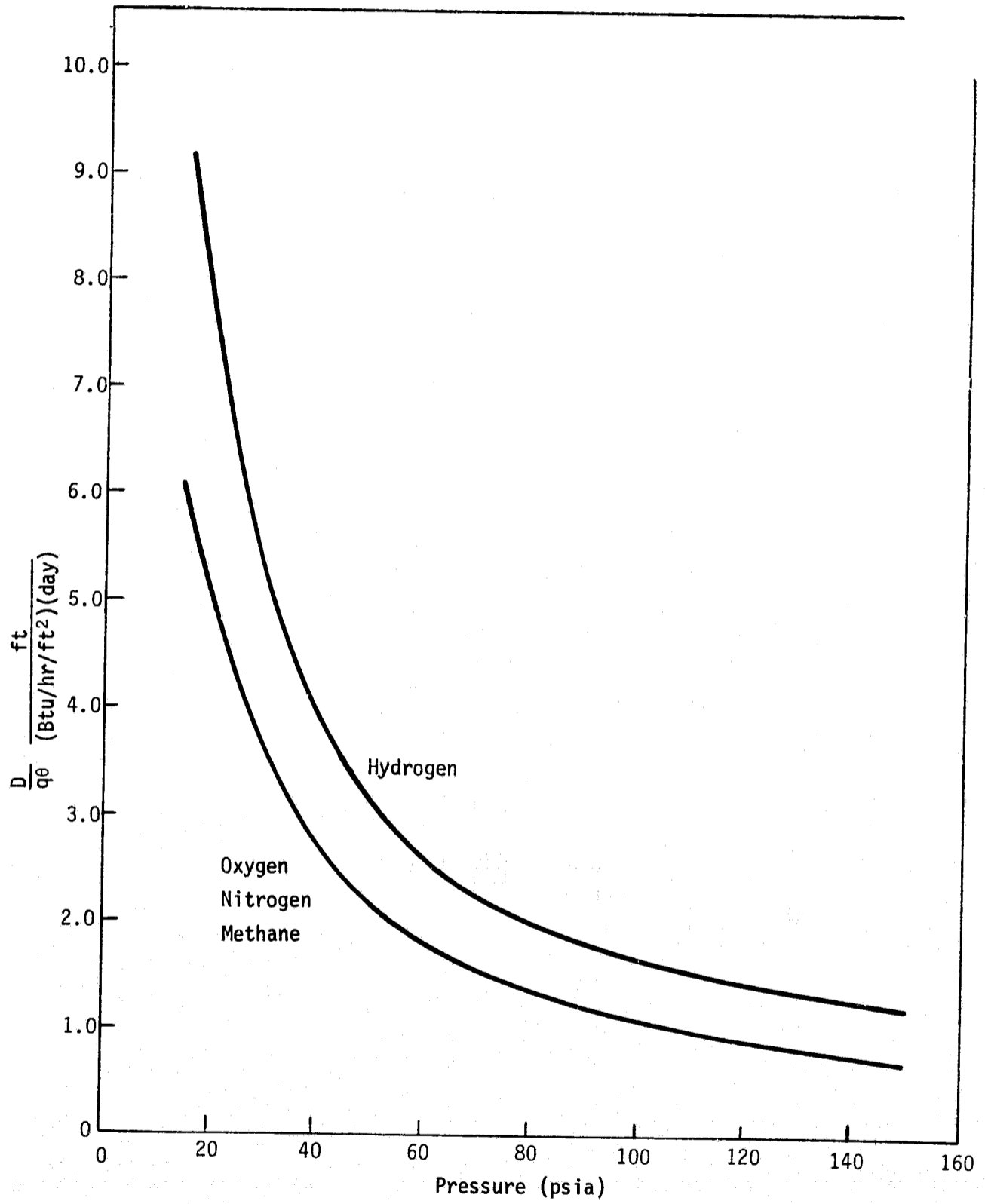
Figure II-13   Spherical Tank Size, Heat Flux, and Depletion Time to Maintain
Steady Conditions within a Cryogenic Storage Tank
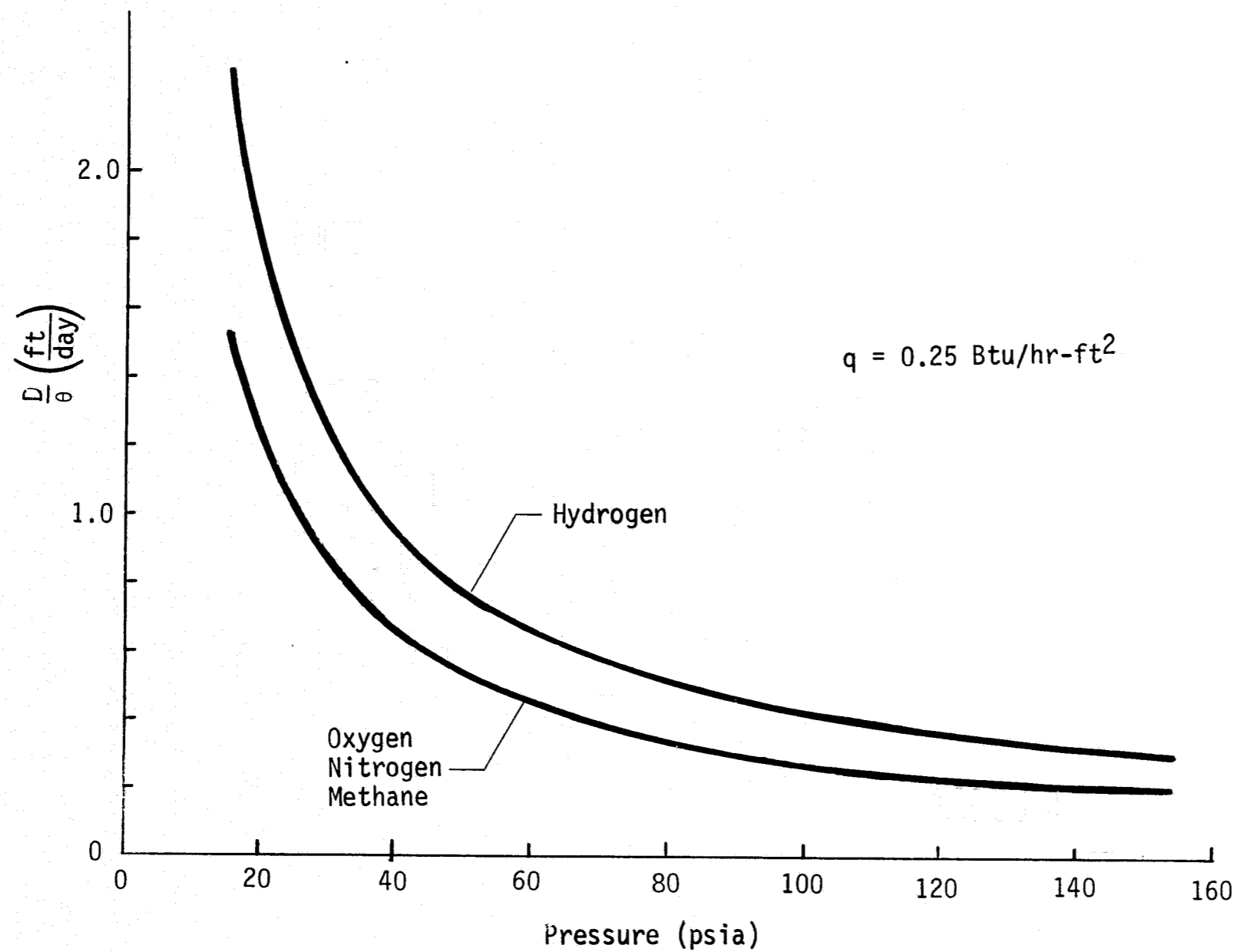
Figure II-14 Spherical Tank Size and Depletion Time to Maintain Steady Conditions within a Cryogenic Storage Tank Heated at the Rate of 0.25 Btu/hr-ft²

### III. DSL ANALYTICAL MODEL

A mathematical model was developed to help assist in the design analysis, parametric study, and the test plan formulation for the DSL retention/expulsion system. Since the model simulates the thermodynamics and heat transfer of a DSL, various modes of operation under specified thermal conditions can be evaluated. The model provides a means to establish the expected thermal performance, rates of change of pressure and temperature, and the limits of applicability of the system. All four cryogens specified in the parametric study can be treated. Their thermodynamic and transport properties are input to the computer program as a function of temperature and pressure. Pressurization with a noncondensible gas, giving a two-component gas mixture is permissible, as are spherical or cylindrical tank configurations. The following modes of operations can be simulated:

1) Pressurization of the system due to external heat input;

2) Pressurization of either the vapor annulus or bulk region with autogenous or inert gas;

3) Venting, with various vent control systems;

4) Liquid outflow.

The analytical model was programmed in FORTRAN IV language for use on the CDC 6500/6600 computer. It was written in subroutine format wherein various options can easily be added or deleted from the program. A brief description of the model, including analysis and program capabilities and limitations, is presented in this chapter.

The thermodynamic and transport properties for the four cryogens and for helium pressurant are calculated from curve fit equations. With the exception of hydrogen, the vapor of the propellant is considered to be an ideal gas. For hydrogen, the Redlich-Kwong equation of state was used. This equation of state was checked out for hydrogen gas and was determined to be within 5% of published data (Ref III-1) for pressures up to 150 psia and for a temperature range of $35^{o}$R to $530^{o}$R.

The program was initially developed to aid in the design of the subscale model by simulating pressurization, venting, and fluid expulsion in a 1-g acceleration environment. Thus the position of the ullage and the liquid in the bulk fluid region was known and a flat interface between the two was assumed. Since hydrostatic head and natural convection heat transfer coefficients are functions of g-level, low-g conditions can be simulated by using an acceleration value near zero. Since the outer annulus is liquid-free and we do not use ullage control in the bulk region, actual low-g liquid/vapor interface shapes are not significant with respect to venting simulation. However, the analytical model will not handle such things as diffusion of a two-component gas mixture in the bulk fluid region during low-g simulation, and condensation and vaporization are assumed to occur at a flat interface.

## A. TANK THERMODYNAMICS AND HEAT TRANSFER

The program considers a complete DSL inside a spherical tank or a cylindrical tank with flat ends (configuration of subscale model). Figure III-1 shows the contents of a spherical tank divided into five nodes corresponding to the following volumes:

VGA     - vapor volume in outer annulus;

VBU     - bulk vapor volume;

VBL     - bulk liquid volume;

VLBU     - inner-annulus volume seeing bulk ullage;

VL     - inner-annulus liquid volume seeing bulk liquid.

A communication port having a screen with a bubble point less than that of the other screens is included to allow for propellant and pressurant mass transfer between the outer annulus and the bulk ullage. The program can handle noncondensible pressurant in both ullage nodes if desired.

A heat and mass transfer analysis is performed for one control volume at a time with new pressures and temperatures calculated at each time step (by a forward differencing technique). New masses are calculated after the amount of vaporization (condensation), liquid outflow, and vapor venting has been determined.

The initial temperature of each of the nodes is input along with the total pressure in the bulk ullage node. The partial pressure of propellant in the bulk ullage node, $P_{VBU}$, is set equal to the vapor pressure of the propellant at the bulk liquid temperature. The residual gas pressure $P_{GBU}$, is the difference between the total ullage gas pressure, $P_{BU}$, and the vapor pressure of the propellant. The initial total gas pressure in the outer annulus, $P_{GA}$, is equal to the bulk gas pressure plus the hydrostatic head for the height of fluid between the liquid-vapor interface in the bulk region and the outer screen, with consideration for the acceleration level being simulated. The partial pressure of propellant, $P_{VGA}$, is set equal to the vapor pressure of propellant at the temperature of the liquid annulus. The residual gas pressure in the outer annulus, $P_{GGA}$, is again the difference between the two.

$$P_{BU} = P_{VBU} + P_{GBU}$$

$$P_{GA} = P_{VGA} + P_{GGA}$$

For ideal gases $P = \frac{MRT}{V}$, and
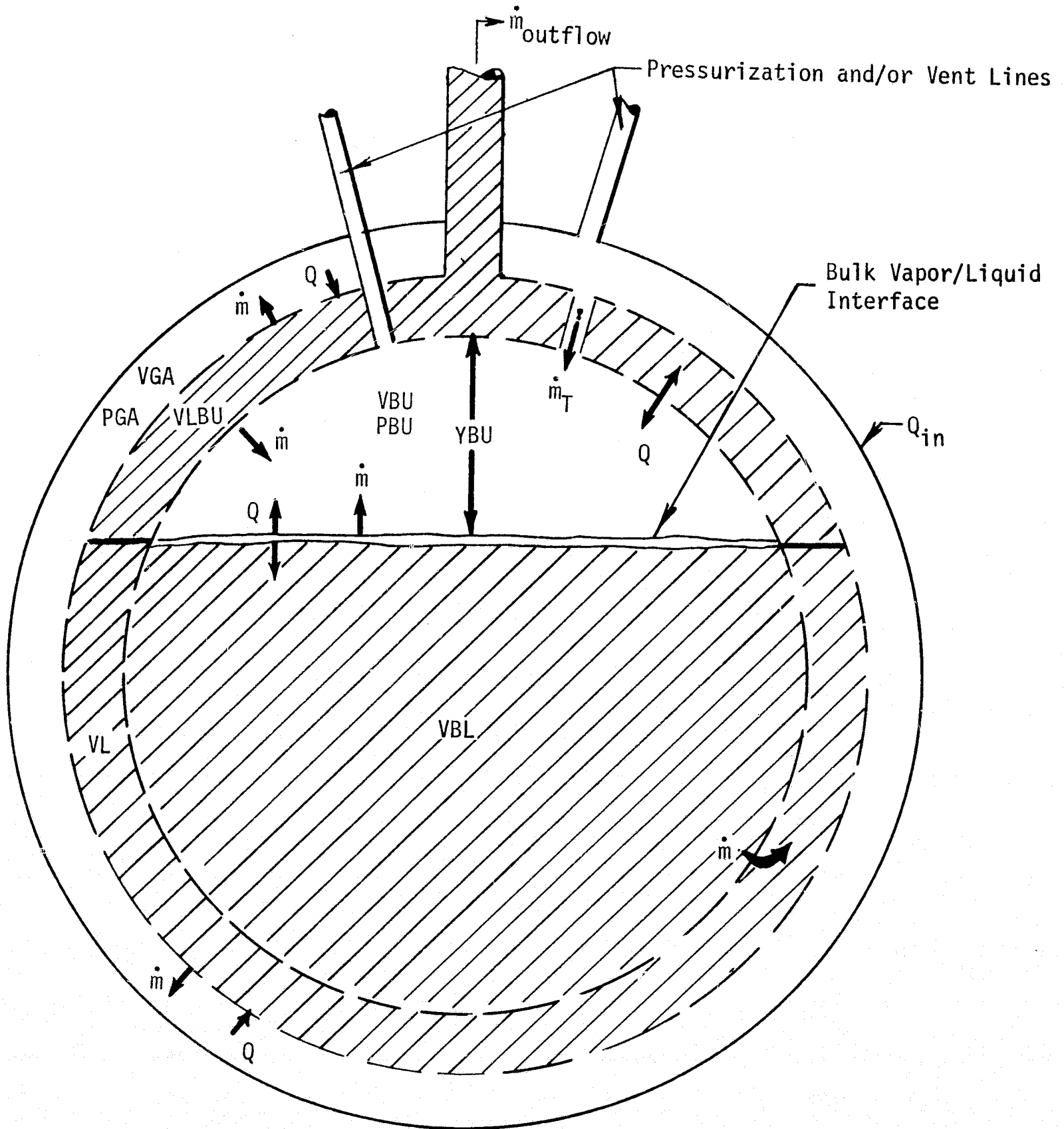
Figure III-1  Heat and Mass Transfer Model for the Baseline DSL

$$\frac{\partial P}{\partial \theta} = P \left\{ \frac{1}{M} \quad \frac{\partial M}{\partial \theta} + \frac{1}{T} \quad \frac{\partial T}{\partial \theta} - \frac{1}{V} \quad \frac{\partial V}{\partial \theta} \right\}. \qquad \text{(III-1)}$$

The pressure in the outer annulus is constrained by the requirement that it must not exceed the pressure in the bulk ullage by more than the retention capability of any of the wetted screens forming the liquid supply annulus. A communication screen is thus provided with a pressure retention capability slightly less than that of the screens forming the liquid annulus. A pressure increase in the outer annulus may relieve itself by breaking down the communication screen to allow gas flow to the bulk ullage rather than breaking down one of the spherical screens allowing vapor bubbles to be ingested into the liquid annulus. Thus

$$P_{GA} - P_{BU} < BPC$$

where BPC is the capillary retention pressure or bubble point of the communication screen.

Let $\Delta P = P_{GA} - (P_{BU} + BPC)$

then $\Delta P \Big|_{\theta}^{\theta + \Delta\theta} = \frac{\partial \Delta P}{\partial \theta} d\theta.$

Assuming that some gas flows across the communication screen in order to satisfy the pressure constraint $\Delta P^{\theta + \Delta\theta} \to 0$ and

$$\frac{\partial \Delta P}{\partial \theta} = -\frac{\Delta P^{\theta}}{d\theta} = DPDT$$

$$\frac{\partial \Delta P}{\partial \theta} = \frac{\partial}{\partial \theta} (P_{GA} - P_{BU} - BPC)$$

$$= \frac{\partial}{\partial \theta} (P_{VGA} + P_{GGA} - P_{VBU} - P_{GBU}).$$

Substituting in Eq (III-1) for each of the above terms,

$$\frac{\partial \Delta P}{\partial \theta} = P_{GGA} \frac{1}{M_{GGA}} \frac{\partial M_{GGA}}{\partial \theta} + P_{VGA} \frac{1}{M_{VGA}} \frac{\partial M_{VGA}}{\partial \theta}$$

$$+ \frac{P_{GA}}{T_{GA}} \frac{\partial T_{GA}}{\partial \theta} - \frac{P_{GA}}{V_{GA}} \frac{\partial V_{GA}}{\partial \theta} \qquad \text{(continued)}$$

$$- P_{GBU} \frac{1}{M_{GBU}} \frac{\partial M_{GBU}}{\partial \theta} - P_{VBU} \frac{1}{M_{VBU}} \frac{\partial M_{VBU}}{\partial \theta}$$

$$- \frac{P_{BU}}{T_{BU}} \frac{\partial T_{BU}}{\partial \theta} + \frac{P_{BU}}{V_{BU}} \frac{\partial V_{BU}}{\partial \theta} = DPDT. \qquad \text{(III-2)}$$

Terms of the form $\frac{\partial M}{\partial \theta}$, $\frac{\partial V}{\partial \theta}$ and $\frac{\partial T}{\partial \theta}$ must be evaluated. The term $\frac{\partial M}{\partial \theta}$ contains the summation of all the mass transfers due to vaporization (condensation), venting, pressurization, and a term $\dot{m}_T$ which represents the amount of gas transferred across the communication screen during breakdown of that screen. The term $\frac{\partial V}{\partial \theta}$ is zero for the outer annulus since this ullage volume is fixed in size. The bulk ullage volume increases due to the decrease in bulk liquid mass when liquid is resupplied to the liquid annulus to replace that vaporized at the screen surfaces.

The rate of change of gas temperature in the ullage nodes, $\frac{\partial T}{\partial \theta}$, is obtained from an energy balance for the total node. The energy terms involved in the balance are related to the following factors:

1) Specific enthalpy and flow rate of the gas entering and vented;

2) Mass transfer between gas and liquid phases;

3) Heat transfer between gas and liquid phases and between the gas and tank walls or screens;

4) Change in internal energy of the gas phase;

5) Work on the propellant.

From the first law of thermodynamics

$$dU = dQ - PdV$$

$$U\frac{\partial M}{\partial \theta} + M\frac{\partial U}{\partial \theta} = \frac{\partial Q}{\partial \theta} + h_1 \frac{\partial M}{\partial \theta} - P\frac{\partial V}{\partial \theta}$$

where $h_1$ represents the enthalpy of mass entering the node at temperature $T_1$. For a near-ideal gas, the enthalpy can be represented by $C_p T$, internal energy by $C_v T$ and internal energy change by $C_v \frac{\partial T}{\partial \theta}$, since $C_p$ and $C_v$ can be considered constant over the temperature ranges encountered.

$$MC_v \frac{\partial T}{\partial \theta} + \frac{\partial M}{\partial \theta} C_v T = (Q_{in} - Q_{out}) + \frac{\partial M}{\partial \theta} C_p T_1 - P \frac{\partial V}{\partial \theta}$$

$$MC_v \frac{\partial T}{\partial \theta} = (Q_{in} - Q_{out}) + \frac{\partial M}{\partial \theta} (C_p T_1 - C_v T) - P \frac{\partial V}{\partial \theta}$$

$$\frac{\partial T}{\partial \theta} = \frac{(Q_{in} - Q_{out}) + \frac{\partial M}{\partial \theta} \left[ C_p (T_1 - T) + PV \right] - P \frac{\partial V}{\partial \theta}}{MC_v} \ .$$

The rate of change of temperature in the liquid nodes is calculated from a similar equation with $\frac{\partial V}{\partial \theta}$ equal to zero since the liquid volumes are fixed in size.

Equation (III-2) can now be solved for $\dot{m}_T$, the amount of gas transferred across the communication screen. The program then returns to the heat and mass transfer calculations for time $\theta = \theta + \Delta\theta$.

The heat transfer in the ullage nodes and in the bulk region is assumed to be of the free convective type given by a general equation of form

$$Q = h \ A \ (\Delta T)$$

where Q = heat transfer rate,

  h = convective heat transfer coefficient,

  A = heat transfer area,   .

  T = temperature differential.

Heat transfer in the liquid annulus is calculated based on an equivalent heat conductivity acting over a fluid layer confined by two parallel surfaces. Heat transfer coefficients and heat conductivity are determined empirically from test data by dimensional analysis and curve fitting. The empirical data of Eckert and Drake (Ref III-2) and Kreith (Ref III-3) were used to calculate the necessary heat transfer coefficients.

### B. PRESSURIZATION AND FLUID EXPULSION

The program has the option of pressurization with autogenous and/or noncondensible (residual) gas pressurant. A fixed flow rate orifice is simulated by using a constant valued mass flow rate table lookup. A regulator operation is simulated by specifying a regulator setting for the bulk ullage pressure and determining if pressurant should be added during a compute interval. The pressurant enters the vapor annulus and the communication port limits the pressure differential between the vapor annulus and the bulk ullage to the bubble point.

The program can consider outflow during blowdown of the tank or outflow under a pressure regulated condition. The outflow rate can be considered a constant or specified as a function of time, such as for a mission duty cycle. Outflow is considered to be completed and the tank assumed to be empty when all the liquid has been depleted from the bulk region. The propellant remaining in the liquid annulus is assumed to be residual.

### C. VENTING

Successful venting of the DSL is dependent on sensitive pressure control in the gas annulus. During venting, the pressure in the gas annulus must not fall below that value required for support of the liquid in the bulk region. (During a coast period in Earth orbit when the drag-induced acceleration vector is known, it may be advantageous to drop the liquid out of the bulk region to allow a preferential rapid venting capability, see Section II.B on DSL operation.) In zero gravity, the pressure in the gas annulus must not fall below the inner ullage pressure. With finite gravity, the gas annulus pressure must exceed the bulk pressure by the liquid hydrostatic head.

The DSL can provide liquid-free venting of vapor from the outer annulus. The mass outflow rate will be either sonic or subsonic depending on the ratio of the total tank pressure to the local atmospheric pressure as compared to the critical pressure ratio for the ullage gas (Mach = 1.0). A mass fraction for the vented gas is computed and the propellant vapor and helium pressurant masses adjusted accordingly. The ratio of specific heats and the critical pressure ratio for the mixed ullage are as follows:

$$\gamma_m = \frac{C_p}{C_v} \; ; \; \text{and}$$

$$PR_{cr} = \left[\frac{2}{\gamma_m+1}\right]^{\left\{\frac{\gamma_M}{\gamma_M-1}\right\}} .$$

The vented flow rate then becomes

$$\dot{m}_{vent} = A_e \sqrt{\frac{2(P_T - P_A) \, g_c P_T M_{WT}}{(1545) \, T_T}} \quad \text{(subsonic)}$$

$$\dot{m}_{vent} = A_e P_T \sqrt{\frac{M_{WT}\gamma_m \, g_c}{(1545)T_T} \left(\frac{2}{\gamma_m+1}\right)^{\left(\frac{\gamma_m+1}{\gamma_m-1}\right)}} \quad \text{(sonic)}$$

where $A_e$ = effective vent orifice area;

$P_T, T_T$ = total pressure and temperature of mixed ullage;

$P_A$ = atmospheric pressure;

$M_{WT}$ = molecular weight of mixed ullage.

Various vent schemes are incorporated into the model to allow for venting when an ullage overpressure condition exists. One vent scheme was analyzed where the outer annulus was vented to the point where it could just support the hydrostatic head of the bulk fluid in one-g (as a result, the allowable pressure decay during venting of the outer annulus will be on the order of 0.1 psi for the subscale model). At this point the vent was closed and pressure increased in the outer annulus until the communication screen broke down and vapor passed from the outer annulus to the bulk region. This continued until the regulated pressure was again reached. An example of this type of vent cycle is shown in Fig. III-2. A heat flux of 5.0 Btu/hr ft$^2$ and a 0.50-in. gas annulus were assumed for a spherical subscale tank filled with nitrogen. The screens forming the liquid annulus were assumed to be made of 325 x 2300 mesh Dutch twill with the communication screen made of 250 x 1370 mesh. The upper curve represents the pressure in the outer annulus, while the lower curve depicts the pressure in the central region.

At time 1, the vent valve has closed and the pressure in the outer region begins to rise. The pressure in the central region is falling at this time because condensation is occurring. At time 2, the pressure difference between the two regions has exceeded the bubble point of the communication screen and gas flows from the outer annulus to the central region. At this time there is an abrupt change in slope of the two pressure curves. As a result of the gas flow from the outer to inner ullage regions, the ullage gas in the central region is superheated and condensation at the liquid-vapor interface occurs continuously. The pressure in the outer region reaches the vent point at time 3. When venting begins, the pressure difference between the two ullage regions falls below the bubble point of the communication screen and flow between the two regions stops. The condensation in the inner region then causes the pressure to fall until flow from the outer region again resumes.

For the case of near-zero gravity the pressure in the gas annulus must not fall below the inner ullage pressure. For this case the allowable pressure decay during venting will be on the order of the bubble point of the communication screen (0.29 psi for nitrogen). Such a case is shown in Fig. III-3 for an acceleration of 0.05 g. For this case the lower set point on the pressure control in the outer annulus was set at 0.05 psi above the inner pressure while the upper set point was fixed.

Another vent scheme would incorporate a vent cycle where venting is initiated before slightly superheated vapor was allowed to break through the communication screen to add some energy to the bulk fluid region. The variation of pressure with time for this case is shown in Fig. III-4.

The tank self-pressurizes and gas is transferred through the communication port until venting is initiated at 0.0045 hours. Both pressure limits for the vent cycle are referenced to the bulk ullage pressure. Venting of the vapor annulus starts when the vapor annulus pressure is 0.25 psi greater than the bulk ullage pressure and ceases after the vapor annulus pressure has dropped to within 0.05 psi of the bulk ullage pressure. Flow between the two gas regions
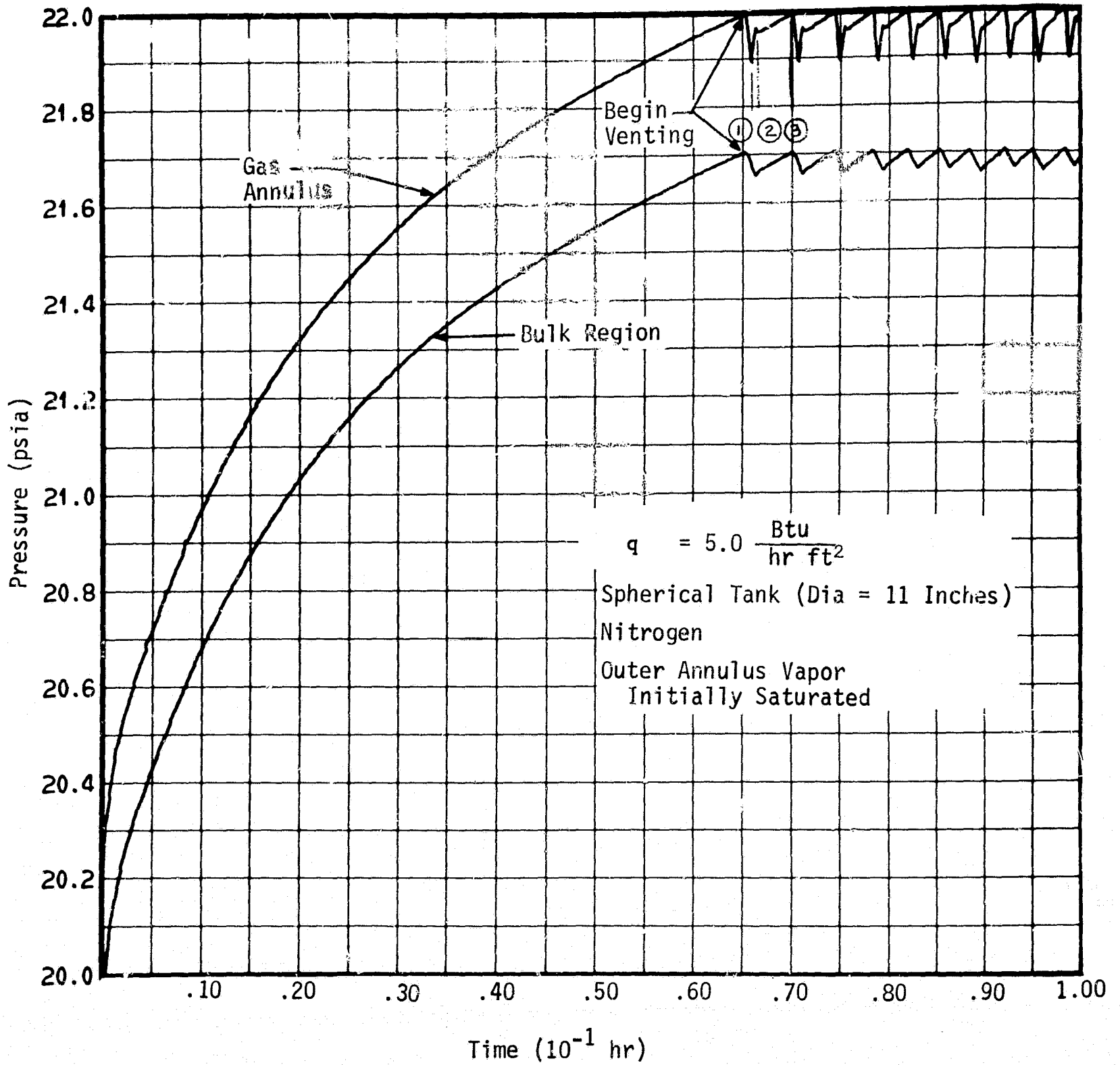
Figure III-2  Vent Cycle for Spherical Tank (1-g)

38
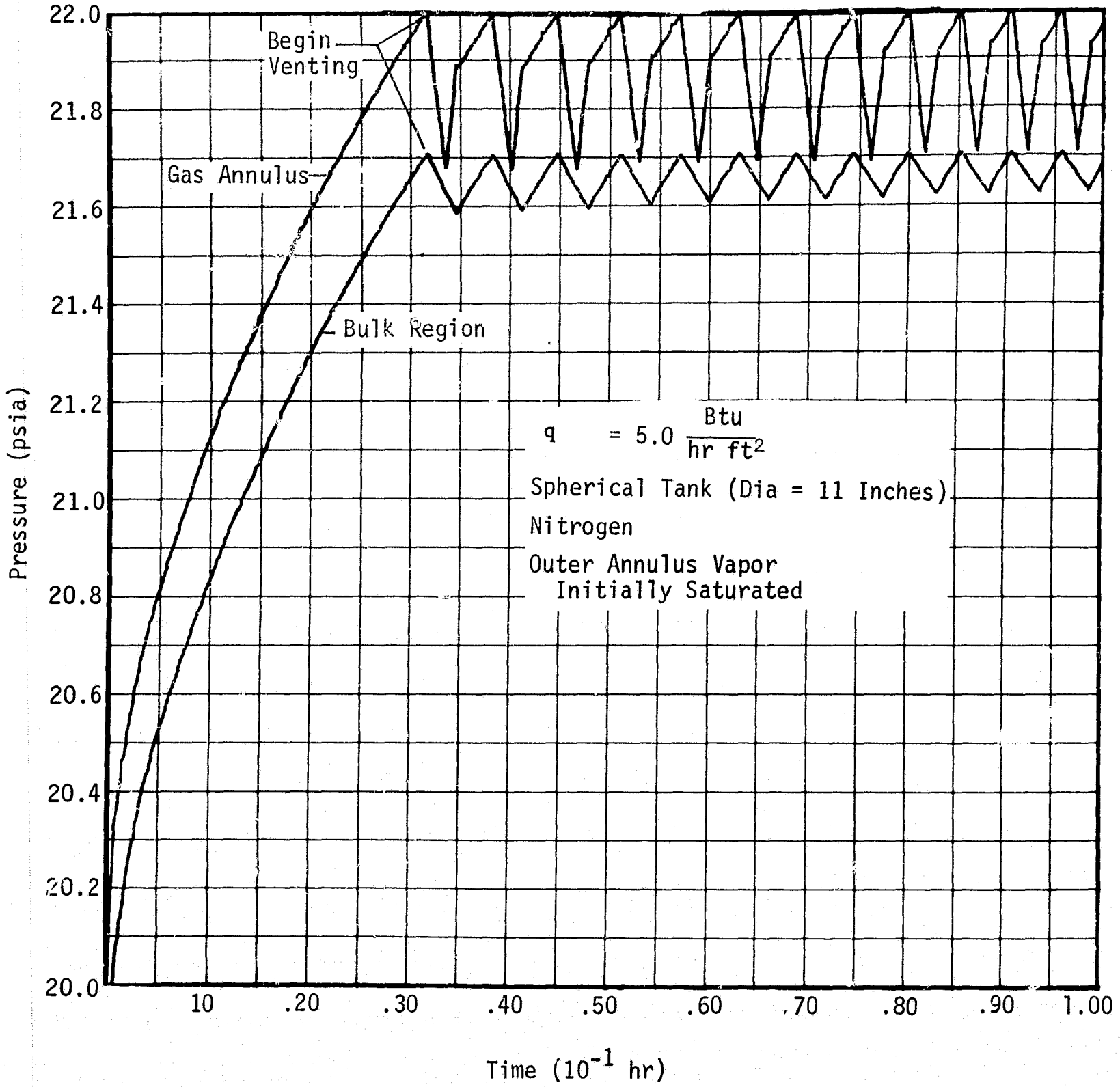


Figure III-3 Venting Cycle for Spherical Tank (0.05 g) with
Flow through Communication Screen
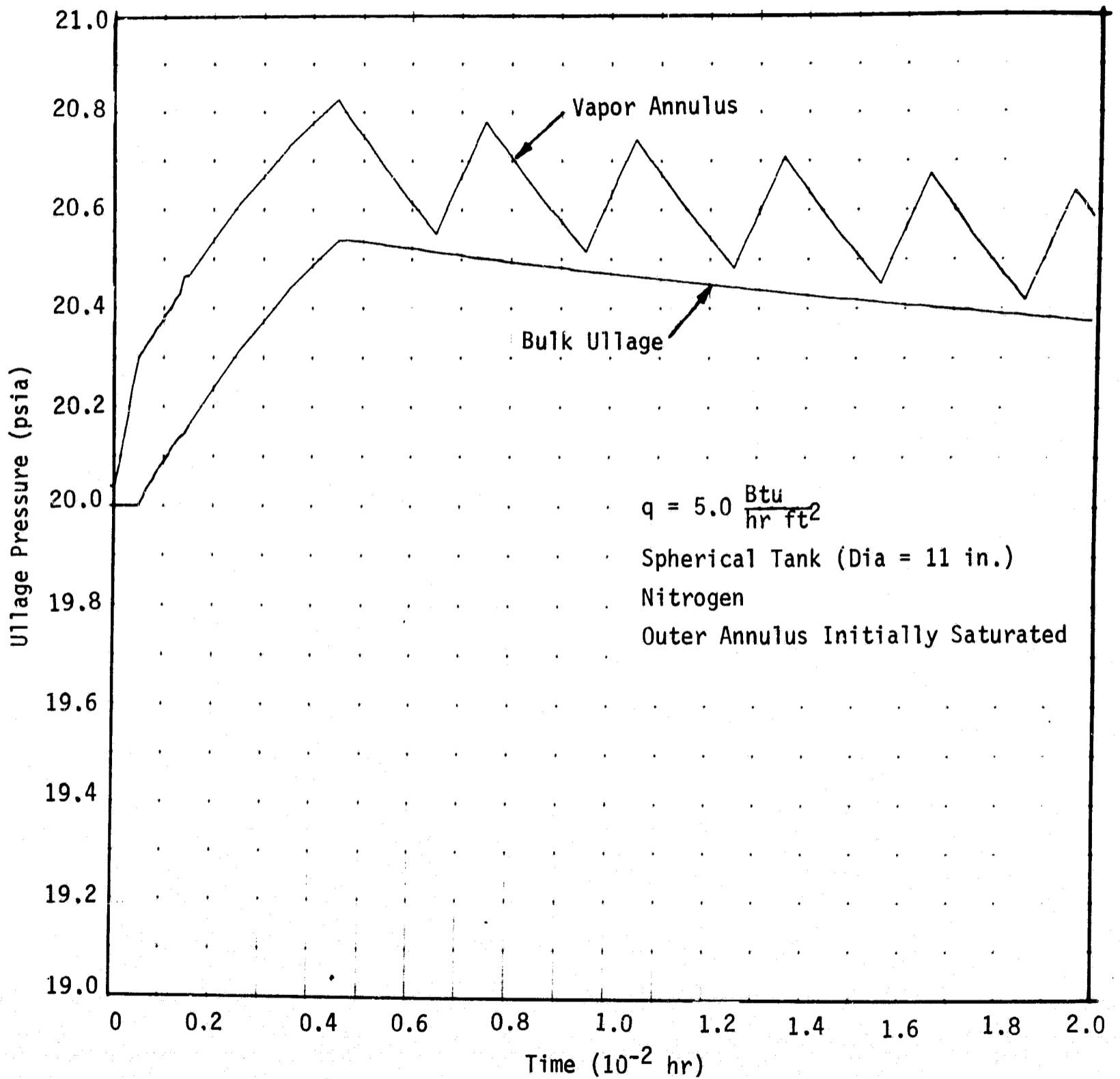
Figure III-4  Vent Cycle for Spherical Tank (0.05 g) with
No Flow through Communication Screen

does not occur during the vent cycle because the differential pressure at which
venting is initiated is less than the bubble point of the screen in the communi-
cation port. By keeping the vapor annulus pressure at least 0.05 psi above the
bulk ullage pressure, the differential will be more than sufficient to support
the hydrostatic head at low-g.

Initially, the bulk ullage pressure decreases somewhat because gas was
flowing through the communication port before venting started. Some collapse
of the bulk ullage due to condensation occurs when venting begins (Fig. III-4).
After approximately 10 minutes, this pressure levels off and begins to rise at
a slow rate (0.6 psi per hour) as shown in Fig. III-5. This is expected because
the vent rate (0.18 $lb_m$/hr) is roughly equivalent to the heat input and venting
is taking place only two-thirds of the time.

It appears that this latter case is an improved mode of venting because
the temperature difference across the liquid annulus is minimized, thus reducing
the conduction heat transfer to the bulk liquid. Also, as a result of the gas
flow through the communication port, condensation occurs continuously in the
former cases. This condensation is a major heat input to the bulk liquid.
Therefore, by minimizing the pressure difference between the two ullage regions,
an adiabatic condition is more closely approached with regard to the bulk liquid.
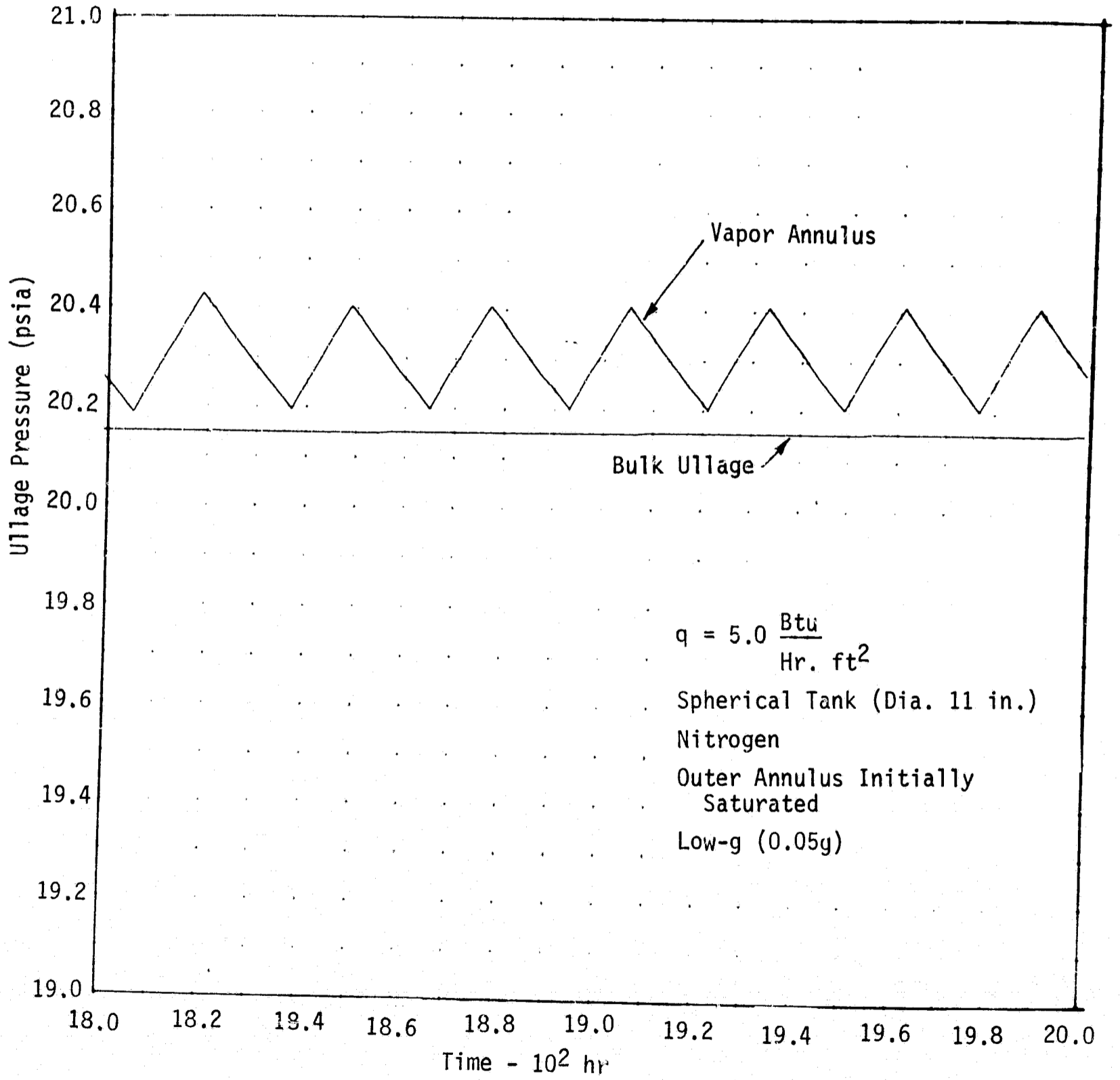
Figure III-5  Venting for Spherical Tank (0.05 g) with no Flow through Communication Screen

## IV. PARAMETRIC STUDY RESULTS

The DSL concept was the baseline passive concept for the parametric analysis. The concept is flexible, as described in Chapter II, and may assume various configurations to satisfy different applications. The range of parameters over which the DSL concept was analyzed is presented in Section A, Study Guidelines, of this chapter.

To satisfy the three design objectives with the DSL, heat transfer and thermodynamics during pressurization, venting, and fluid expulsion were considered. Of prime importance was the stability of the DSL under both hydrostatic and hydrodynamic conditions over a range of operating parameters. Material selection and system weight, along with screen cleaning and inspection, are important to the fabrication and assembly of any capillary device. These considerations are discussed in the following sections.

### A. STUDY GUIDELINES

The parametric study guidelines are presented in Table IV-1. The range of parameters include relatively small tank volumes and low flowrates (life support and auxiliary power systems), as well as large tankage and high flowrates that are applicable to the Shuttle orbiter propulsion system.

Parametric Study Guidelines

| Fluids | Oxygen | Hydrogen | Methane | Nitrogen |
|---|---|---|---|---|
| Volume Flow Rate | 5 to 10,000 $ft^3$<br>0 to 20 $lb_m/hr$<br>0 to 100 $lb_m/sec$ | 5 to 10,000 $ft^3$<br>0 to 3 $lb_m/hr$<br>0 to 20 $lb_m/sec$ | 5 to 10,000 $ft^3$<br><br>0 to 30 $lb_m/sec$ | 5 to 500 $ft^3$<br>0 to 20 $lb_m/sec$ |
| Pressure: | 14.7 to 150 psia (Pressure relief is nonpropulsive). | | | |
| L/D: | L/D = 1 for all volumes (5 to 10,000 $ft^3$)<br>L/D $\leq$ 5 for volume of 500 $ft^3$<br>L/D $\leq$ 10 for volumes of 1000 $ft^3$ and greater | | | |
| Heat Leak: 0.25 Btu/hr-$ft^2$ (all fluids) | | | | |
| Acceleration: Positive: 0→7 g<br>Negative: 0→0.02 g<br>Lateral: 0.01 g<br>Pitch: 4°/sec | | | | |
| Propulsion Duty Cycle:<br><br>Restarts: 0 → 20<br>Burntime: 1 sec → Depletion | | | | |

The DSL appears suitable for storage of each of the four cryogens considered--hydrogen, oxygen, methane, and nitrogen. The surface tension, density, kinematic surface tension, heat of vaporization, and bubble point for the cryogens are presented in Table IV-2.

Table IV-2   Cryogen Properties

| Liquid | $\sigma$ Surface Tension, $(lb_f/ft)$ | $\rho$ Density, $(lb_m/ft^3)$ | $\beta$ Kinematic Surface Tension, $(ft^3/sec^2)$ | $\Delta h$ Heat of Vaporization, $(Btu/lb_m)$ | $\Delta P_c$ Maximum Capillary Pressure $\Delta Pc(psi)$ (325x2300 Screen) |
|---|---|---|---|---|---|
| $N_2$ | $5.8 \times 10^{-4}$ | 50 | $3.7 \times 10^{-4}$ | 84 | 0.34 |
| $O_2$ | $8.7 \times 10^{-4}$ | 70.5 | $4.0 \times 10^{-4}$ | 90 | 0.53 |
| $H_2$ | $1.2 \times 10^{-4}$ | 4.3 | $9.0 \times 10^{-4}$ | 189 | 0.08 |
| $CH_4$ | $9.15 \times 10^{-4}$ | 26.3 | $11.2 \times 10^{-4}$ | 211 | 0.56 |

The properties for the cryogens correspond to saturation at 20 psia. The capillary pressure difference, $\Delta P_c$, was calculated from the measured value for 325 x 2300 Dutch twill screen using methanol (Ref IV-1). This value is 26-in. of water. As shown in the table, $LH_2$ affords the smallest capillary pressure difference, only about 15% of that for $LO_2$ for the same pore size.

The less-dense hydrogen and methane have high kinematic surface tension values and, therefore, tend to be more easily stabilized and controlled passively when compared to the oxygen and nitrogen.

B.   TANK PRESSURE RELIEF

In Chapter II.C, the thermodyanamic performance of the DSL pressure relief technique* was compared to the liquid vent system over the parametric study pressure range of 14.7-to-150 psia. For the relatively low system pressures of a Space Shuttle orbiter (less than 4 atmospheres) the DSL system compared favorably to the liquid vent system. For the higher storage pressures, a more detailed comparison of the DSL and liquid vent systems is needed (with regard to reliability, efficiency, and weight for each application) to select the preferred concept.

The various DSL venting schemes are discussed in Chapter II.C. During the fine venting scheme, the pressure in the gas annulus must not fall below that required for support of the liquid in the central (bulk) region. In zero-g, when there is little or no hydrostatic head, the pressure in the gas annulus must not fall below the inner-ullage pressure. Another way of stating this is that with a finite gravity, the gas annulus pressure must exceed the inner pressure by the bulk liquid head. Conversely, the pressure in the gas annulus cannot be allowed to rise above the bubble point of the screen which forms the outer surface of the liquid annulus.

*The DSL pressure relief method is nonpropulsive, i.e., it does not require a settling force to achieve venting.

44

To prevent the pressure in the gas annulus from breaking down the
screens that form the liquid annulus, a connection between the two gas
regions is provided that has a lesser bubble point than the liquid annulus
boundaries. As a result, the allowable pressure decay during venting of the
outer annulus will be only about 0.5 psi or less. The analysis presented in
the following paragraphs confirms that such a pressure decay may be accomplished
in a reasonable time with practical annular volumes, and outflow rates. The
pressure relief results for the four cryogens are presented along with a
discussion of the effect of gas annulus gap size on system pressure and venting.

## 1. Pressure Response

Consider a gas volume with mass addition at the rate $\dot{m}_e$, which results
from evaporation and a vent rate of $K\dot{m}_e$. An energy balance on the system

$$(\dot{m}_e h_1 - K\dot{m}_e h)d\theta = dU = Udm + mdU \tag{IV-1}$$

where it has been assumed that the heat transfer into the gas annulus is equal
to that transferred out at the liquid interface (and which results in the
evaporation rate $\dot{m}_e$). If it is assumed that the temperature rise of the gas
above saturation is small*, then $h_1 \approx h$ and Eq (IV-1) becomes

$$\dot{m}_e h d\theta (1-K) = Udm + mdU \tag{IV-1a}$$

the change in mass of the gas is

$$dm = \dot{m}_e (1-K) d\theta \tag{IV-2}$$

the change in internal energy may be written

$$dU = C_v dT \tag{IV-3}$$

where introducing the gas law in Eq (IV-3) yields

$$dU = \frac{C_v V}{R} (dP - \frac{P}{m} dm). \tag{IV-3a}$$

Combining Eq (IV-1a), (IV-2), and (IV-3a) yields

$$\frac{1 + C_v/R}{C_v/R} \frac{dm}{m} = \frac{dP}{P} \tag{IV-4}$$

and integrating from $m_o$ to $m$ and $P_o$ to $P$ results in

$$\frac{P}{P_o} = \left[\frac{m}{m_o}\right]^\gamma \tag{IV-5}$$

---

*This can be confirmed by the solution to Eq (II-8).

where

$$\gamma = \frac{1+C_v/R}{C_v/R} = \frac{C_p}{C_v} .$$

Then writing

$$\left[\frac{m}{m_o}\right]^\gamma = \left[\frac{m_o - \dot{m}_e(1-K)\theta}{m_o}\right]^\gamma = \left[1 - \frac{\dot{m}_e}{m_o}(1-K)\theta\right]^\gamma \tag{IV-6}$$

and expanding the right hand side of Eq (IV-6) by the binomial theorem and retaining only the first two terms yields[†]:

$$\frac{m^\gamma}{m_o} = 1 - \frac{\gamma \dot{m}_e(1-K)\theta}{m_o} \tag{IV-6a}$$

also,

$$\frac{P}{P_o} = 1 - \frac{\Delta P}{P_o} . \tag{IV-7}$$

Expressing the evaporation rate in terms of the heat flux, area, and latent heat of vaporization

$$\dot{m}_e = \frac{qA}{\lambda} = \frac{qV}{\lambda \Delta R}$$

where the thickness of the gas layer, $\Delta R$, is equal to the ratio of gas layer volume-to-surface area. Combining Eq (IV-5), (IV-6a), (IV-7), and (IV-8) yields

$$\Delta R = \frac{q\theta(k-1)}{\Delta P} \frac{RT_o\gamma}{\lambda} \tag{IV-9}$$

The property group $\dfrac{RT_o\gamma}{\lambda}$ is tabulated below for the four study fluids.

| Fluid | $\dfrac{RT_o\gamma}{\lambda}$ (ft-$lb_f$/Btu) |
|---|---|
| Hydrogen | 255 |
| Nitrogen | 131 |
| Oxygen | 125 |
| Methane | 128 |

---

[†] Note that this restricts the analysis to cases where $m/m_o \approx 1$.

Equation (IV-9) is plotted for $N_2$ in the form of $\Delta R$ versus $q\theta/\Delta P$ on Fig. IV-1. Values of $\Delta R$ for $O_2$, $H_2$, and $CH_4$ may be obtained by multiplying ratios of the above constants times values obtained from Fig. IV-1. For an example, let the heat flux to a nitrogen tank be 2.0 Btu/hr $ft^2$, and it is desired to drop the pressure by 0.1 psi in a period of 10 sec, $q\theta/\Delta P = 200$ (Btu/hr $ft^2$)(sec)/ ($lb/in^2$). Then from the figure, $\Delta R$ must be 0.12 in. when K = 1.2 and 0.6 in. when K = 2. If K = 10, $\Delta R$ must be 5.4 in. Thus, if a 1 in. gas layer were specified, the control valve must be sized to modulate flow rates of about twice the boiloff rate.

### 2. Vent Cycle Comparison

The DSL was evaluated to determine the effect of the gas annulus gap and volume and vent flowrate. The low-g acceleration condition was 0.05 g. The baseline configuration was a spherical tank with a volume of 500 cu ft (59-in. radius). The case considered was for the tank to be approximately 10% full of liquid nitrogen with the heat input 0.25 Btu/hr $ft^2$. A liquid annulus gap of 1 in. (constant) was used. Each case started with a saturated condition at 140°R and sufficient helium to pressurize the bulk ullage to 20 psia. Venting of the gas annulus was initiated when its pressure became 0.25 psi greater than the bulk ullage pressure. Venting was terminated when this pressure was reduced to 0.05 psi above the bulk ullage pressure.

The effect of gas annulus gap is shown in Fig. IV-2 thru IV-4 with respective gap widths of 3 in., 1.5 in. and 0.5 in. The vent rate was 1.08 $lb_m$/hr for each case. Venting was directly from the vapor annulus to prevent breakdown of the communication screen, thus allowing a nearly adiabatic condition for the bulk region. A comparison of the three figures shows an increase in vent frequency with a decrease in annulus width (and volume). This is due to the lower superheat capacity available with the smaller vapor volumes. The outer screen is at saturation temperature corresponding to the partial pressure of propellant vapor in the outer annulus. The liquid in the liquid annulus shows a slight degree of subcooling.

A dimensionless ratio, K,

$$K = \frac{\dot{m}_{vent}}{Q/\Delta h} \tag{IV-10}$$

was used to relate the vent flow rate, $\dot{m}_{vent}$, to the heat flux, Q, and the heat of vaporization, $\Delta h$. For the case discussed thus far, K was equal to 1.2. Figure IV-5 presents another illustration of the gas annulus width effect on the vent frequency (for K=1.2). The upper line shown is the amount of time the vent valve remains open during the vent cycle. The lower line is the amount of time required for the total vent cycle (vent valve closed-to-vent valve closed). Not shown are the values for a 9-in. gas annulus width, determined to be 67 minutes vent valve open, and 105 minutes total cycle time.
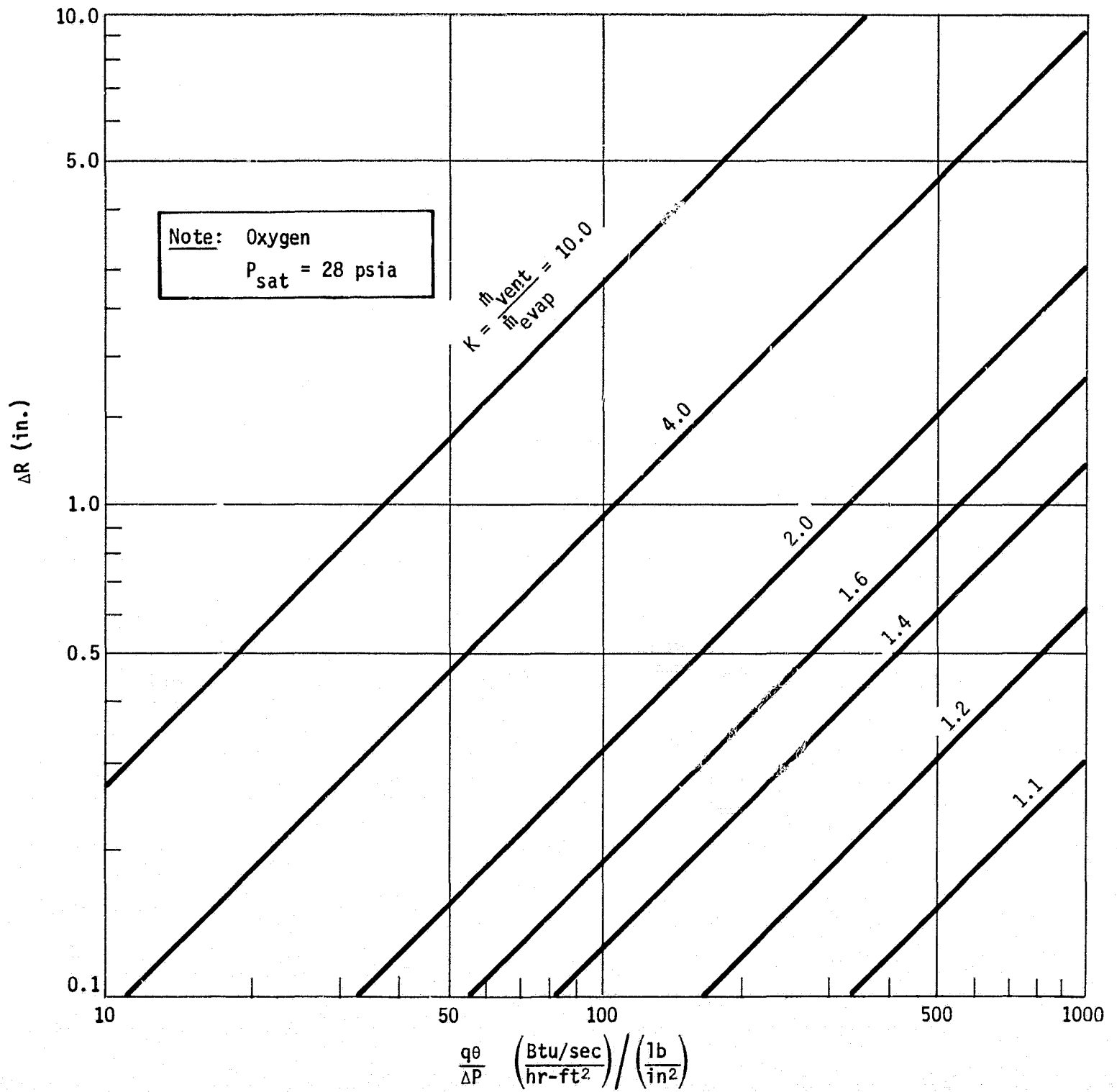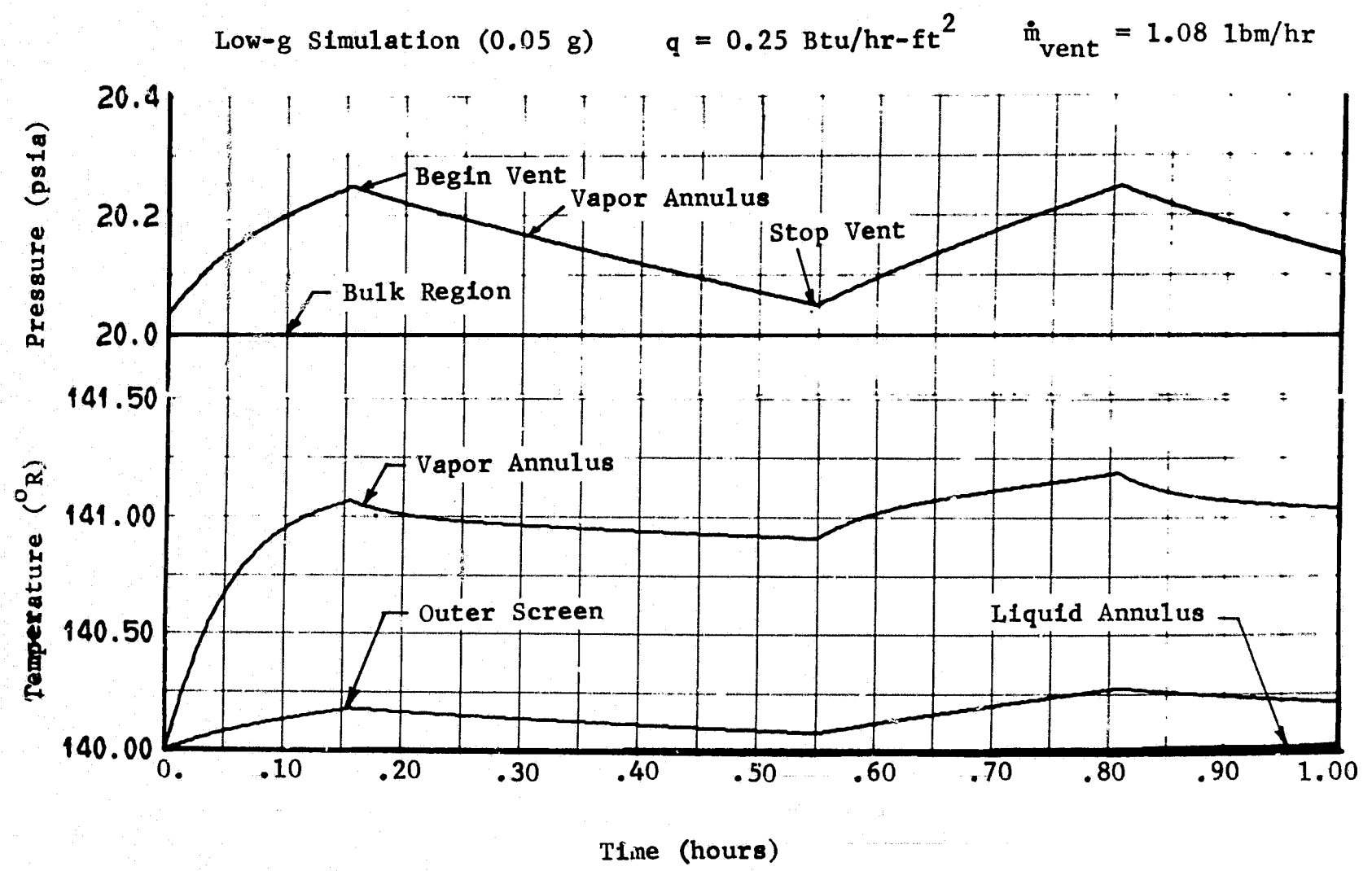
Figure IV-1  Pressure Response during Venting (DSL)

Figure IV-2 Low-g Venting - 500 ft$^3$ Spherical Nitrogen Tank ($\Delta R$ = 30 in.)
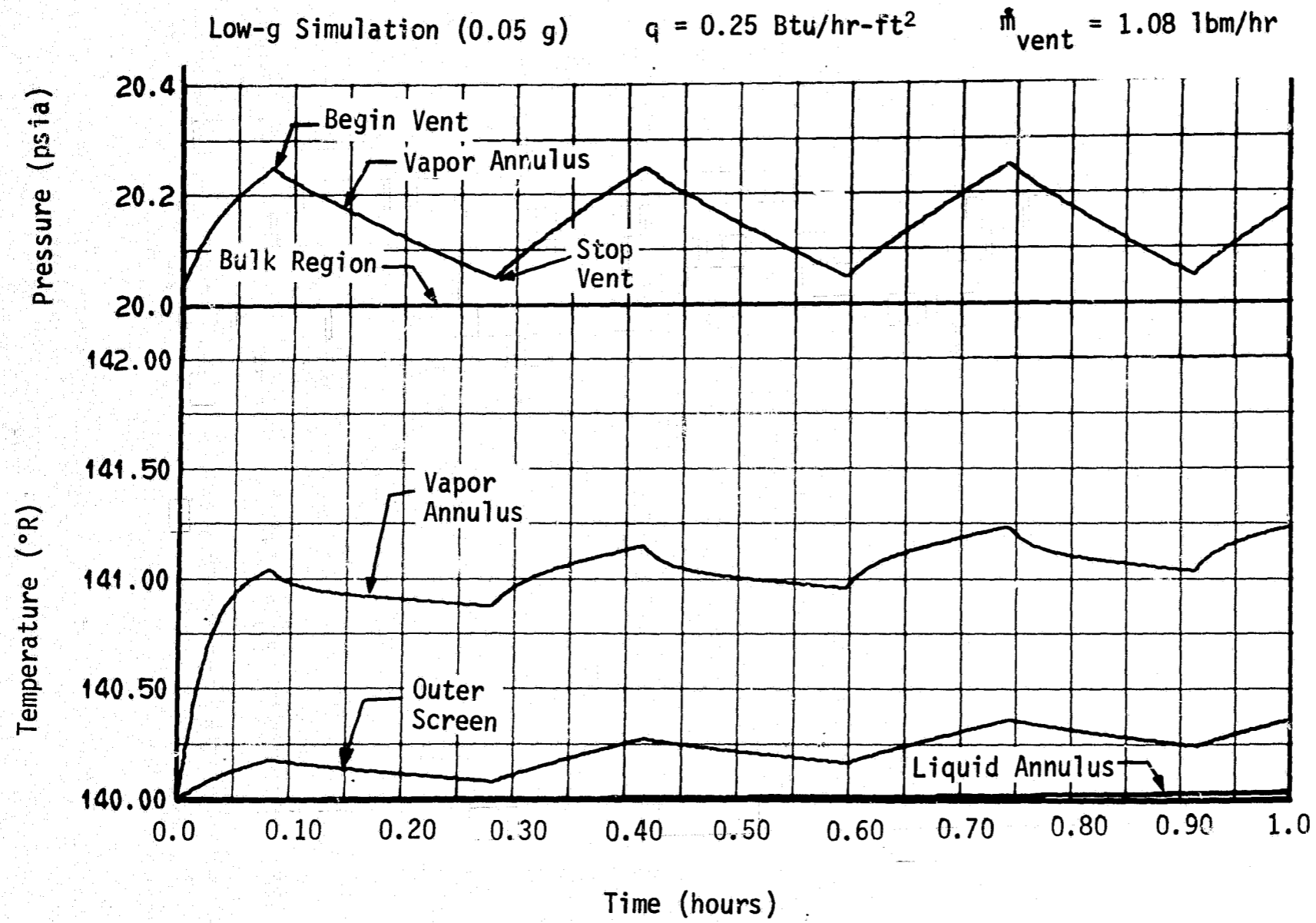
Figure IV-3  Low-g Venting - 500 ft$^3$ Spherical Nitrogen Tank ($\Delta R$ = 1.5 in.)
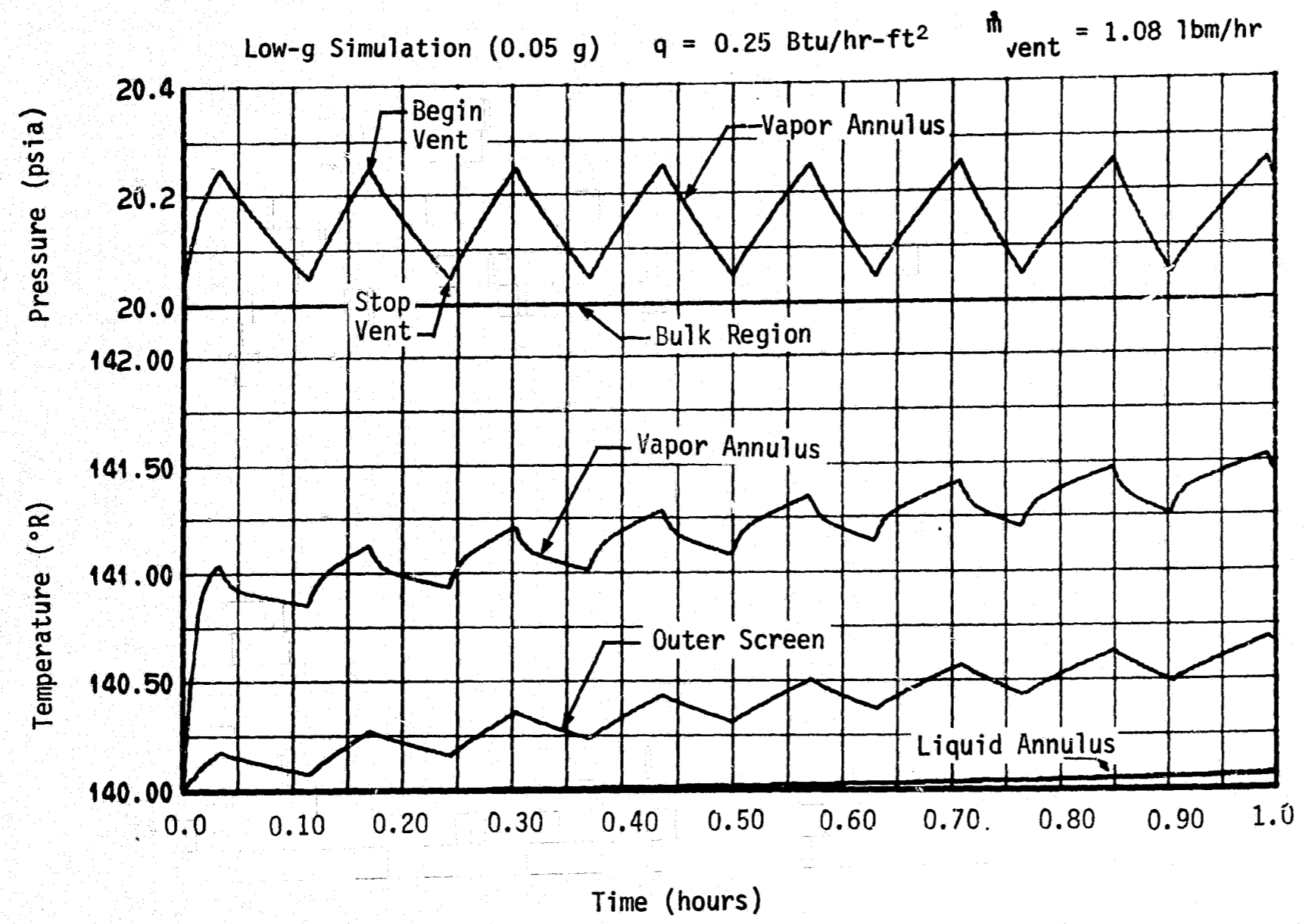
Figure IV-4  Low-g Venting - 500 ft$^3$ Spherical Nitrogen Tank ($\Delta R$ = 0.5 in.)
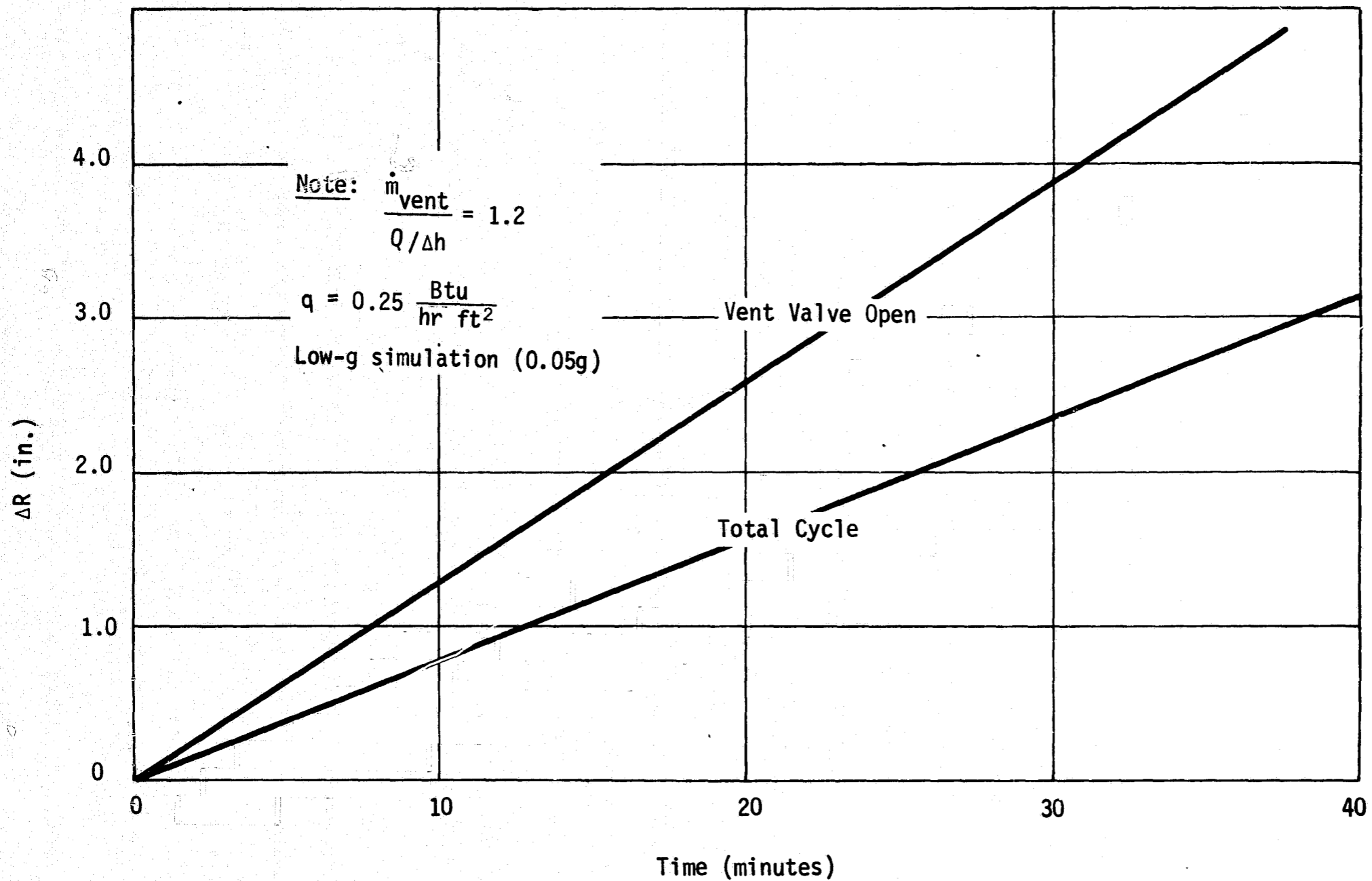
Figure IV-5   Vent Cycle Duration - 500 ft$^3$ Nitrogen Tank

The effect of variations in the vent flow rate, or K, for two different gas annulus widths is shown in Fig. IV-6. Again, the total vent cycle times for each condition are presented. These two curves, Fig. IV-5 and IV-6, can be used to estimate typical vent cycle times. (Only a period of 1 hr was evaluated; long-term variations in the cycle rate were not evaluated.) Note that Fig. IV-5 and IV-6 were constructed from Fig. IV-2 thru IV-4, which are intermittent vent cases, and that K=1.0 is not a continuous vent.

The rate at which the bulk pressure increases during low-g storage with venting was evaluated during steady-state heat input over a period of 3 hr using the DSL computer program. These results were extrapolated to determine the possible long-term (7 day) effect on the tank pressure. A 500-cu ft spherical tank (59-in. radius) with a liquid annulus gap of 0.5 in. and a gas annulus gap of 1.5-in. was evaluated for each of the four fluids. The tank was 50% full and the heat input was 0.25 Btu/hr ft$^2$. Venting was accomplished by keeping the gas annulus pressure between an upper and lower limit (Table IV-3), which is referenced to the bulk ullage pressure. Gas flow from the gas annulus through the communication port was not permitted.

The pressure rise rate and the amount of mass vented for each fluid is listed in Table IV-3. Again, the K value is used to express the relationship between vent rate and heat input. With K = 1.0 for hydrogen, the gas annulus pressure continued to rise, necessitating use of a larger K for this case. Plots of the vent cycles for each case are shown in Fig. IV-7. Since vent cycle time increases (number of cycles decreases) with increased gas annulus gap, the results in Fig. IV-7 show the need for an increased gap width in the hydrogen tank. The larger gap tends to permit use of a lower K value which also may increase vent cycle time (see Fig. IV-6).

This preliminary investigation tends to show that tank pressure can be satisfactorily controlled even with the rather low vent flow rate considered. If a smaller pressure rise were desired, it could be accomplished using a higher vent rate. One important factor not considered here is the effect of outflowing liquid from the tank, which reduces tank pressure and minimizes venting (see Fig. VII-6 where liquid outflow can be assumed to be liquid vent). The study results tend to show also that for a given mission profile, vent flow rate can be optimized to provide desired pressure control, i.e., a minimum amount of mass vented overboard.

Another vent scheme considered using the DSL computer program was a continuous vent. For certain applications this may be desirable (for example, supplying gas for a life support system). The same configuration discussed in the previous paragraphs was also considered here for oxygen and nitrogen, except that no helium pressurant was used. The vapor was saturated at the liquid interface temperature. It was assumed that a constant vent rate (for each) of approximately 0.3-lb$_m$/hr was desired.
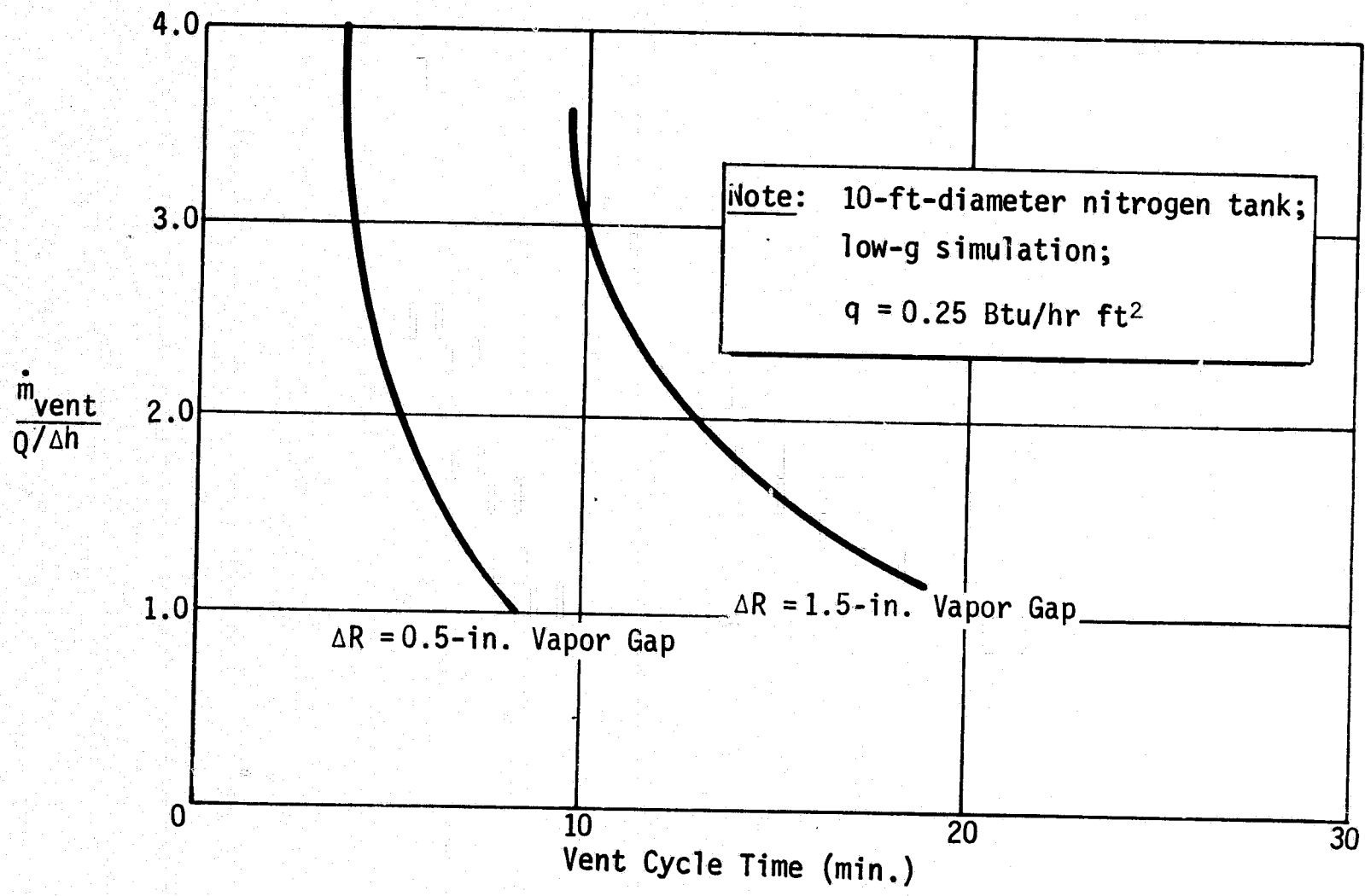
Figure IV-6 Effect of Vent Flow Rate on Vent Cycle Time

## Table IV-3  Vent Results for Parametric Study

| Fluid | Vent Rate $\dot{m}$ vent $q/\Delta h$ | Control Limits | | 3 Hour Vent Period | | | Extrapolated to 7 Days | |
|---|---|---|---|---|---|---|---|---|
| | | Upper (psi) | Lower (psi) | Pressure Rise Rate (psi/hr) | Mass Vented Vapor (1bm) | Mass Vented Helium (1bm) | Pressure Rise (psi) | Vapor Mass Vented (1bm) |
| Oxygen | 1.05 | .45 | .05 | .051 | 1.124 | 0.056 | 8.54 | 62.8 |
| Methane | 1.00 | .45 | .05 | .029 | 0.397 | 0.031 | 4.81 | 22.2 |
| Nitrogen | 1.24 | .25 | .05 | .013 | 1.488 | 0.064 | 2.23 | 83.3 |
| Hydrogen | 1.98 | .07 | .01 | .044 | 0.742 | 0.542 | 7.33 | 41.5 |
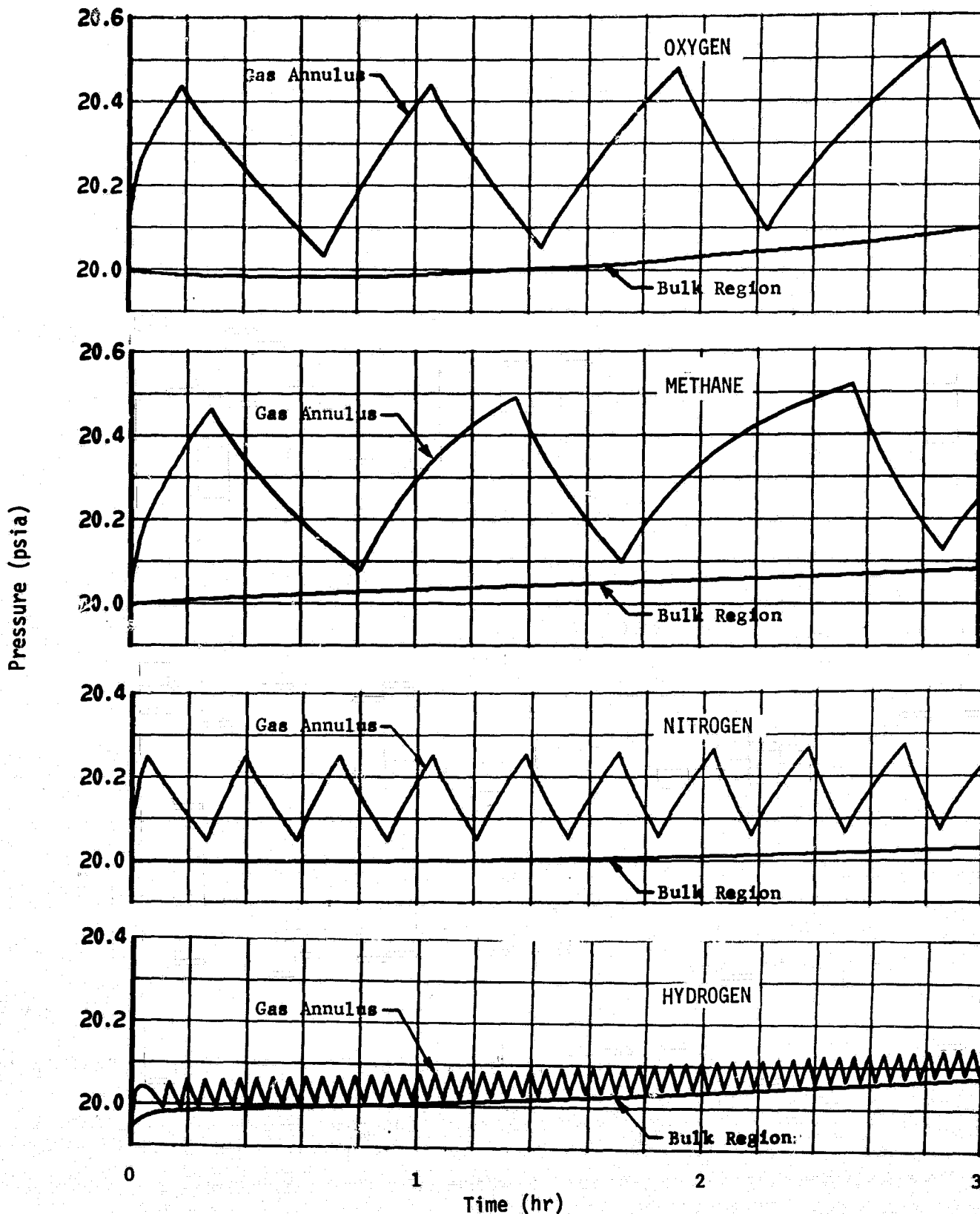
Figure IV-7  Parametric Vent Results for Oxygen, Methane, Nitrogen and Hydrogen.

To control the gas annulus pressure within the control limits, the continuous vent rate had to be augmented, i.e., additional venting was required. The storage system vent rate (total) is then the sum of the two vent rates. The effect of using this type of venting is shown in Table IV-4 for the nitrogen and oxygen, respectively. A relatively large amount of mass is vented, but approximately one-third of that amount is being used by the life support system. Since a relatively large amount of mass is vented, the pressure control does not appear to present any problem. Plots of the vent cycles are shown in Fig. IV-8. The K value for both cases was near unity. For nitrogen, this tends to cause a very long vent cycle, as shown.

## C. LIQUID EXPULSION

Several factors must be considered in the design of the passive systems to provide desired expulsion efficiencies of 99% or more. First, however, expulsion efficiency must be defined. The term is usually defined as the percentage of the loadable propellant which is usable, i.e., that percentage which can be expelled as gas-free liquid. For this program, the following relationship was used for simplicity:

$$\eta_e (\%) = \frac{\text{Tank Vol} - \text{Residual Propellant Vol}}{\text{Tank Vol}} \times 100. \qquad \text{(IV-11)}$$

A slight difference exists between this relationship and the usual expulsion efficiency definition, stated earlier, because tank volume is not the loadable propellant volume. They differ because of the volume displaced by components within the tank, such as the DSL, and the initial ullage volume. Additionally, for cryogenic storage, vaporized propellant will also contribute to this difference. In particular, vaporized propellant that is vented overboard can be a significant contribution.

Residual propellant for the DSL can be determined directly because it is the volume of the liquid annulus. The annulus is formed by the two concentric or eccentric screen liners or by a number of separate channels, as described earlier and pictured in Fig. II-1 thru II-3. Gas-free liquid expulsion depends on the ability of the screen forming the liquid annulus to prevent pressurization gas and propellant vapor from entering the liquid annulus through the screen pores. The resistance to this gas breakthrough depends on the interface stability provided by the capillary pressure difference, $\Delta P_c$, which is a function of the pore size and surface tension. The capillary pressure difference cannot be exceeded without ingesting some gas into the liquid annulus. The breakdown phenomenon occurs when the sum of the differential pressures associated with (1) hydrostatic head, (2) viscous losses due to flow through the screen, (3) additional viscous losses due to flow in the liquid annulus, and (4) the static pressure change in the annulus due to velocity head, exceed the capillary retention capability of the screen.* These pressure losses are additive as shown by:

$$(\Delta P_c)_{max} \geq \Delta P_{vh} + \Delta P_f + \Delta P_a + \Delta P_h \qquad \text{(IV-12)}$$

---

*Additionally, a screen dryout consideration is discussed on page 70.

Table III-4. Pressure Rise Rate and Mass Vented
During Continuous Venting

| Fluid | Vent Rate | | 5 Hour Vent Period | | Extrapolated to 7 Days | |
| | Continuous ($lb_m$/hr) | Augmented ($lb_m$/hr) | Pressure Rise Rate (psi/hr) | Mass Vapor Vented ($lb_m$) | Pressure Rise (psi) | Vapor Mass Vented ($lb_m$) |
| --- | --- | --- | --- | --- | --- | --- |
| Nitrogen | 0.31 | 0.58 | 0.00078 | 4.402 | 0.131 | 149.0 |
| Oxygen | 0.31 | 0.67 | 0.00565 | 3.942 | 0.945 | 132.5 |

58
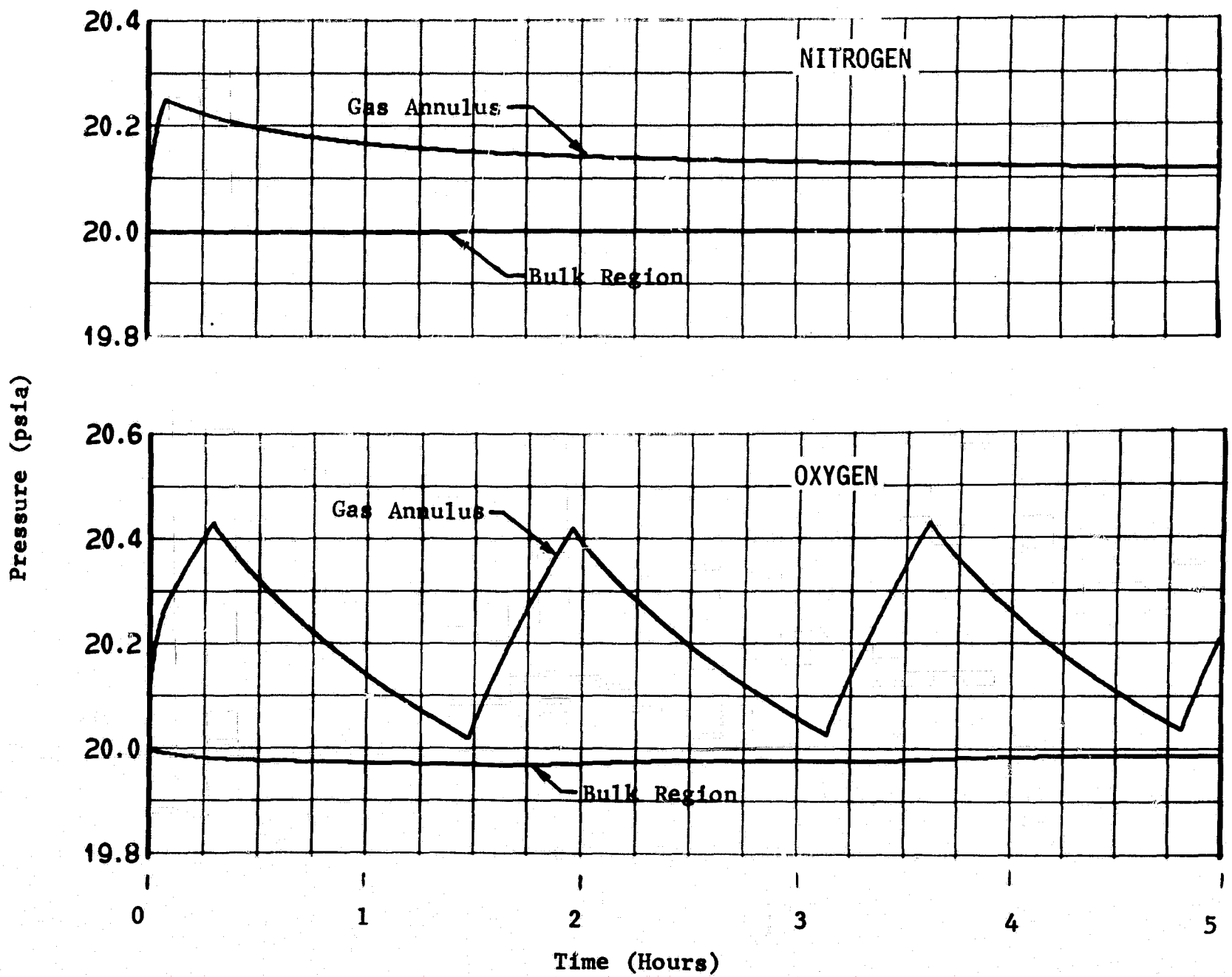


Figure IV-8  Continuous Venting Results for Nitrogen and Oxygen

where

$\Delta P_c$    = Capillary retention pressure (maximum);

$\Delta P_{vh}$  = Static pressure change due to dynamic head;

$\Delta P_f$    = Annulus viscous losses (flow);

$\Delta P_a$    = Screen viscous losses (entrance losses);

$\Delta P_h$    = Hydrostatic head pressure difference.

The four terms cn the righthand side of the equation are the adverse pressure differences previously mentioned. Each of these terms is calculable using the empirical relationships presented in Ref IV-2 for metal cloth and the measured flow loss data presented in Martin Marietta Report TM-1661-66-12, "Liquid Outflow Tests of Surface Tension Systems under Minus One-g," December 1966.

During expulsion, the bulk liquid level recedes and the screen area exposed to liquid flow from the bulk volume to the liquid annulus is decreased. As this occurs, the pressure drop for flow through the screen, $\Delta P_a$, increases due to the increased flowrate per unit area. Good design practice will permit all of the bulk liquid to be expelled (at which point gas in ingested into the liquid annulus). Thus, the volume within the liquid annulus, as mentioned, is unavailable propellant. It is, therefore, desirable to design the smallest possible liquid annulus while still satisfying the liquid flow rate requirements and flow losses. Figure IV-9 shows expulsion efficiencies attainable as a function of annulus gap size for spherical tanks, assuming the liquid annulus is a complete spherical shell. Higher values of expulsion efficiency can be obtained if the liquid annulus comprises discrete channels. In special cases, such as the Shuttle orbiter (Chapter V), the acceleration vector during reentry can be used to achieve expulsion efficiencies of nearly 100%.

For an actual system design, such as the 500-cu-ft $LO_2$ tank and the 2000-cu-ft $LH_2$ tank of the low crossrange Shuttle orbiter, once a liquid annulus gap size is selected, a limiting liquid outflow rate can be obtained. Figure IV-10 presents expulsion efficiency as a function of liquid flowrate. An expulsion efficiency of 100% represents the limiting condition of a zero gap size, no liquid outflow rate, and no pressure loss due to fluid flow. For the Shuttle point design, discussed in Chapter V, the $LO_2$ and $LH_2$ tank outflow rates were 14 $lb_m$/sec and 3.5 $lb_m$/sec respectively, yielding an expulsion efficiency greater than 99% (for each). Even for a $LO_2$ flowrate of 100 $lb_m$/sec and a $LH_2$ flowrate of 20 $lb_m$/sec (see Parametric Study Guidelines, Table IV-1) expulsion efficiencies of 97.5 and 98% can be obtained.
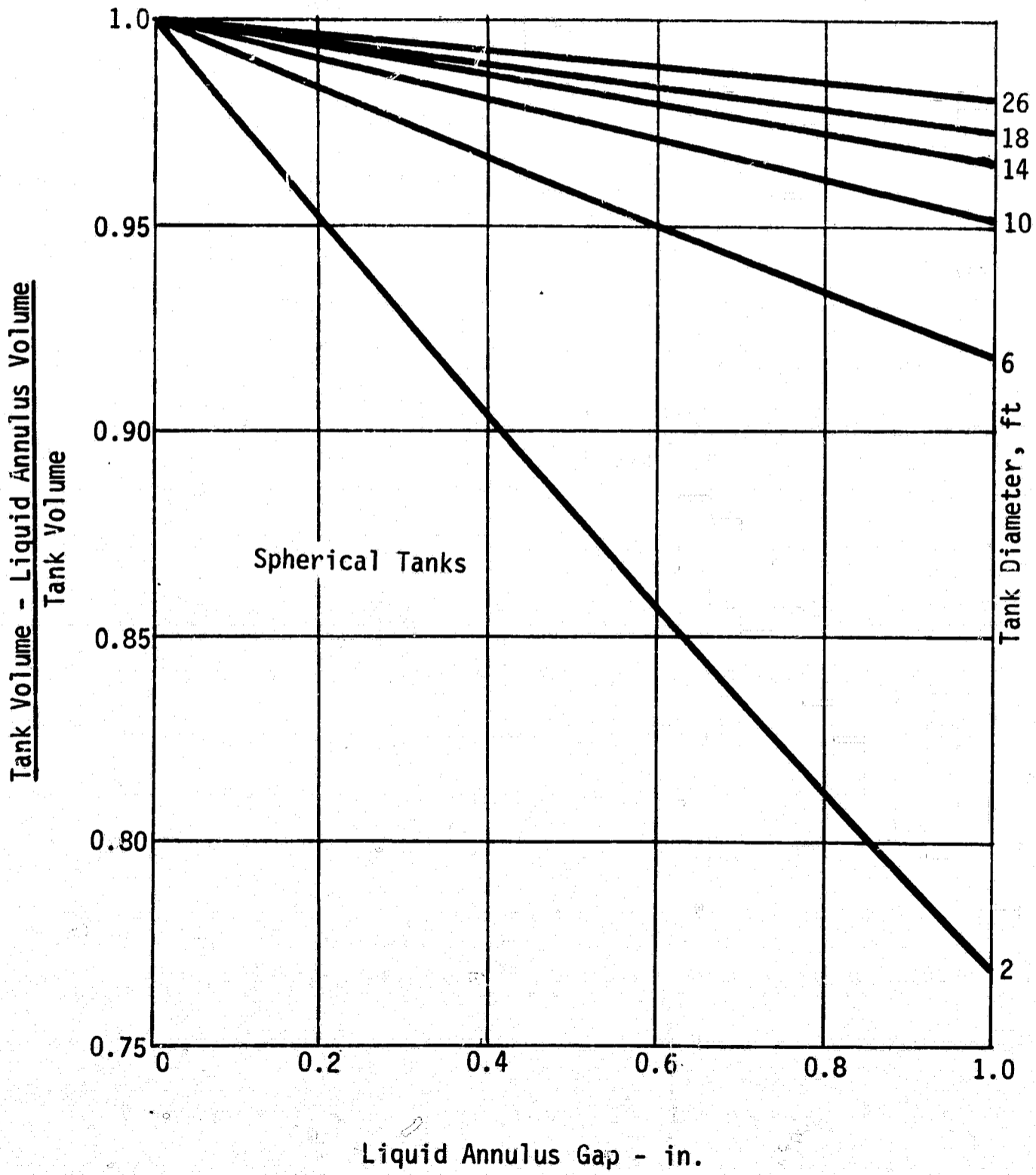
Figure IV-9 Tank Volume Efficiency vs Liquid Annulus Gap Size
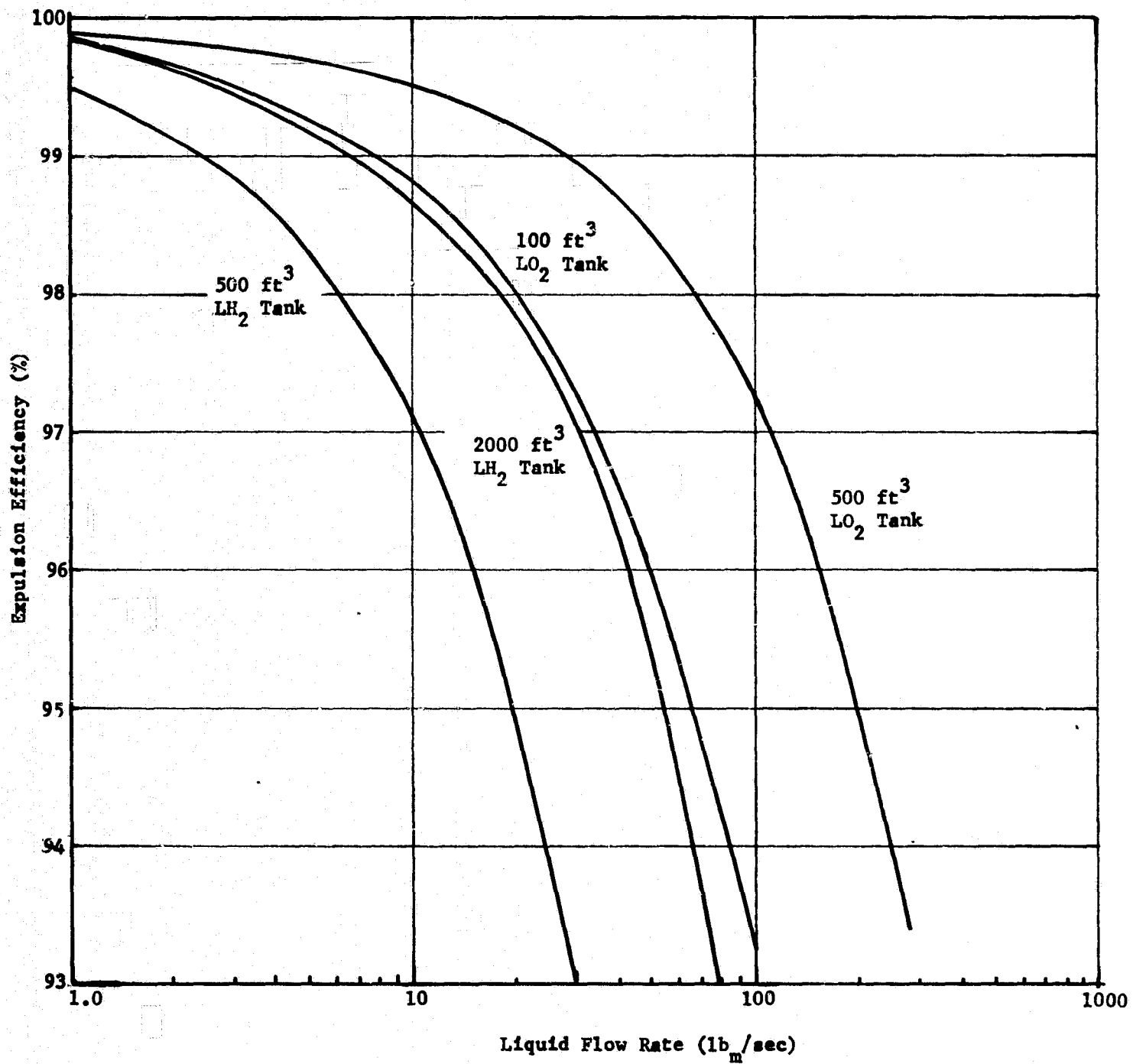
Figure IV-10 Expulsion Efficiency vs Liquid Flow Rate

### D. PROPELLANT CONTROL

The DSL concept affords control of the bulk propellant by keeping it off the tank wall during low-g storage. The DSL also stabilizes and controls the liquid annulus region to assure gas-free liquid expulsion. The bulk liquid control is desired because it tends to minimize stratification effects, if any, and reduces propellant vaporization and resultant vented mass. To positively control the bulk propellant, however, the foraminous material must completely enclose the propellant. This total liner within the tank is the unique difference between the DSL and other capillary concepts. The total liner can contain communication ports between the vapor annulus and the central ullage, as shown in Fig. II-1; however, the bulk liquid is contained within the total liner during low g.

Stability for a capillary system is defined as the system's ability to maintain liquid-vapor separation at the surface of the perforated material under the acceleration and thermal environment for the mission. Stability under the different axial and lateral accelerations, due to powered maneuvers, and fluid motion during unpowered phases (e.g., drag and docking) are important design considerations, particularly for the reusable Shuttle orbiter. Because the capillary forces are small,* they will not be dominant during the prelaunch and launch phases; however, during low g they will tend to dominate and control the fluid.

An additional stability consideration with cryogenic storage is the ability of the screen and perforated plate material to remain wetted under the thermal environment. Interface stability is afforded only with the wetted condition. Heat leak into the propellant from various sources must be considered: (1) through the wall and structure supporting the foraminous assembly; (2) soakback from the propellant feedline; and (3) warm pressurization gas. Screen dryout and resultant stability loss are critical to any passive system, including the DSL, and are reviewed later in this section.

As discussed in Section C of this chapter, the maximum capillary pressure difference is usually measured experimentally (bubble point) for different foraminous material, perforated plate, square, and twilled weave screen. It is the important criterion in selecting the foraminous material. The selection of the material to form the liquid annulus and the total liner is based on;

$$\Delta P_c \geq \rho a h \qquad \qquad \text{(IV-13)}$$

---

\* The magnitude of these forces is so small that they are commonly neglected in the design of fluid systems for Earth applications. For example, the tension exerted by a liquid hydrogen surface along an intersection of about 3 ft in length is less than $0.02\text{-lb}_f$.

for the low-g storage case of interest. As seen, it is merely a question
of selecting material that assures the proper bubble point to stabilize
the liquid in the annulus and the bulk propellant under the low-g acceleration.
The maximum hydrostatic head, h, that can be supported by different screen mesh
sizes under accelerations to 10 g is presented in Fig. IV-11 thru IV-14 for hydrogen,
oxygen, nitrogen, and methane, respectively. Stability under an orbital drag
acceleration condition of $10^{-5}$ g, or so, can easily be provided with a single-layer
screen. For example, at an acceleration level of 0.01 g, a 165 x 800 mesh stain-
less steel screen will support about 950 in of $LH_2$ (Fig. IV-11).

Stability of the liquid annulus during prelaunch and launch must also be
considered when selecting the mesh size. For example, during a 7-g boost phase,
a single-layer 325 x 2300 mesh screen will support only about 4-1/2 in of $LH_2$.

If the liquid annulus protrudes above the bulk propellant by more than 4-1/2 in
during launch, the screen will break down and ullage will be ingested into the
liquid annulus. It may be necessary to select a finer mesh size than that
dictated by the low-g acceleration environment. If this does not resolve the
instability, a calendered screen or more than one layer of screen may be needed
for the liquid annulus screen surface exposed during boost. The calender process
entails deforming the screen with heavy rollers. A resultant increase of about
15% in the capillary pressure retention can be realized using this method
(Ref IV-3).

For applications where a marked increase in pressure retention above that
afforded by the single-layer foraminous material are desired, several layers of
screen may be needed. With proper spacing between the layers, the capillary
pressure retention for each layer can be used, additively. In other words, if
the retention requirement is 0.1 psi, five layers of screen, each with a
contribution of 0.02 psi, are adequate for stability (Ref IV-1).

The venting and liquid expulsion phases during storage also present
additional propellant control and stability considerations which influence
the selection of foraminous material. As discussed in Section C of this chapter,
viscous effects are considerations for achieving desired liquid expulsion
efficiencies. Therefore, in addition to the capillary pressure retention,
the weave of the screen is important because a tortuous path for flow will
produce higher pressure drops. Square-weave screen, for example, presents a
lesser loss to flow than does the twilled metal cloth. As discussed in Section B,
Chapter II, the sensitivity of the pressure relief cycle is dictated, in part,
by the capillary pressure difference of the screen (either the communication screen
or that forming the liquid annulus). Briefly, a coarser screen material dictates
a more narrow band on the vent pressure relief.

It is desirable that the bulk propellant be contained within the total
liner during low-g maneuvers, pitch and roll, and lateral and axial accelerations
tending to produce bulk liquid motion and slosh. Damping and control of liquids
were studied under a recent NASA program (Ref IV-1). The experimental results
show that the Weber number (We) can be used to predict damping as afforded by
foraminous material. The critical Weber number, $We_{cr}$, a ratio of inertia-to-
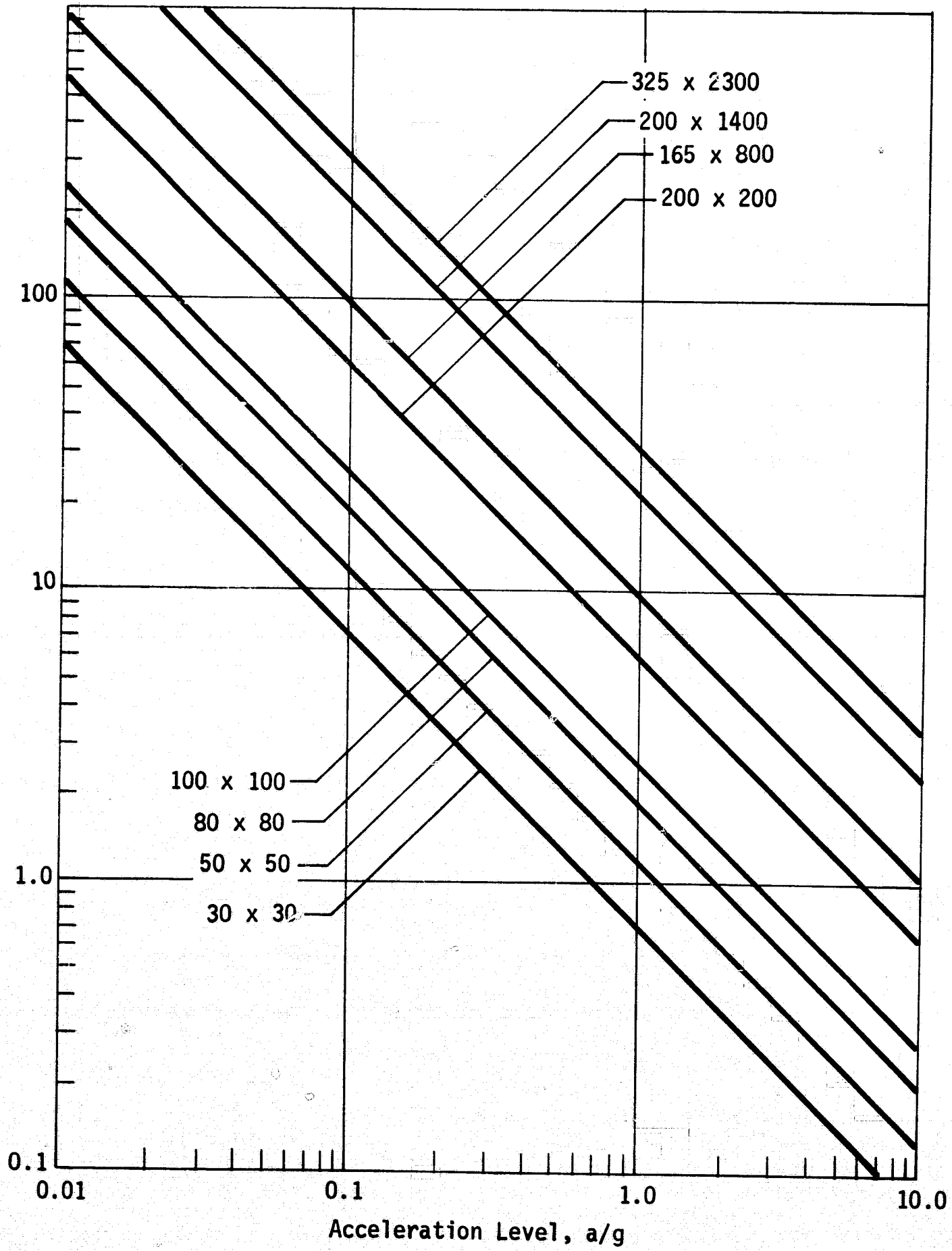
Figure IV-11  Maximum LH$_2$ Hydrostatic Head vs Acceleration Level
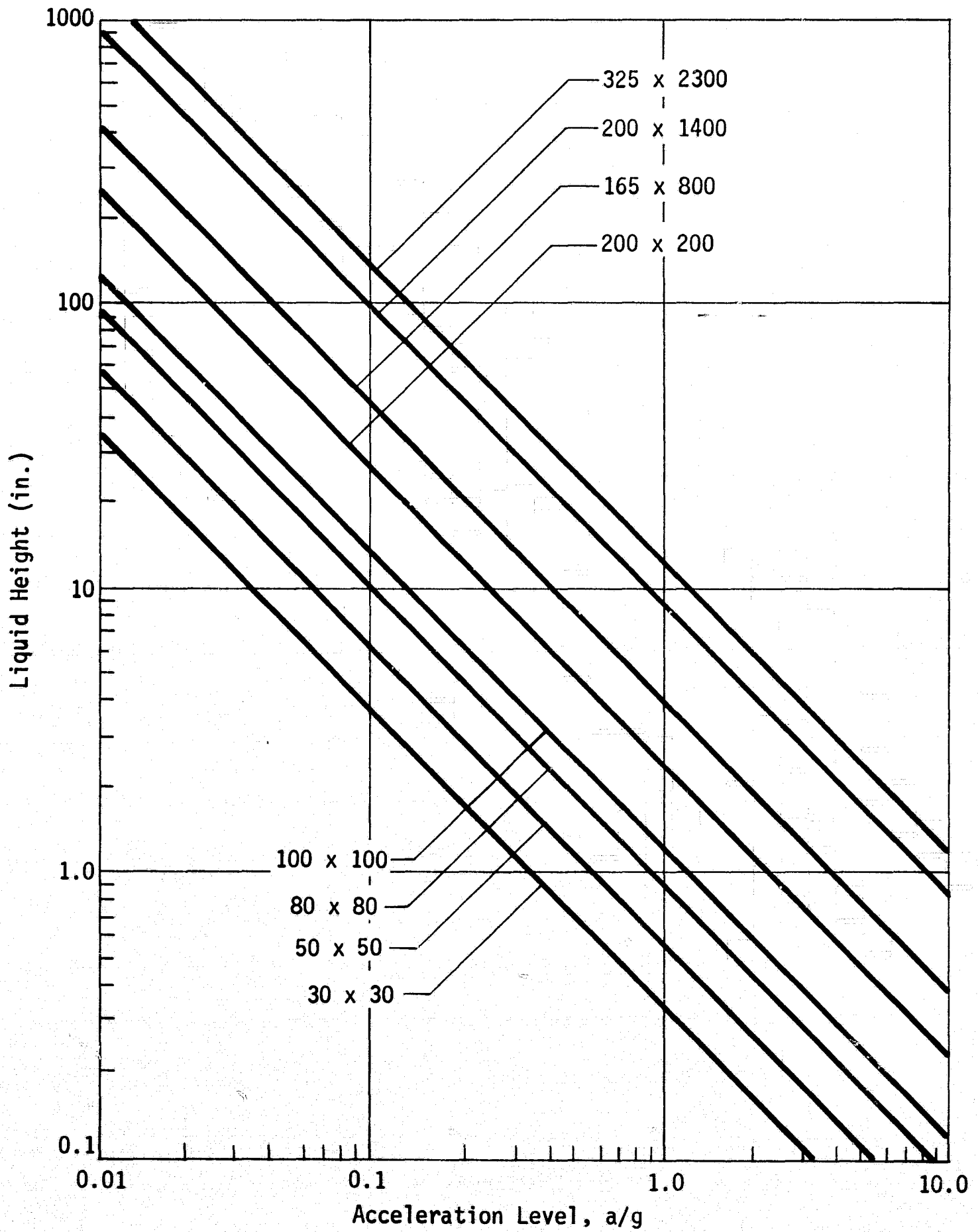
Figure IV-12   Maximum LO$_2$ Hydrostatic Head vs Acceleration Level
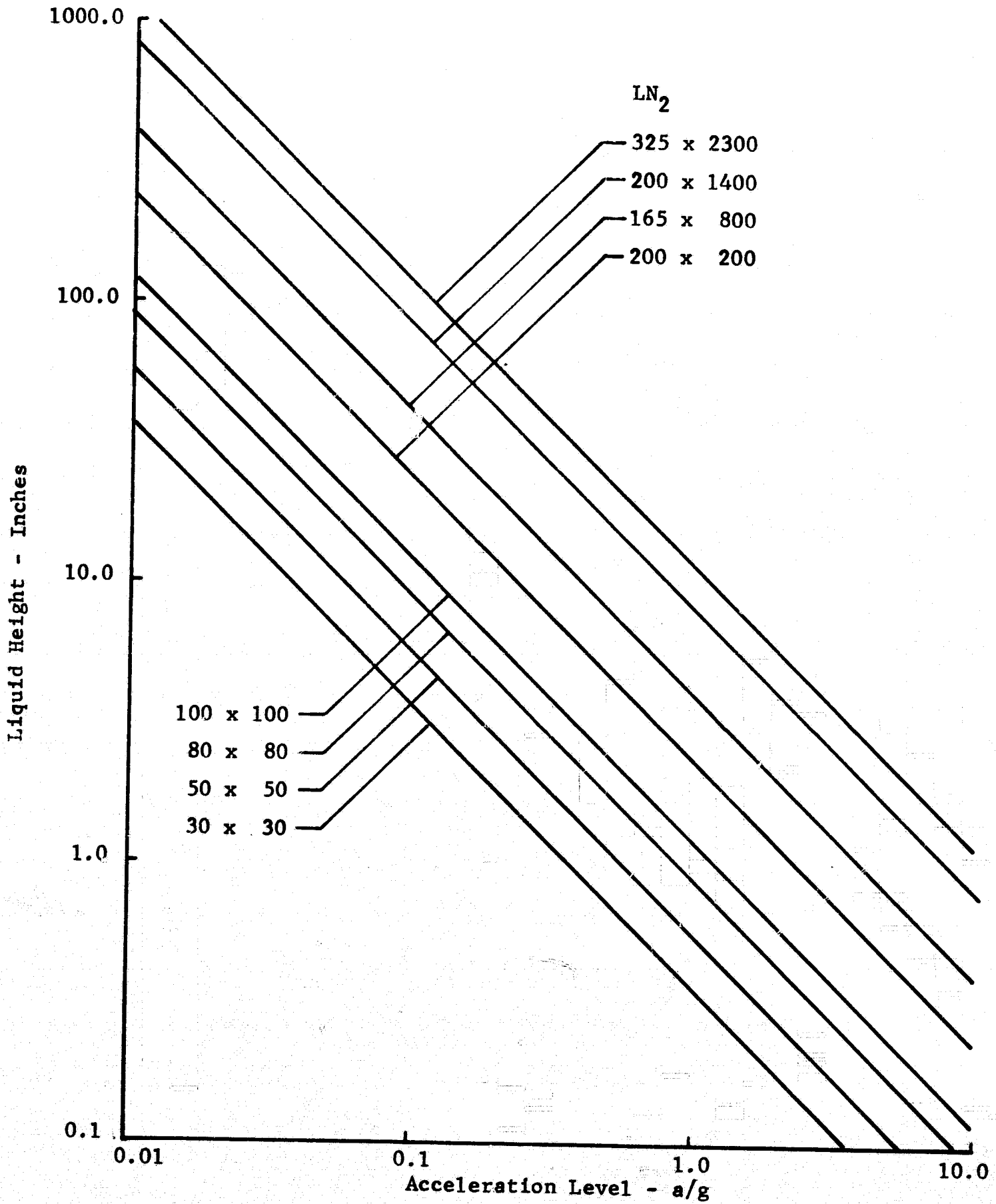
Figure IV-13  Maximum LN$_2$ Hydrostatic Head vs Acceleration Level
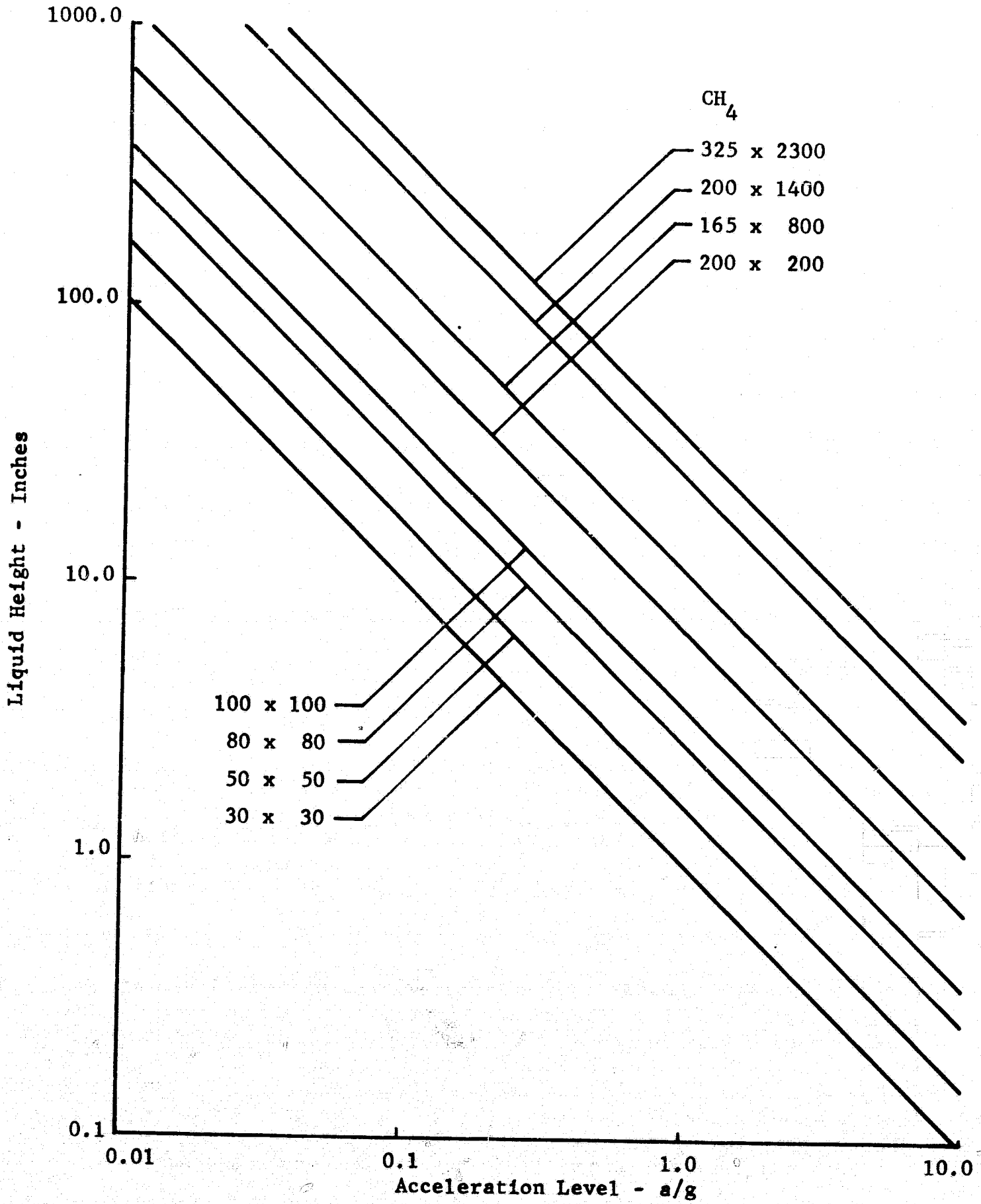
Figure IV-14   Maximum Liquid Methane Hydrostatic Head vs Acceleration Level

68

capillary forces, may be expressed as:

$$We_{cr} = \frac{v_{cr}^2 L}{\beta} \qquad \text{(IV-14)}$$

where L is the characteristic dimension of the foraminous material (pore radius, for example), $v_{cr}$ is the liquid impingement velocity, and $\beta$ is the kinematic surface tension. To a lesser extent, the effect of open-to-total area ratio for the material was assessed in the drop tower study.

Various foraminous configurations, including single- and double-layer perforated plate and screen, were evaluated in the Martin Marietta 2.1-sec drop tower. The tests were conducted over a range of settling Bond numbers* from 30.4 to 135.0, based on the radius of the cylindrical tanks. Liquid was settled against different perforated barrier configurations and containment was observed. For example, complete damping (containment) was verified experimentally at Weber numbers $\leq 0.02$ for single-layer Dutch twill cloth.

As shown in Fig. IV-15, the Dutch twill weave can effectively damp and control liquid. Single screen layers of various mesh sizes, 165 x 800, 200 x 1400, and 325 x 2300, are shown along with square-weave screen. The complex weave of the twilled material greatly aids in preventing the liquid from passing through the barrier. The test liquids, methanol, Freon TF, and carbon tetrachloride, were (before the drop) some distance below the barrier. At drop initiation, a near-constant, axisymmetric, axial acceleration settled the liquid against the foraminous material. The excellent damping results as pictured for the twilled screen are just prior ($\Delta\theta = 1.9$ sec) to termination of the drop test. This type of containment is representative of that achievable with the twilled total liner of the DSL.

The DSL tends to maintain a gas layer between the tank wall and the outer-screen liner with liquid between the two screens during low-g. During most of the low-g duration, therefore, a liquid/vapor interface will exist at the screen nearest the tank wall. The heat leak into the cryogenic liquid tank is intercepted at this screen surface by vaporization of liquid. If the outer-screen were to dry out, boiling may result, causing vapor formation in the liquid annulus. The introduction of hot pressurant into the tank is another design consideration because it may cause vaporization and dryout of the screen.

Simple analyses, as presented here, indicate that screen will not dry out unless the heat flux at the screen surface reaches levels ranging from $10^4$ to $10^5$ Btu/ft$^2$hr. Tests conducted under an independent research task (Ref IV-4), also tend to support this range of heat flux, although the results are qualitative. The apparatus used for the tests is pictured in Fig. IV-16. The aquarium-like device was approximately 6 x 4 x 2 in. The test liquid was pentane. The two parallel screens, representative of the DSL concept, were 200 x 1400 stainless positioned about 1/8-in apart. The vapor annulus,

---

*Bond number is a ratio of acceleration-to-capillary forces.
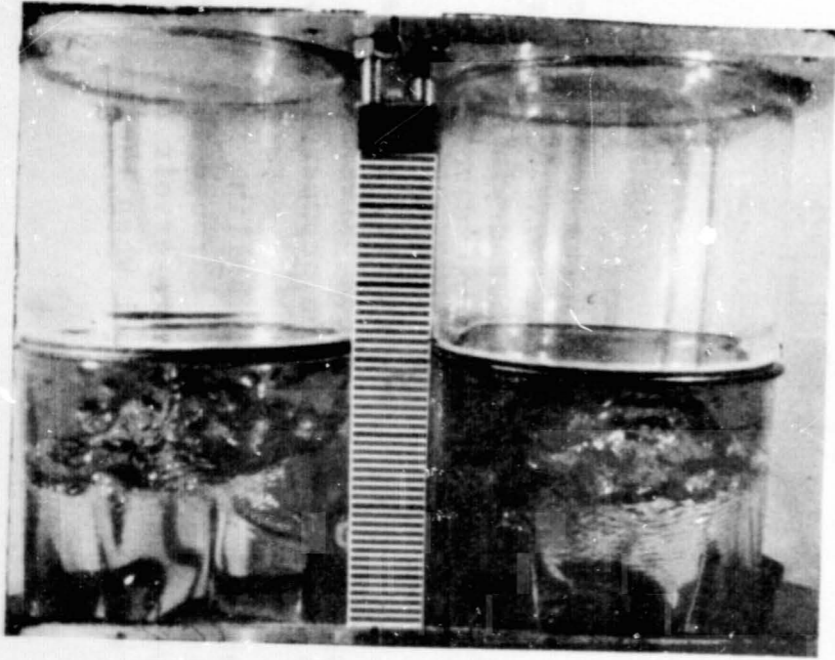
$\triangle$t = 1.9 sec

(325 x 2300 Mesh on Left; 200 x 1400 on Right)
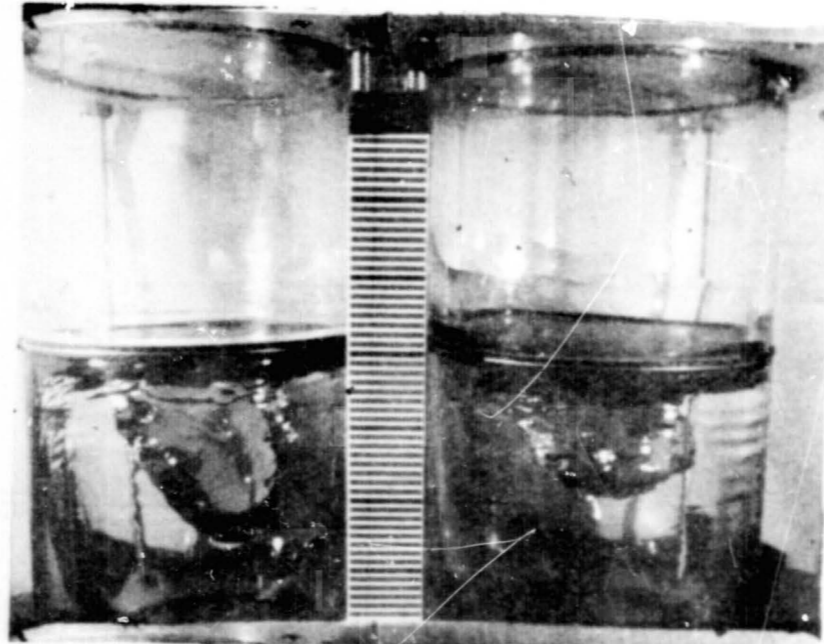
$\triangle$t = 1.9 sec

(165 x 800 on Left; 50 x 50 on Right)
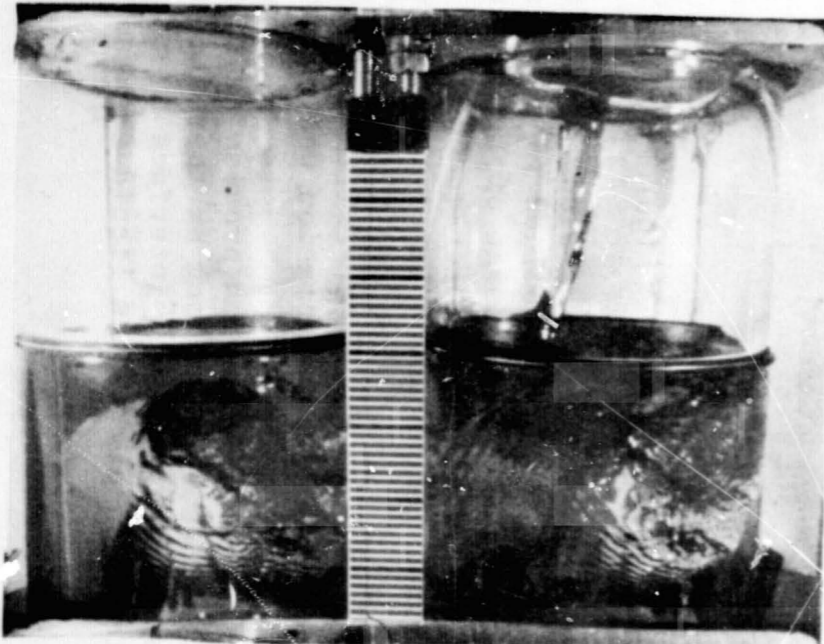
$\triangle$t = 1.9 sec

(165 x 800 on Left; 50 x 50 on Right)
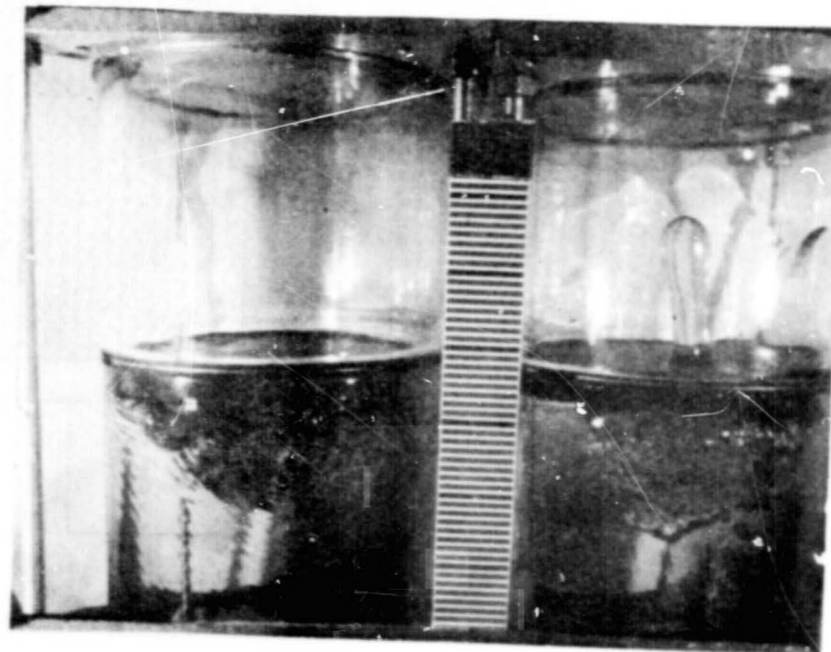
$\triangle$t = 1.9 sec

(165 x 800 on Left; 50 x 50 on Right)

Figure IV-15  Typical Screen Containment Results (Ref IV-1)

70
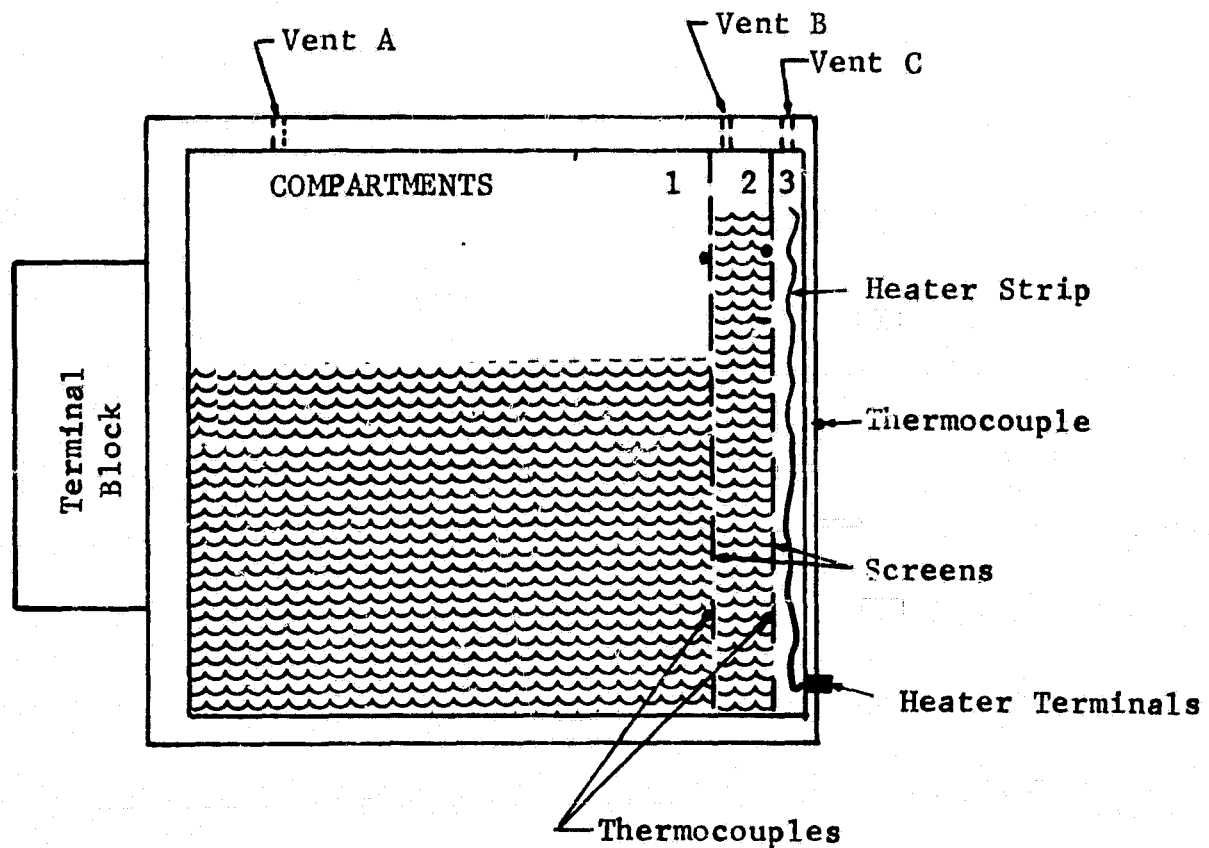


Figure IV-16  Screen Liner Test Model

compartment No. 3, was also about 1/8-in.  The one-g test results demonstrated
that when heat was applied to the system, the liquid in compartment 3 vaporized,
emptying the compartment of liquid in less than 120 sec without drying the
screen separating compartments 2 and 3.  After compartment 3 was devoid of
liquid, its pressure level was controlled (to a minimum) by venting vapor
out of the test specimen through vent C.  The latter was a simple, cylindrical
port with a wetted screen (lower BP) acting as a passive check valve.  Again,
no pentane vapor formation was observed in the liquid annulus, compartment 2.

The vaporization process at the screen surface prevents boiling in the
liquid annulus as long as there is sufficient flow of liquid through the screen
to the vapor-liquid interface in the individual pores.  The reservoir for this
liquid supply is the liquid annulus.  The screen will dry out when the pressure

loss caused by the friction flow through the screen equals the maximum capillary pressure difference afforded by the screen pores. The analytical results presented here are based on the correlation of data for frictional losses for flow of liquid through fine mesh screens, as presented in Ref. IV-4:

$$\Delta P_f = (0.45 \times 10^{-10}) \frac{(Ns+Nw)^2}{d} \frac{\mu q}{\Delta h \rho} ,$$ (IV-15)

where

$Ns$ = number of shute wires/inch,

$Nw$ = number of warp wires/inch,

$d$ = mean wire diameter = $(Ns ds + Nw\ dw)/(Ns + Nw)$,

$ds$ = diameter of shute wires (in.),

$dw$ = diameter of warp wires (in.),

$\Delta h$ = heat of vaporization (Btu/lb$_m$),

$q$ = heat flux (Btu/ft$^2$hr),

$\mu$ = viscosity (centipoise),

$\rho$ = density (lb$_m$/ft$^3$),

$\Delta P_f$ = pressure loss (psi).

Equating $\Delta P_f$ to the maximum capillary pressure difference for a given screen mesh yields the heat flux at which the screen will dry out for a given propellant. The results of this analysis for three different screen meshes are presented below.

| Cryogen | 325 x 2300 | 250 x 1370 | 200 x 1400 |
|---------|------------|------------|------------|
| Nitrogen | 36,000 $\frac{Btu}{ft^2 hr}$ | 132,000 $\frac{Btu}{ft^2 hr}$ | 110,000 $\frac{Btu}{ft^2 hr}$ |
| Oxygen | 68,000 | 250,000 | 200,000 |
| Hydrogen | 23,600 | 80,000 | 68,000 |

The Shuttle orbiter maneuvering system (OMS) tanks probably will use a warm autogenous pressurization. Typical pressurant flow conditions during $\Delta V$ engine burns are hydrogen gas at 200°R and 0.035 lb$_m$/sec and oxygen gas at 300°R and 0.16 lb$_m$/sec. The heat flux to the screen liner (assumed uniform) is then during pressurization 40 Btu/ft$^2$hr for the hydrogen tank and 30 Btu/ft$^2$hr for the oxygen tank. These values are several orders of magnitude below the calculated estimates. The natural heat leak through the tank walls is nominally 0.25 Btu/ft$^2$hr. Clearly, these heat sources are not sufficient to dry out the screen.

## E. FABRICATION AND ASSEMBLY

Fine mesh screen fabrication to date has been limited to relatively small sizes, particularly when the shape of the device is of compound curvature. The latter have been limited to only about 1 ft., or less, in size (Ref IV-5). The systems were usually fabricated for use in ground tests, as with the DSL subscale model described in Chapter VII, which limit system size due to hydrostatic heads. The Agena sump device, comprised of fine mesh twilled metal cloth which has flown successfully (Ref IV-6), is in this size range.

There have been larger capillary devices built, such as the umbrella trap arrangement used in the Apollo CSM (Ref IV-3) and the finger-like galleries used in the 62-in. diameter tank (Ref IV-6); however, neither is of the compound curvature that may be required for the fine-mesh DSL system. The relatively large tankage of the Shuttle orbiter, on the order of 10-ft, by size alone, presents a significant challenge with regard to fabrication, inspection, cleaning, handling, and maintenance. The experience available today shows no insurmountable problem associated with the large cryogenic storage systems; however, work is required in this area to substantiate this. Again, the reusability requirement of the Shuttle orbiter places even a greater importance on inspection, cleaning, handling, and maintenance.

Because the capillary characteristics of the screen depend on the pore size, the fabrication of curved surfaces must be accomplished with minimum distortion. Martin Marietta has developed manufacturing technology for forming high-quality, compound curvature surfaces of plain or pleated screen. An "orange peel" or "gore" section technique has been developed for manufacturing plain surfaces. For pleated surfaces, a two-stage procedure has been developed in which a singly curved surface is formed first with the compound curvature developed from the singly-curved one. A compound curvature screen device formed in this manner is shown in Fig. IV-17.

Before any fabrication process is performed, the screen is thermally conditioned to ensure that the capillary retention capability of the screen will be only minimally degraded during the forming process. Pleated screens formed by Martin Marietta to date have been of cylindrical, spherical, or partial-spherical shapes. The largest size to date has been 10-inches. The ultimate percentage of elongation of the screen material must be considered. This value is 55% for stainless steel and 35% for the less ductile aluminum. This is an important consideration when selecting an appropriate bend radius. Further, stainless steel screens are available in considerably smaller mesh sizes than aluminum screens, and therefore are more attractive from the standpoint of capillary retention capability.

The fabrication of screen-to-screen and screen-to-plate presents certain limitations such as; contamination areas must be minimized (particularly when $LO_2$ is involved), and screen integrity should not be destroyed by excessive heating or loads applied during joining. Based on the Martin Marietta experience (Ref IV-7), mechanically formed joints are not acceptable. Screen-to-screen
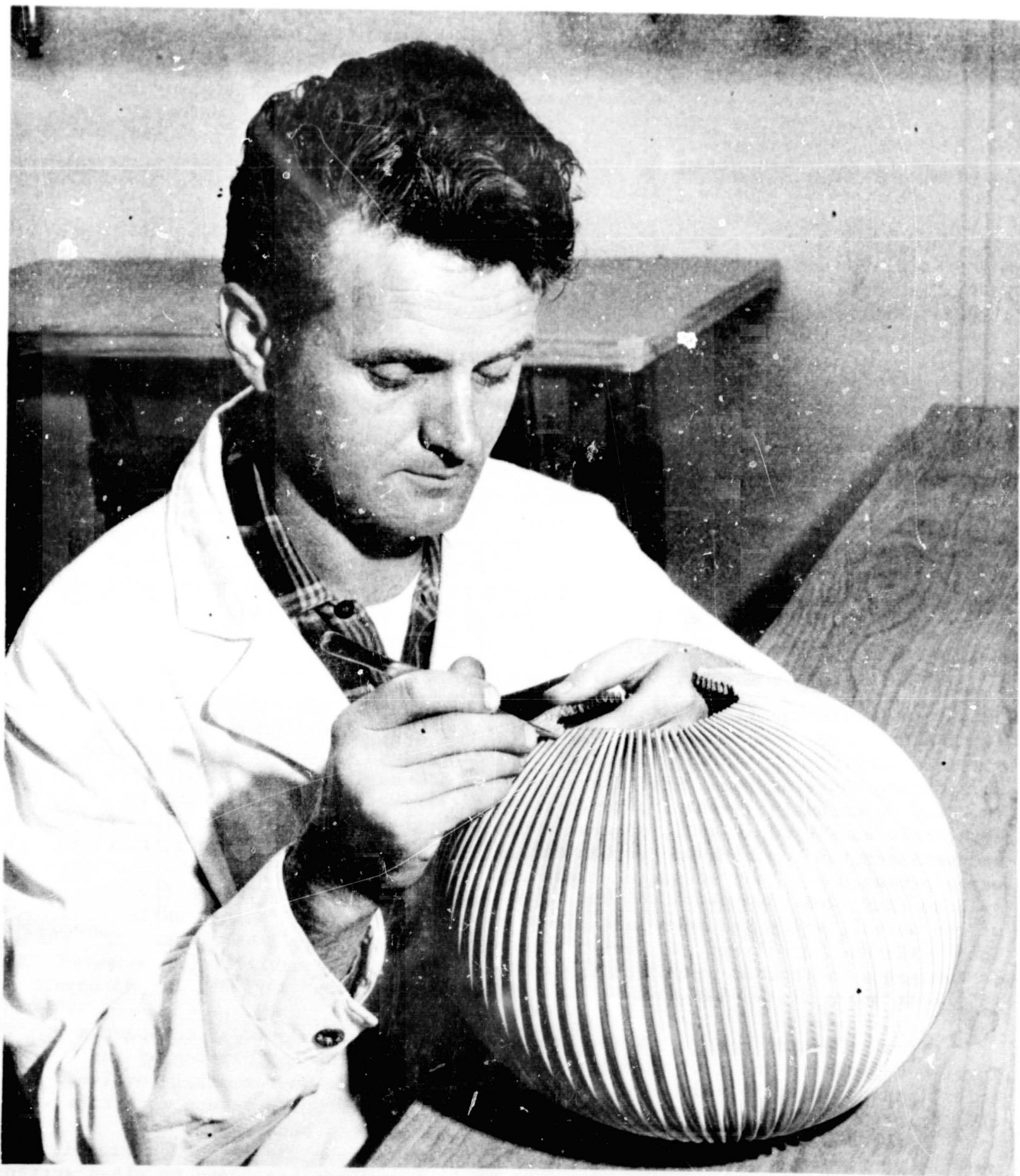
Figure IV-17   Martin Marietta Technician Inspecting 10-in.-dia.-Sphere
of 250x1370 Dutch-Twill Screen Formed with 72 Pleats (1/4 in. deep).

joining has been successfully accomplished with resistance seam welding. Resistance seam welding produces a narrow weld that is easily cleaned. Joining screen-to-plate can be accomplished by either brazing or welding. Brazing is the simpler method. Wicking of the screen material by the braze alloy in the area adjacent to the joint is avoided by applying a "stop-off" material before the brazing operation. For stainless steel, a gold/nickle braze and Yttrium Oxide (Y O$_3$) "stop-off" have been used effectively. Resistance welding can also be used to join screen-to-plate, but the joint is more difficult to clean. When this type joint is fabricated the joint should fill with molten metal. Fusion welding can supply sufficient molten metal, but there is a high possibility of melting the screen wires before the plate area is sufficiently softened to weld properly. Electron beam welding can join screen-to-plate satisfactorily because the heat input can be closely controlled. With this method the wire melts only in the area of the joint. Because of the complexity of most screen-to-plate joints, brazing is the preferred technique.

Pleated screen liners for full dual screens have been fabricated in quarter-spherical sections. Thus, two of these sections are required to form a hemisphere. The sections are joined with two screen-to-screen resistance seam welds. The pole and equatorial regions of the hemispheres are then machined on an electrical discharge milling machine to the proper size for joining by brazing to the outflow cup and girth plate, or in the case of a partial liner or trap, to the outflow cup and cover plate assembly. When practical, individual screen sections are checked for their capillary retention capability with a bubble point test before they are assembled; quite often a bubble point check is not possible until the entire screen device has been assembled.

### 1. Cleaning and Inspection

Even though capillary retention systems fabricated from fine mesh screens (with pore sizes on the order of only a few microns) contain great numbers of possible contaminant entrapment sites, no problems are anticipated with regard to cleaning these devices, including those for LO$_2$ service. This conclusion is based on extensive Martin Marietta screen cleaning experience, including a recently completed in-house program where cleaning procedures were developed and demonstrated for cleaning screen devices for use with LF$_2$. Liquid fluorine usage presents the most stringent cleaning requirements for any fluid. The program (Ref IV-8) demonstrated that the 2300 mesh Dutch twill screen (12-15 micron pores), which had been formed into test sample screen devices using both resistance and inert gas fusion welding techniques, could be cleaned of contaminants so that no reduction in capillary retention capability (as measured by bubble point tests) was recorded after continuous exposure to LF$_2$ for 35 days.

Normal cleaning techniques for propellant tanks and associated components involve degreasing and acid cleaning before assembly. The composition of the acid cleaning solution and the specific procedure depends on the metal involved and the propellant to which it is to be exposed. However, the screen materials used in the DSL systems cannot be cleaned by this process because the acid would remove an amount of metal sufficient to degrade the retention capability of the screens. Therefore, a vacuum annealing process has been used to clean screens.

This is normally performed after assembly of the device and completion of the bubble point tests. The stainless steel screens used in the fluorine tests mentioned previously were cleaned in this way. The standard method for inspecting screen devices to ensure conformity to capillary retention specifications is the bubble point test. The pressure retention capability range for various screen mesh sizes, as determined by Martin Marietta using the bubble point technique, is presented in Table IV-5.

Table IV-5  Martin Marietta Screen Pressure Retention Data

| Screen Material | Screen Mesh | Bubble Point, BP (in. of $H_2O$) | | |
| | | As Received | Vapor Degreased | Ultrasonic Cleaning |
|---|---|---|---|---|
| Stainless Steel | 30x30 | 0.68 (2)* | 0.68-0.69 (3) | -- |
| Stainless Steel | 50x50 | 1.19-1.20 (2) | 1.22-1.23 (6) | -- |
| Stainless Steel | 80x80 | 1.75-1.80 (2) | 1.80-1.85 (6) | -- |
| Stainless Steel | 100x100 | 2.20-2.28 (4) | 2.20-2.22 (5) | -- |
| Stainless Steel | 150x150 | 2.73-3.20 (4) | 3.10-3.12 (5) | -- |
| Stainless Steel | 200x200 | 3.75-4.60 (11) | 3.89-4.40 (12) | -- |
| Aluminum | 120x120 | 2.06-2.24 (13) | 2.17-2.55 (16) | -- |
| Aluminum | 30x250 | 2.50-2.70 (6) | 2.63-2.71 (7) | -- |
| Aluminum | 200x1400 | 16.30-16.40 (2) | -- | -- |
| Stainless Steel | 24x110 | 1.99-2.09 (5) | 1.96-2.12 (12) | -- |
| Stainless Steel | 30x250 | 2.58-2.65 (5) | 2.54-3.00 (15) | -- |
| Stainless Steel | 80x700 | 6.37-6.48 (5) | 6.28-6.36 (6) | -- |
| Stainless Steel | 165x800 | 7.82-8.30 (17) | 7.90-8.23 (14) | 7.85-8.16 (15) |
| Stainless Steel | 200x1400 | 16.70-17.40 (18) | 16.70-17.04 (15) | 17.08-17.25 (17) |
| Stainless Steel | 250x1370 | 21.10-22.83 (12) | 20.80-22.20 (13) | 21.40-22.40 (20) |
| Stainless Steel | 325x2300 | 24.80-26.75 (18) | 25.15-26.40 (16) | 25.82-26.70 (21) |

Note: Samples tested in methanol.

*Numbers in parentheses are numbers of samples tested.

The data presented in Table IV-5 were obtained using methanol as the test liquid. Using these data, the pressure retention for a given screen material and mesh size can be determined for other liquids from:

$$(BP)_\ell = \frac{\sigma_\ell}{\sigma_{Methanol}} (BP)_{Methanol} \qquad \text{IV-16)}$$

where the subscript, $\ell$, refers to the other liquid.

Because of the limited scope and funding of this program, no detailed structural analyses of the DSL subscale model were made. However, a detailed design of the DSL subscale model was made and the design is presented in Chapter VII. A preliminary effort was made, however, to uncover any major design problems for large-scale cryogenic tankage. Some of this effort, which uncovered no insurmountable problems, is presented in the following paragraphs.

One conceptual design for the construction of a screen liner subassembly
is shown in Figure IV-18.  The rib and stringer structure provides for the
inner screen to be mounted on its inside with the outer screen on the outside,
as shown.  The structure, itself, provides the liquid annulus gap.  All members
of the structure are fabricated from perforated plate so the structure affords
little interference with flow in the annulus.

A possible scheme for mounting the liner subassembly within the tank is
shown in Figure IV-19.  Wires are used to support the liner within the tank.
A sufficient number of laces is provided so that the anticipated loads on the
liner can be supported by suspension.  By using thin wire only, the amount of
heat transferred by the wire from the wall to the liner is minimized.  This
method of supporting the liner can be used for any tank configuration.

## 2.  System Mass

Expulsion device mass (dry), though only a small part of the total tank and
propellant mass, becomes more and more significant as tank size increases.  For
small sizes, say 5 ft$^3$ for example, the complete DSL may be only a small fraction
of the total mass and have little impact on mission payload potential.  As tank
size becomes larger, the DSL mass becomes a key consideration.

Fortunately, a wide variety of materials is readily available for capillary
system fabrication.  In addition, configuration selection is virtually unlimited,
permitting designs that are attractive for most space missions considering
expulsion performance, as well as weight.

Foraminous material of stainless steel, aluminum, titanium, and many alloys
are commercially available "from the shelf."  Perforated plate, square weave,
and Dutch twill screen are readily available in materials compatible with most
propellants.  For the cryogenic fluids of concern during this study, either
stainless steel or aluminum is attractive.

The point design study made for the Shuttle orbiter considered aluminum
tankage.  It is desirable to use the same material for the passive device and
tank to avoid problems associated with dissimilar metal joints.  Aluminum per-
forated plate and square weave screen are available in pore and mesh sizes
common to stainless steel, but the finest Dutch twill screen is available in
stainless steel only.  The finest Dutch twill presently available in aluminum
is 200 x 1400 mesh.  Aluminum possesses the strength required in the present
weaving processes to yield mesh sizes finer than 200 x 1400.  A mesh size of
325 x 2300 is commercially available in stainless steel.  Finer screens, e.g.,
450 x 2750, have been woven in stainless steel, but not without excessive
defects and cost (twice as many defects and three times the cost of the 325 x
2300).

Dry mass estimates for the baseline DSL using stainless steel Dutch twill
screen are presented in Fig. IV-20 and IV-21 for both spherical and cylindrical
tanks.  Two complete liners were assumed with the inner liner pleated.  For
simplicity, it was assumed that the surface area of the outer liner was the
same as the tank in which it was installed and the pleated inner liner was
twice the tank area.

stringer

support eyelet (see detail)

rib

eyelet

outer screen

rib

inner screen

stringer
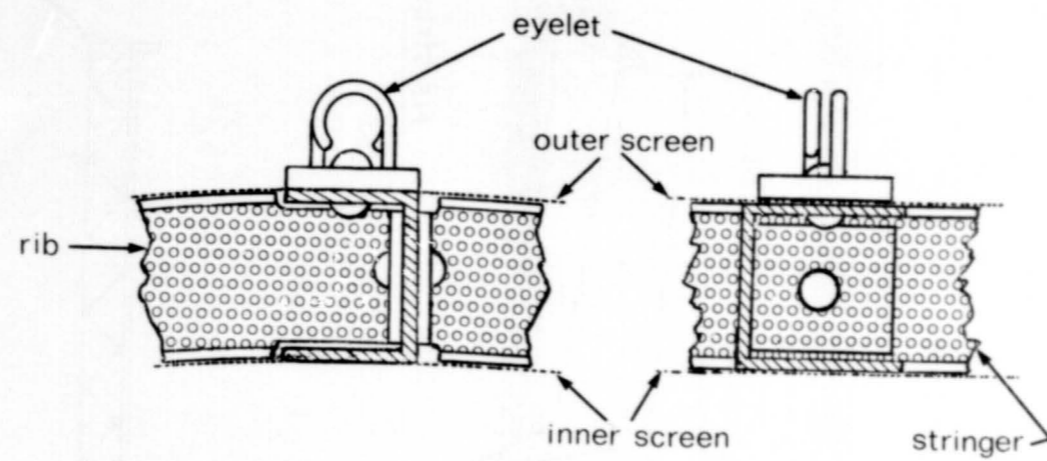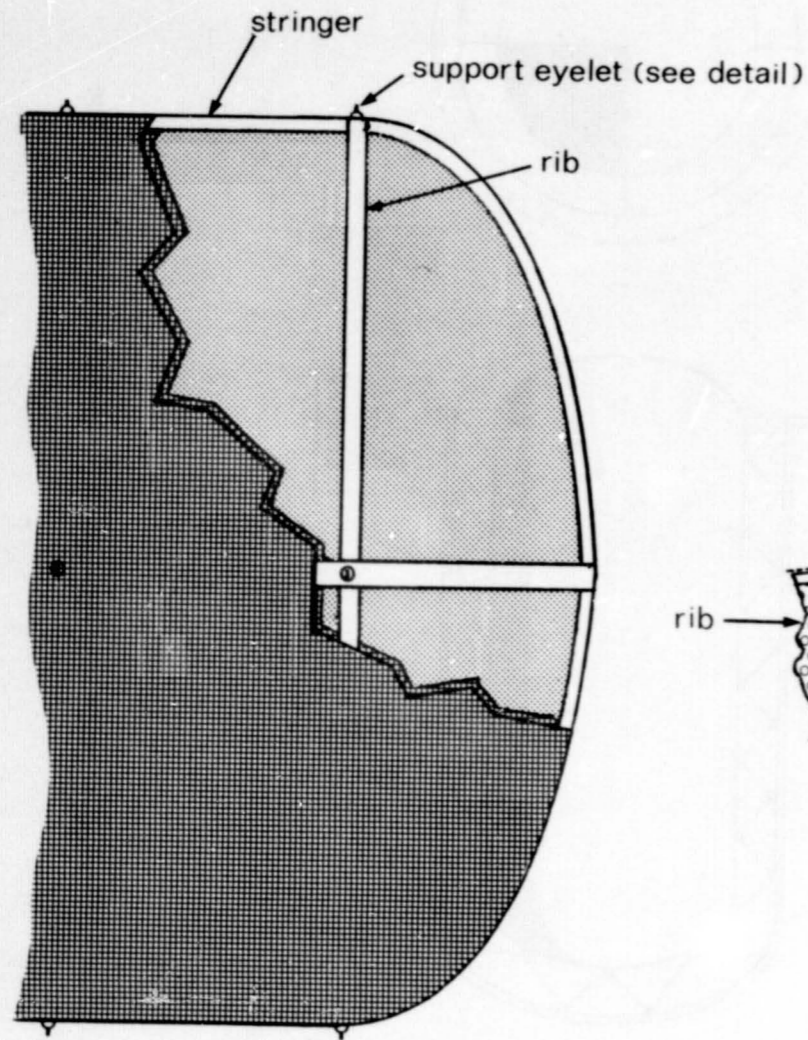
**Eyelet & Frame Detail**

Figure IV-18   Dual-Screen-Liner Construction

77

tank

wire

**Pre-strung**

screen liner

**Installed**
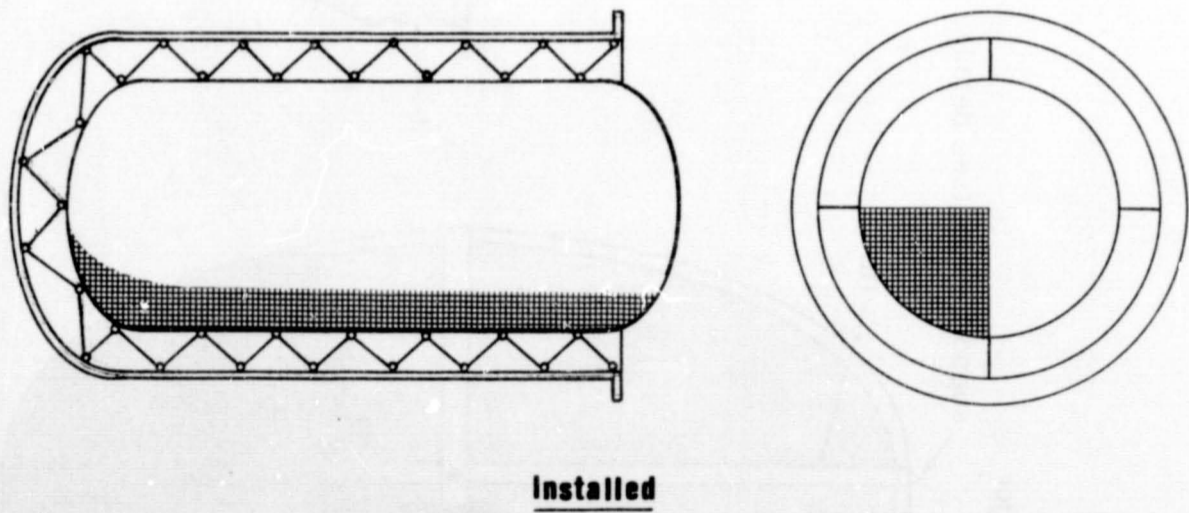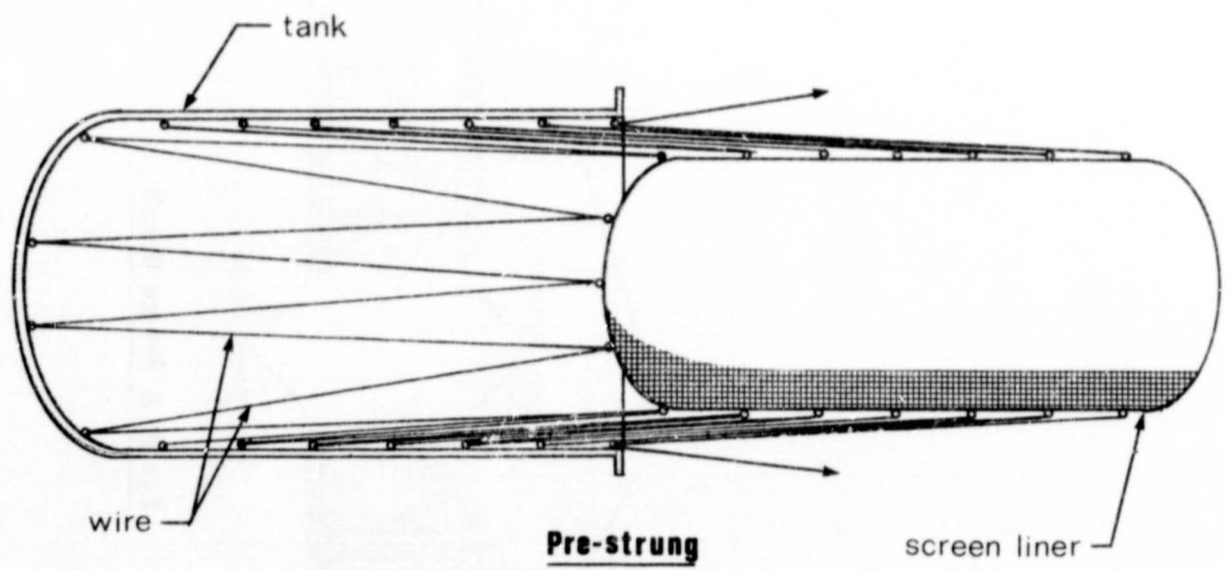
Figure IV-19 "Speed-Lace" Liner Suspension Technique
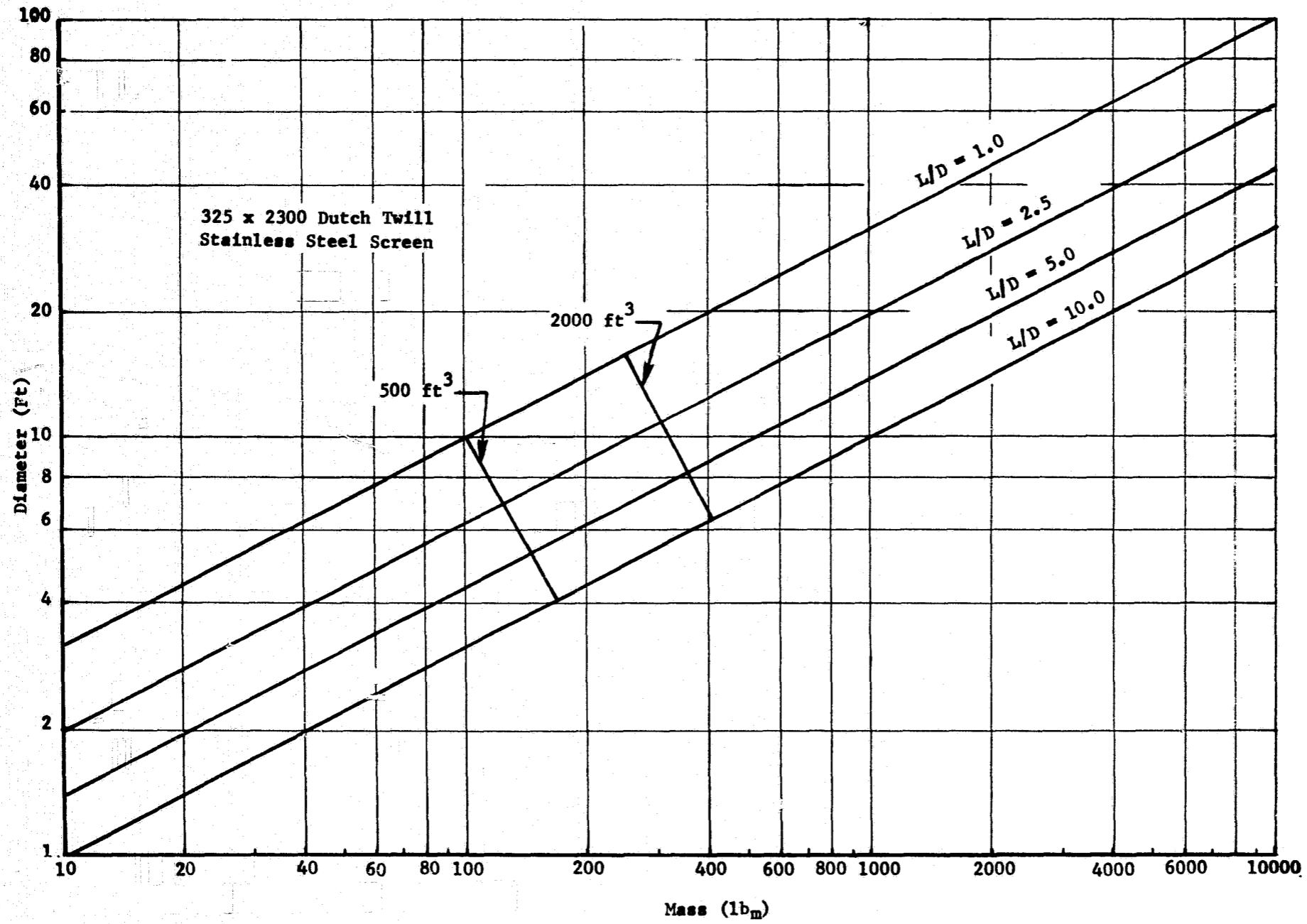
Figure IV-20  Estimated DSL System Mass (Dry), 325x1300 Mesh Screen
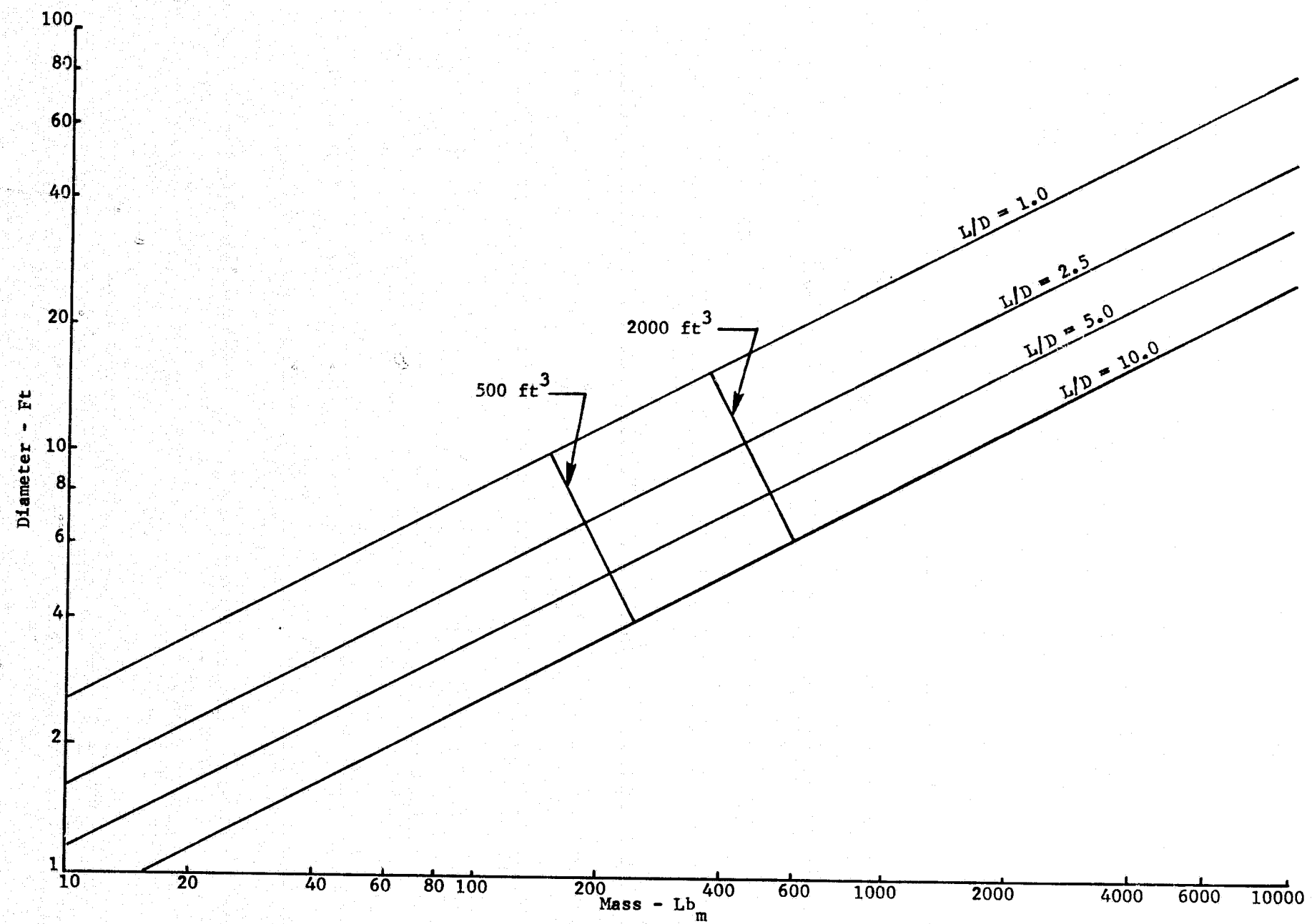
Figure IV-21. Estimated DSL System Mass (Dry), 200x1400 Mesh Screen

An additional 10% was added to the screen mass to account for joints, tube outlets, and support structure, such as the "speed lace" concept in Fig. IV-19. The estimates presented in Fig. IV-20 are for 325 x 2300; Fig. IV-21 for 200 x 1400 mesh stainless steel. The system mass estimates for 200 x 1400 mesh aluminum Dutch twill weave screen are presented in Fig. IV-22. The assumptions used for stainless steel also apply to these estimates. System estimates for the DSL using square weave screen in both stainless and aluminum are presented in Fig. IV-23 thru IV-26. These estimates are based on the same assumptions used for Dutch twill weave.

The DSL mass becomes increasingly significant with increased tank volume. For a 2000-ft$^3$ tank, for example, the DSL weight can vary from 70 to 600 lb$_m$ depending on material selection and tank configuration. Modifications to the DSL can also be employed to reduce the expulsion device weight with little or no impact on the system performance. One variation of the DSL that significantly reduces system mass is that pictured as Example A in Fig. II-3. The flow channels are manifolded at the top and bottom of the tank. All liquid outflow enters the flow channels from the bulk region. The lower flow channel manifold is connected to the tank outlet. Vapor venting is achieved from the annulus formed by the complete liner and tank wall as with the baseline DSL. System mass estimates for different DSL concepts are also presented in the point design effort, Chapter V.

## F.  GENERAL CONCLUSIONS

The results of the parametric study tend to show that the DSL concept is applicable to the wide range of cryogenic storage applications studied, including the Shuttle orbiter. It appears to be adaptable to the four cryogens of interest, oxygen, hydrogen, methane, and nitrogen. As discussed earlier in Part C of Chapter II, the DSL pressure-relief method is efficient when compared to other venting techniques for storage pressures to about four atmospheres. For higher pressures, a more detailed comparison of the DSL and the other systems is needed with regard to reliability, efficiency, and weight to select the preferred concept for each application. In this regard, it is also recommended that the specific storage requirement be thoroughly evaluated before selecting the best DSL concept. A specific point design was made to illustrate this. The results for the 50,000-lb$_m$ straight-wing low-crossrange orbiter design effort are presented separately in the next chapter, Chapter V.
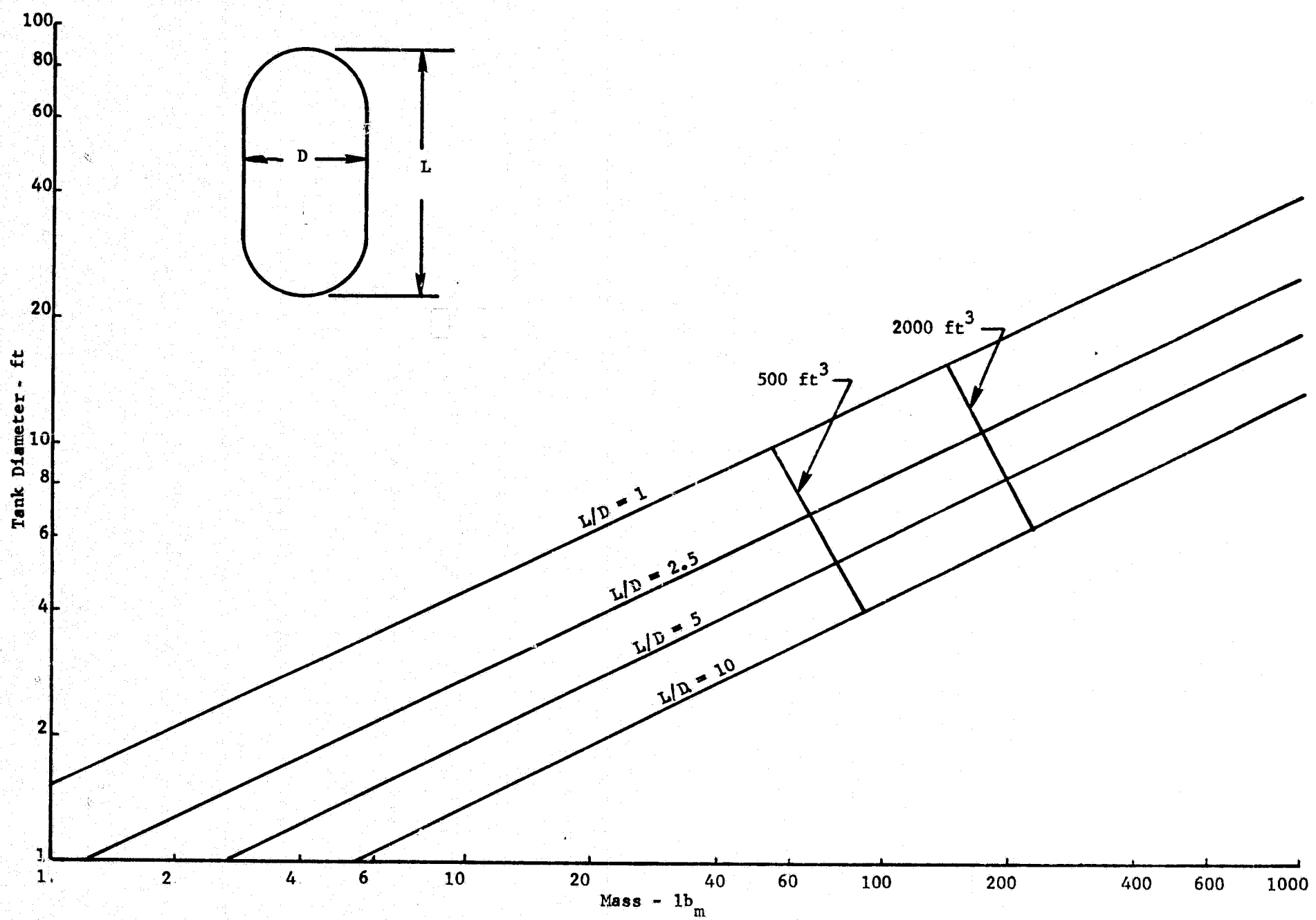
Figure IV-22  Estimated Mass of DSL as a Function of Diameter and L/D for Cylindrical Tanks with Hemispherical Domes (200x1400 Aluminum Screen)
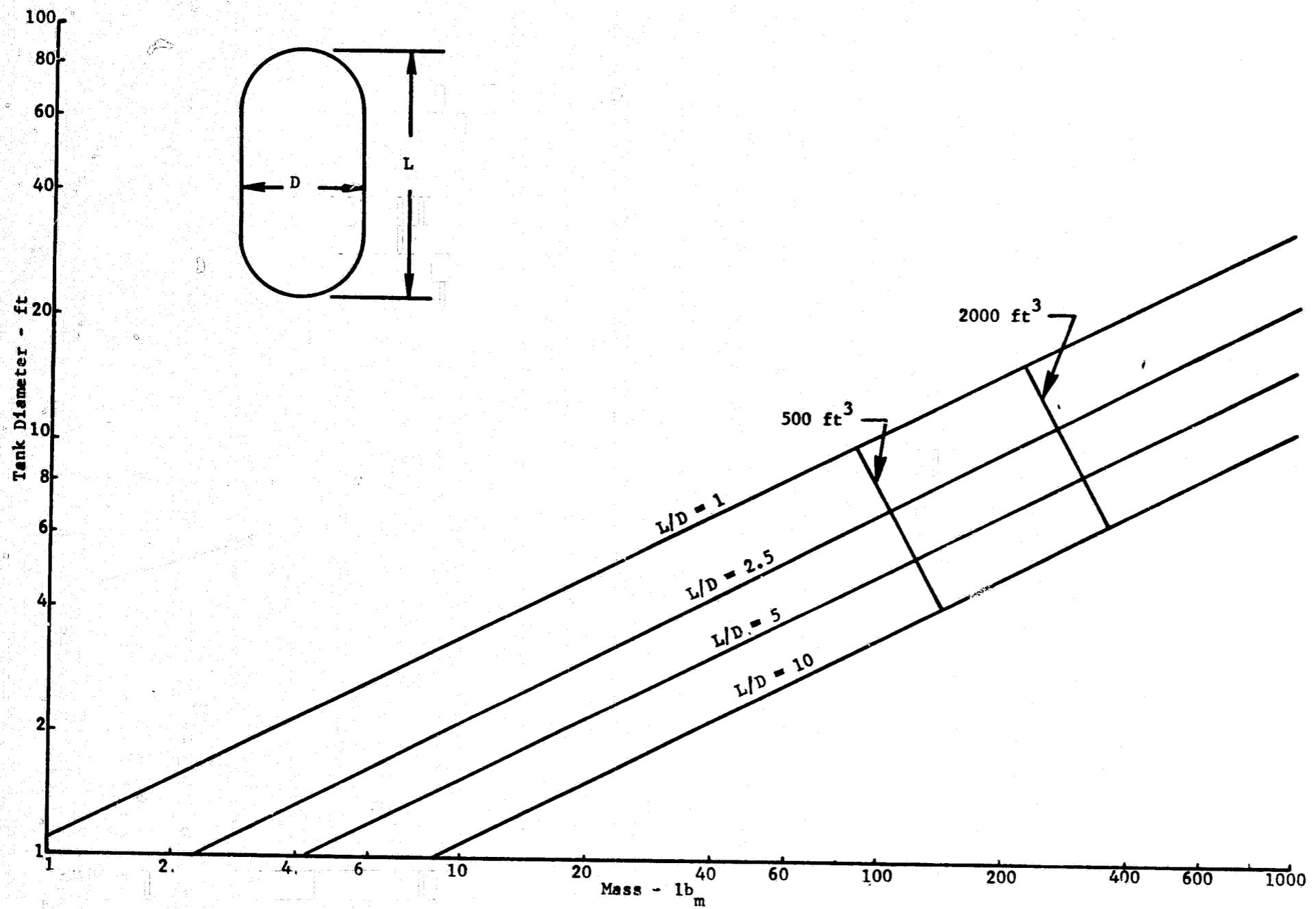
Figure IV-23 Estimated Mass of DSL as a Function of Diameter and L/D for Cylindrical Tanks (200x200 Stainless Screen)
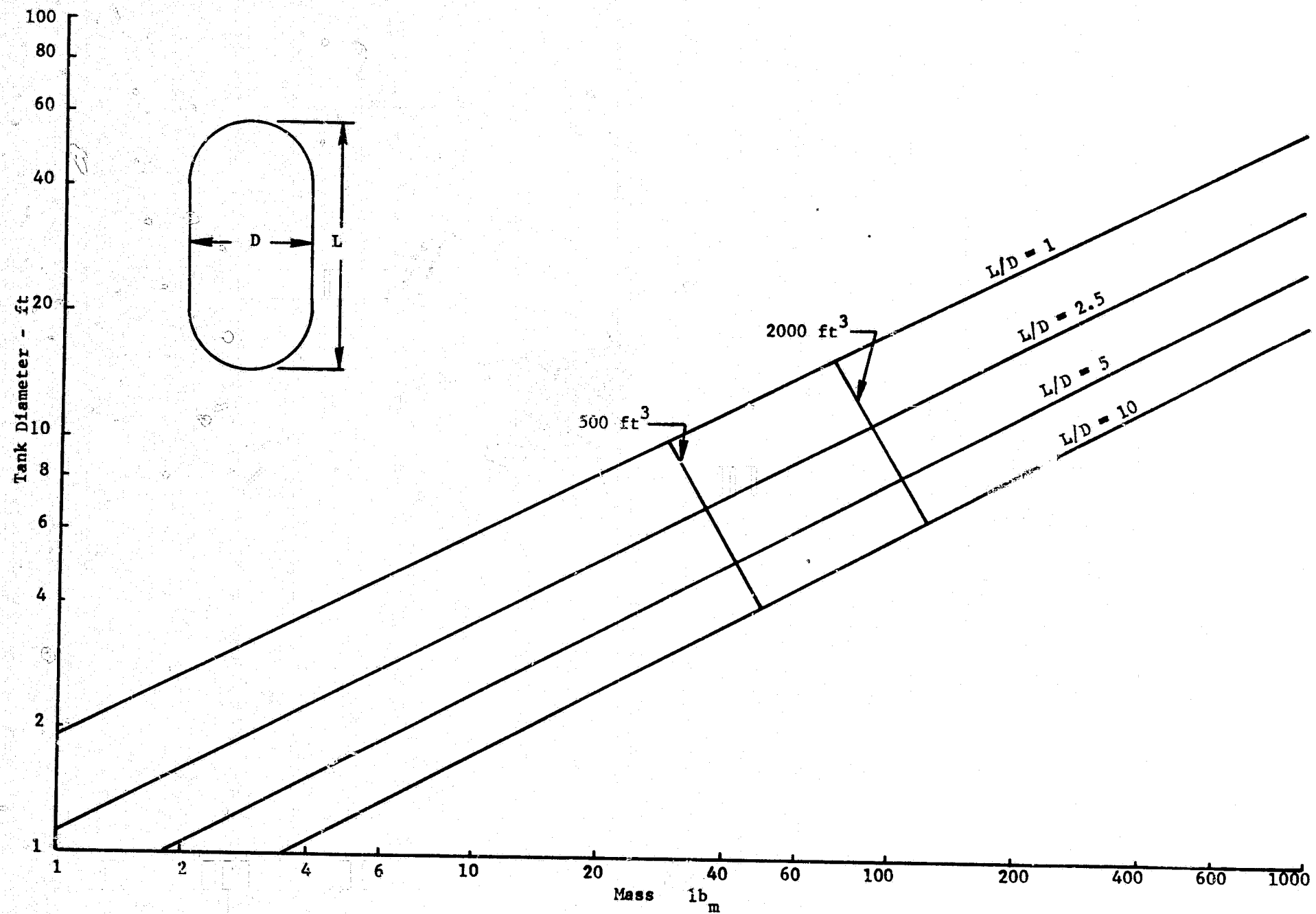
Figure IV-24  Estimated Mass of DSL as a Function of Diameter and L/D for Cylindrical Tanks with Hemispherical Domes (200x200 Aluminum Screen)
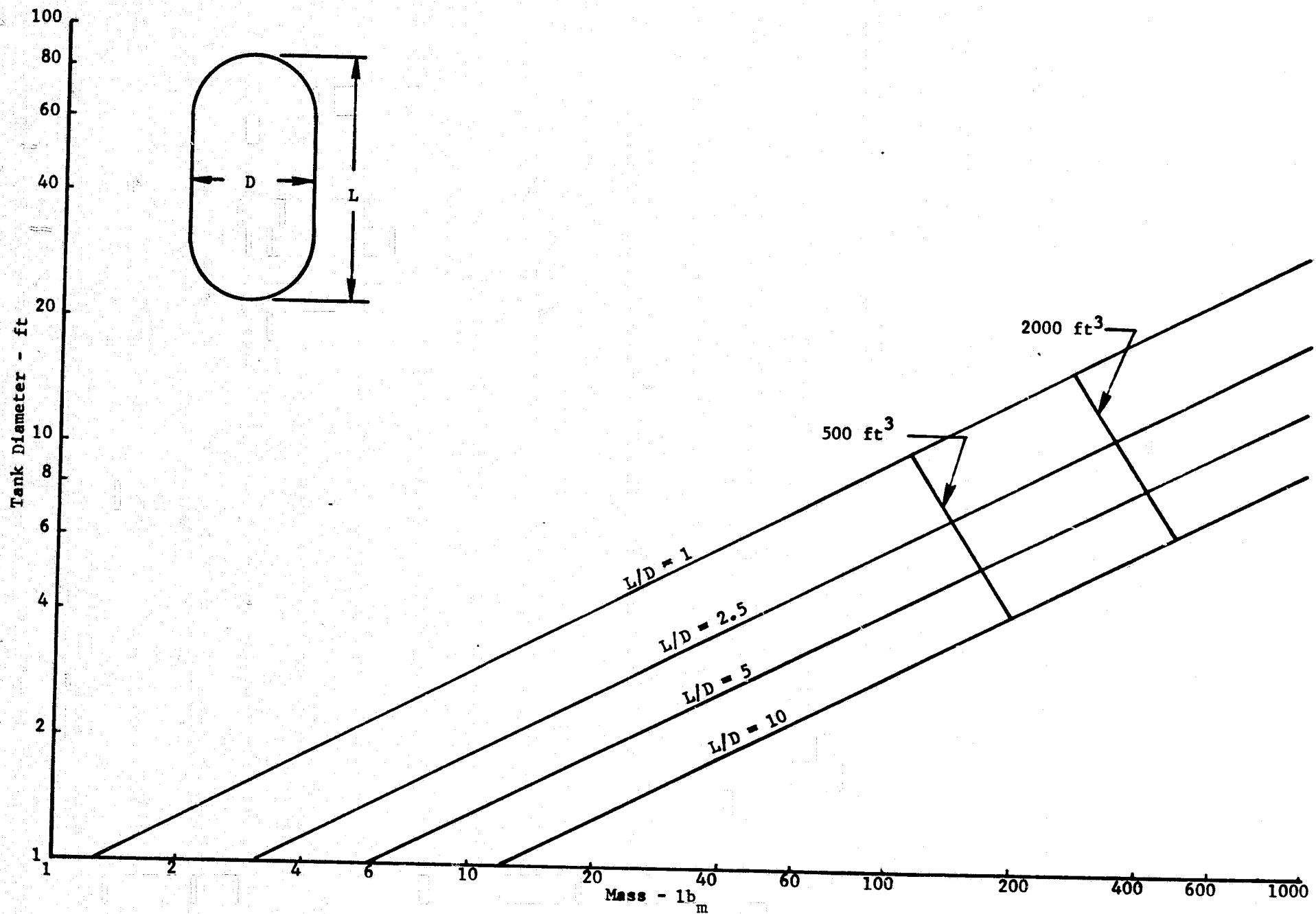
Figure IV-25 Estimated Mass of DSL as a Function of Diameter and L/D for Cylindrical Tanks (100x100 Stainless Screen)

Figure IV-25 Estimated Mass of DSL as a Function of Diameter and L/D for Cylindrical Tanks (100x100 Stainless Screen)
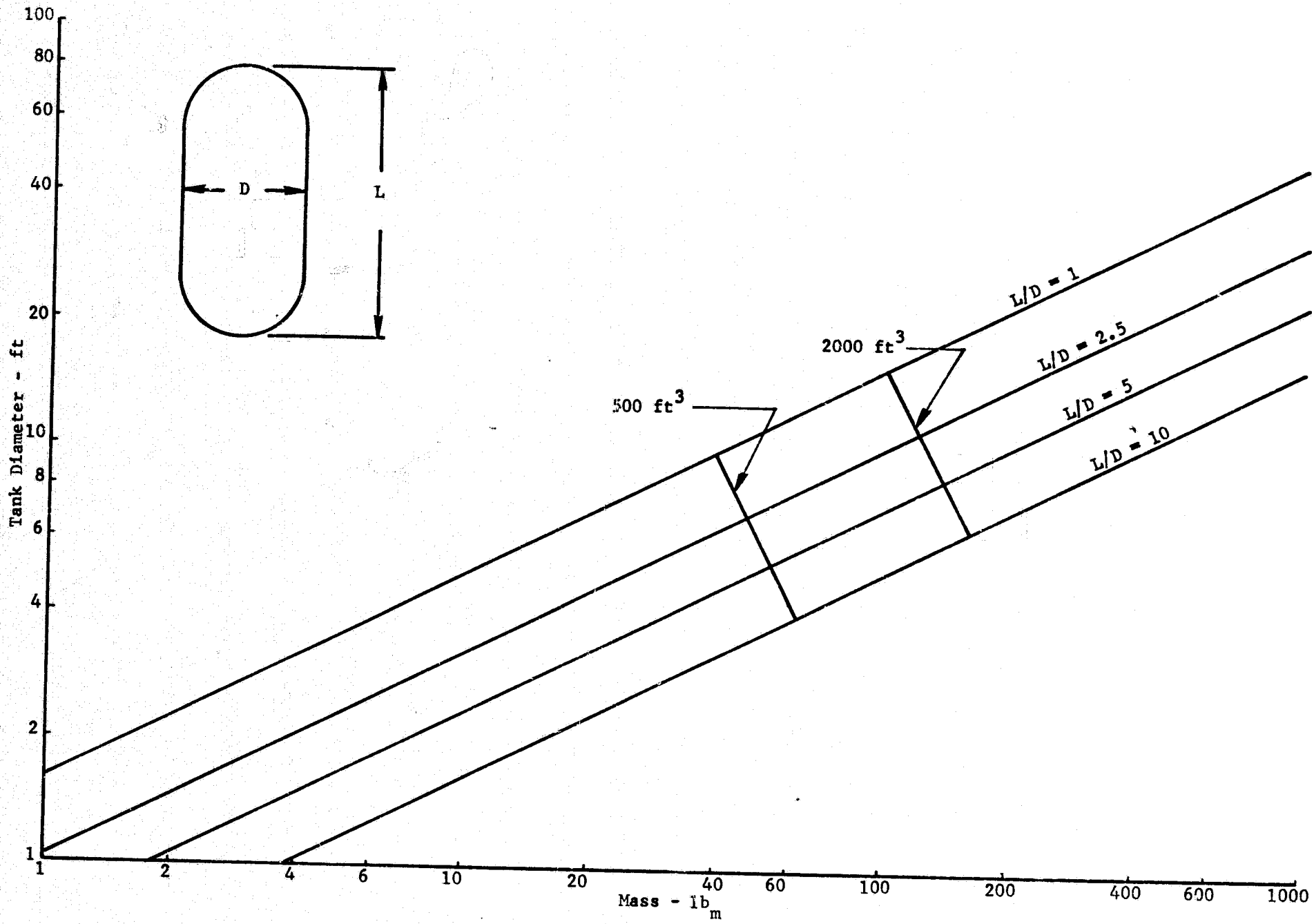
Figure IV-26  Estimated Mass of DSL as a Function of D and L/D for Cylindrical Tanks (100x100 Aluminum Screen)

# V.  SPACE SHUTTLE ORBITER CAPILLARY SYSTEM DESIGN

A preliminary design of a propellant management system for a Space Transportation System (STS) was conducted.  The configuration used in the analysis carried a 50,000-lb orbiting payload with $LH_2$ and $LO_2$ propellants. The primary objectives of this preliminary design effort were:

1) Evaluate the STS design criteria and mission duty cycle with respect to the propellant management system;

2) Select and evaluate candidate capillary propellant management systems;

3) Recommend a propellant management system design for the STS cryogen tankage.

Events that used propellants were orbit injection, orbit change, on-orbit attitude control, rendezvous, docking, reentry, and reentry attitude control. The vehicle was characterized by relatively large tank sizes and lateral accelerations that were an order of magnitude higher than the longitudinal accelerations.  These lateral accelerations occur in a $360^o$ plane, approximately normal to the longitudinal axis.

## A.  DESIGN CRITERIA AND APPROACH

The baseline straight wing orbiter configuration and duty cycle were considered for the design effort.  The engines are high $P_c$ gaseous thrusters requiring relatively long burn times for vehicle velocity changes ($\Delta V$) due to the low thrust.  The 22 thrusters, located forward, aft, and on the wings of the vehicle, are used for both $\Delta V$ and attitude control (ACPS) maneuvers.  The propulsion system schematic is shown in Fig. V-1.

The primary function of the propellant management system is to supply gas-free liquids on demand to the pumps of the propellant conditioning system. The conditioning system recharges the high-pressure gaseous accumulators which supply gases to the thrusters on demand.  Propellant outflow from the storage tanks can be either short or long duration.  The $\Delta V$ and ACPS maneuvers impart acclerations to the propellant tanks that vary both in magnitude and direction. These varying accelerations and outflow requirements together with the relatively large propellant tanks produce stringent design requirements.  In addition, the propellant management system must satisfy the venting requirement during coast periods.  The acceleration during coast periods was considered to be approximately $10^{-5}$ g.

A summary of the three-day orbiter duty cycle is presented in Table V-1, which shows propellant outflow rates, propellant quantities, and acceleration magnitudes and directions for both propellant tanks.  The $\Delta V$ duration times range between 13 and 540 sec.  The ACPS maneuvers are 6 sec in duration. Propellant outflow rates for the $\Delta V$ maneuvers are about twice those for the ACPS maneuvers.
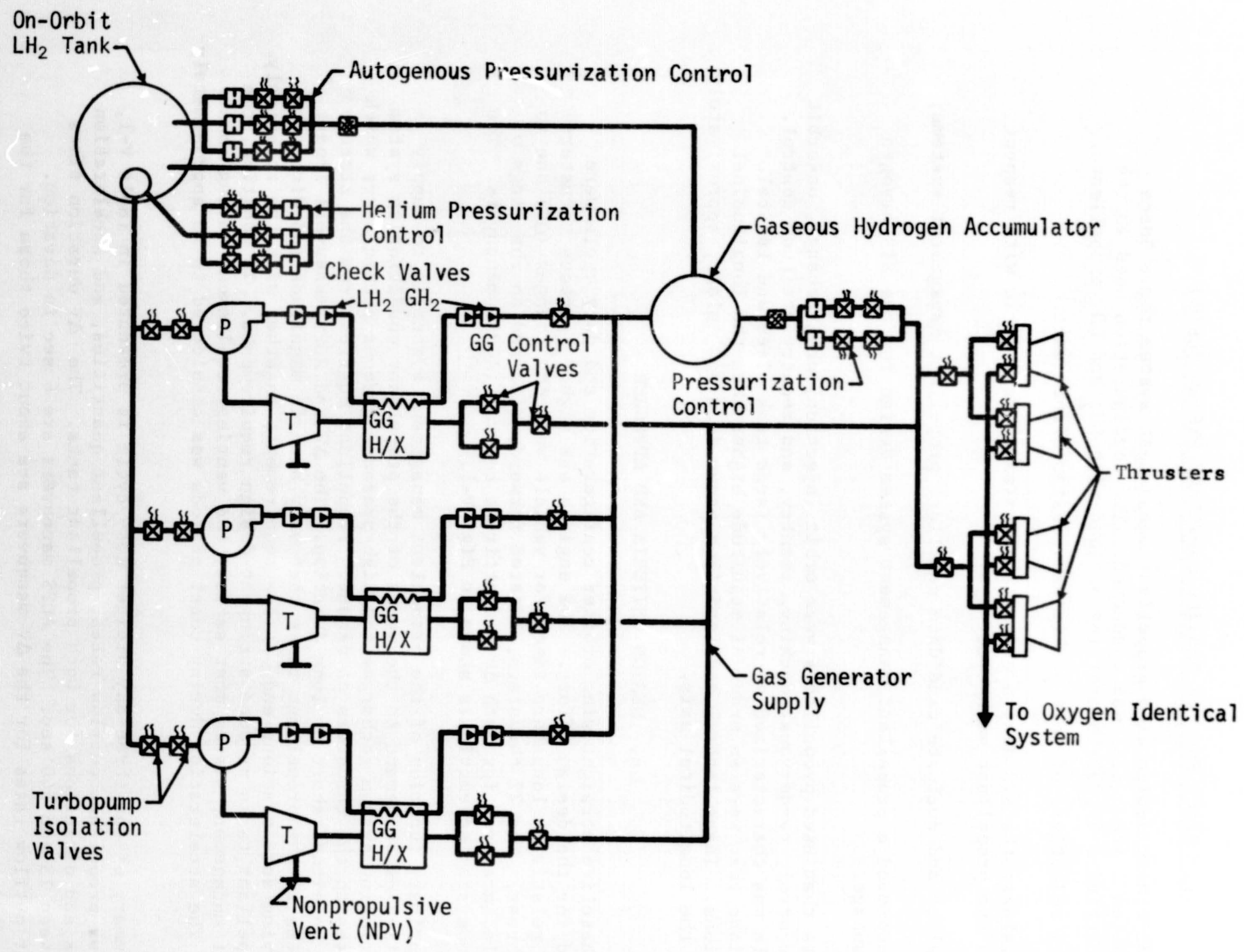
Figure V-1  Shuttle Orbiter Propulsion System Schematic

Table V-1  STS Orbiter Mission Duty Cycle

89

| EVENT | MISSION TIME (hr:min) | EVENT DURATION (sec) | LIQUID OXYGEN TANK | | LIQUID HYDROGEN TANK | | ACCELERATION | |
|---|---|---|---|---|---|---|---|---|
| | | | FLOW RATE (lb_m/sec) | PROPELLANT MASS (lb_m) | FLOW RATE (lb_m/sec) | PROPELLANT MASS (lb_m) | LEVEL | DIRECTION |
| Launch | 0:00 | | | 25877 | | 6506 | | |
| ΔV | 0:49 | 426 | 14.0 | 19877 | 3.5 | 5016 | .027,(.144)* | +x,(±y or ±z) |
| RCS | 0:56 | 6 | 7.0 | 19835 | 2.0 | 5004 | .141 | ±y or ±z |
| RCS | 2:49 | 6 | 7.0 | 19793 | 2.0 | 4992 | .141 | ±y or ±z |
| RCS | 4:49 | 6 | 7.0 | 19751 | 2.0 | 4980 | .141 | ±y or ±z |
| RCS | 6:49 | 6 | 7.0 | 19709 | 2.0 | 4968 | .141 | ±y or ±z |
| RCS | 8:49 | 6 | 7.0 | 19667 | 2.0 | 4956 | .141 | ±y or ±z |
| ΔV | 9:49 | 70 | 14.0 | 19387 | 3.5 | 4886 | .027,(.144) | +x,(±y or ±z) |
| RCS | 9:50 | 6 | 7.0 | 19345 | 2.0 | 4874 | .141 | ±y or ±z |
| RCS | 10:11 | 6 | 7.0 | 19303 | 2.0 | 4862 | .141 | ±y or ±z |
| ΔV | 10:12 | 20 | 14.0 | 19013 | 3.5 | 4792 | .027,(.144) | +x,(±y or ±z) |
| RCS | 12:11 | 6 | 7.0 | 18971 | 2.0 | 4780 | .141 | ±y or ±z |
| RCS | 14:11 | 6 | 7.0 | 18949 | 2.0 | 4768 | .141 | ±y or ±z |
| RCS | 16:11 | 6 | 7.0 | 18887 | 2.0 | 4756 | .141 | ±y or ±z |
| RCS | 18:11 | 6 | 7.0 | 18845 | 2.0 | 4744 | .141 | ±y or ±z |
| RCS | 20:11 | 6 | 7.0 | 18803 | 2.0 | 4732 | .141 | ±y or ±z |
| RCS | 22:13 | 6 | 7.0 | 18761 | 2.0 | 4720 | .141 | ±y or ±z |
| ΔV | 22:14 | 307 | 14.0 | 14461 | 3.5 | 3660 | .027,(.144) | +x,(±y or ±z) |
| ΔV | 23:00 | 260 | 14.0 | 10811 | 3.5 | 2750 | .027,(.144) | +x,(±y or ±z) |
| RCS | 23:05 | 6 | 7.0 | 10769 | 2.0 | 2738 | .141 | ±y or ±z |
| ΔV | 24:34 | 24 | 14.0 | 10429 | 3.5 | 2654 | .027,(.144) | +x,(±y or ±z) |
| RCS | 24:35 | 6 | 7.0 | 10387 | 2.0 | 2642 | .141 | ±y or ±z |
| ΔV | 24:46 | 19 | 14.0 | 10142 | 3.5 | 2576 | .027,(.144) | +x,(±y or ±z) |
| RCS | 24:47 | 6 | 7.0 | 10080 | 2.0 | 2564 | .141 | ±y or ±z |
| ΔV | 24:56 | 10 | 14.0 | 9940 | 3.5 | 2529 | .027,(.144) | +x,(±y or ±z) |
| ΔV | 25:08 | 10 | 14.0 | 9800 | 3.5 | 2494 | .013,(.142) | -x,(±y or ±z) |
| RCS | 25:09 | 6 | 7.0 | 9758 | 2.0 | 2482 | .141 | ±y or ±z |
| ΔV | 25:10 | 13 | 14.0 | 9578 | 3.5 | 2437 | .013,(.142) | -x,(±y or ±z) |
| ΔV | 25:11 | 13 | 14.0 | 9398 | 3.5 | 2392 | .013,(.142) | -x,(±y or ±z) |
| ΔV | 25:13 | 5 | 14.0 | 9328 | 3.5 | 2374 | .027,(.162) | ±y,(±y or ±z) |
| ΔV | 25:15 | 5 | 14.0 | 9258 | 3.5 | 2356 | .027,(.162) | ±z,(±y or ±z) |
| RCS | 25:38 | 6 | 7.0 | 9216 | 2.0 | 2344 | .141 | ±y or ±z |
| ΔV | 25:39 | 10 | 14.0 | 9076 | 3.5 | 2309 | .013,(.142) | -x,(±y or ±z) |
| ΔV | 67:20 | 10 | 14.0 | 8936 | 3.5 | 2274 | .013,(.142) | -x,(±y or ±z) |
| RCS | 70:00 | 6 | 7.0 | 8894 | 2.0 | 2262 | .141 | ±y or ±z |
| ΔV | 70:20 | 540 | 14.0 | 1394 | 3.5 | 362 | .027,(.144) | +x,(±y or ±z) |
| RCS | 70:54 | 6 | 7.0 | 1352 | 2.0 | 350 | .141 | ±y or ±z |
| Start Reentry | 71:32 | † | 7.0 | † | 2.0 | † | 2.3 | +y |
| Full Reentry | 72:09 | † | 7.0 | † | 2.0 | † | 2.3 | +y |
| Transition | 72:20 | † | 7.0 | † | 2.0 | † | 1.75 | +y |
| T.D. | 72:34 | | | | | | | |

*The acceleration levels and directions enclosed by parenthesis are those resulting from an RCS maneuver superimposed on the regular ΔV maneuver which lasts for only 1 second.

†Specific duration times and propellant consumption schedule were not available for this three reentry maneuvers.

Legend:

x   Roll Axis,
y   Yaw Axis,
z   Pitch Axis.

+y

+x

+z
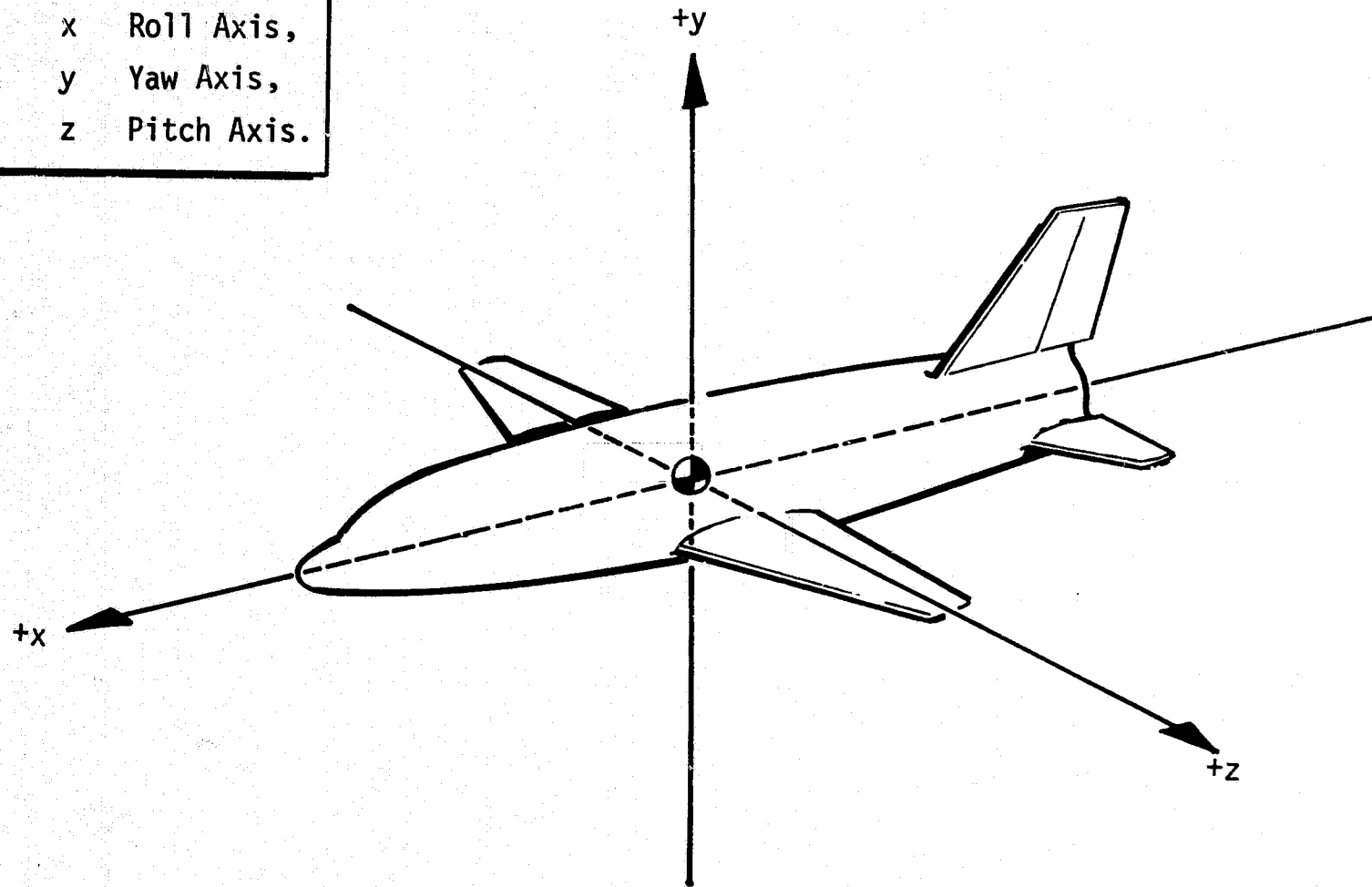
Figure V-2   Shuttle Orbiter Coordinate System

The vehicle coordinate system used to describe acceleration directions is shown in Fig. V-2. The highest vehicle accelerations are encountered during reentry. The reentry accelerations range between 1.7 and 2.3 g and always act approximately in the +y direction, tending to settle propellant in the -y direction. The $\Delta$V maneuvers accelerate the vehicle in the +x, $\pm$y, and $\pm$z directions at 0.027 g. An acceleration of 0.013 g results from $\Delta$V maneuvers in the -x direction. For ACPS maneuvers only, the acceleration on the propellant tanks is 0.14 g, acting either in the +y or $\pm$z direction. A 1-sec ACPS maneuver can occur during a $\Delta$V maneuver. When this occurs, the acceleration increases to 0.144 g for longitudinal $\Delta$V maneuvers and 0.16 g for lateral $\Delta$V maneuvers; these accelerations can act in either the +y or $\pm$z direction. Therefore, the lateral accelerations are approximately 5 to 6 times greater than longitudinal accelerations. This large difference is due primarily to both the location of the propellant tanks and the ACPS thrust levels. Both propellant tanks are located approximately on the x-axis and 50 ft from the vehicle center of gravity (the $LO_2$ tank is forward and the $LH_2$ tank is aft); this results in relatively large angular velocities and accelerations during ACPS maneuvers.

Two propellant management concepts were initially selected and evaluated for application to the orbital maneuvering propulsion system. Each concept was then modified as required. The two concepts selected were the DSL passive retention/expulsion system and a conventional propellant trap. The DSL concept would control both gas and liquid volumes in such a way that single phase fluid (either gas or liquid) could be expelled from the tank on demand. The propellant trap would control only the liquid and would require a thermodynamic vent system to satisfy both the propulsion system and the venting requirements.

After selecting these concepts, preliminary analysis and evaluation of each concept was conducted and modifications were made as required to satisfy the design criteria. Following any modifications, the operating characteristics were defined and preliminary system weights were calculated. A comparison of the two systems was made resulting in the selection of the best system. A qualitative evaluation was made on the effects of design criteria changes on the selected system.

B. MODIFIED DUAL-SCREEN-LINER SYSTEM

## 1. Description and Operating Characteristics

The basic DSL system evaluated in this study is shown in Fig. II-1. For this application, the liquid flow annulus to the outlet is formed between the two screens. Initially, the outer annulus is liquid; but, due to the incident heat flux at the tank wall, vaporization occurs causing pressure buildup which forces the liquid out of this annulus. This outer annulus becomes the gaseous volume in which subsequent pressure buildups occur due to heating and propellant vaporization from the liquid annulus. These pressure buildups can be relieved by venting directly from the outer annulus. Liquid outflow for propellant feed is provided from the inner liquid annulus which is fed by the bulk liquid region.

A preliminary evaluation was conducted to determine the feasibility of using the DSL in the orbiter propellant management system. The evaluation considered a complete DSL with 325 x 2300 mesh stainless steel screens in the $LO_2$ tank because it presents the most severe retention requirements. For this 10-ft-diameter tank, a liquid annulus gap of 1/2-in. was used. The calculations showed that approximately 10% of the liquid annulus volume could break down (capillary retention capability of the screen would be exceeded) under the highest lateral acceleration. This represents a maximum loss of approximately 110 $lb_m$ of $LO_2$ from the liquid annulus. During a 6-sec ACPS maneuver, the $LO_2$ requirement of 42 $lb_m$ cannot be satisfied if 110 $lb_m$ of $LO_2$ is displaced from the portion of the liquid annulus connected to the tank outlet. Under these conditions, the DSL would not meet the primary design requirement. For the hydrogen tank, the liquid annulus breakdown is not as severe because the same screen can retain approximately three times more hydrostatic head of $LH_2$. However, some breakdown in the liquid annulus would still occur in this 16.25-ft-diameter tank.

Following this evaluation, it became apparent that modifications to the DSL concept would be required to circumvent the problems described. The primary modification was directed toward eliminating breakdown in the controlled liquid volume which provides liquid outflow for propellant feed. Another modification that resulted was an increase in the controlled gas volume which is vented. These modifications resulted in the two designs shown in Fig. V-3 and V-4. Both designs have three spherical-screen compartments which provide gas-free liquid expulsion during all of the flight. Liquid is expelled from the small central compartment. This compartment is designed so that it remains gas-free until the total liquid volume becomes less than the compartment volume.

The dual feedline design is shown in Fig. V-3. Except during reentry, liquid is expelled from the central compartment through the feedline located approximately on the x-axis of the vehicle. During reentry, the screens will break down and liquid remaining in the tank settles over the reentry outlet and is expelled through the feedline, which is parallel with the y-axis of the vehicle. This axis corresponds to the approximate reentry acceleration vector.

The single feedline design is shown in Fig. V-4. For this design, the outer and middle screens are the same as those for the dual feedline design. The central spherical compartment, however, consists of a screen hemisphere and a thin-wall hemispherical dome with an outlet. This single outlet is parallel to the orbiter y-axis. During reentry, the liquid remaining is retained in the central compartment.

The operating characteristics for these two designs are essentially the same. Following boost and prepressurization, most of the liquid is contained within the outer screen. The outer controlled gas volume is equal to the initial ullage volume. When the first expulsion event is initiated, liquid flows out of the central compartment and pressurant gas enters the outer gas volume. The liquid contained within the outer screen will flow into the
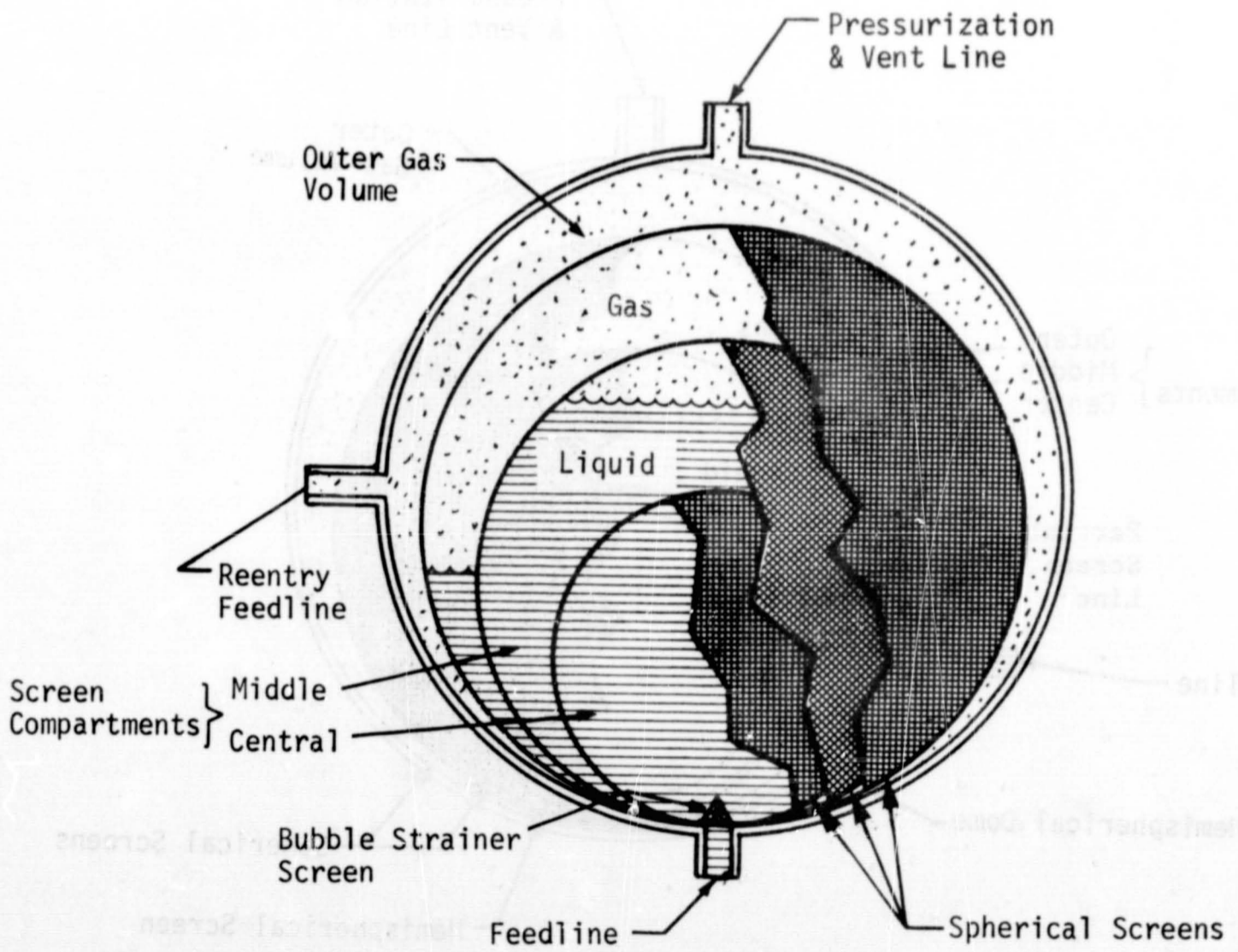
Figure V-3  Modified DSL Dual-Feedline Design

94
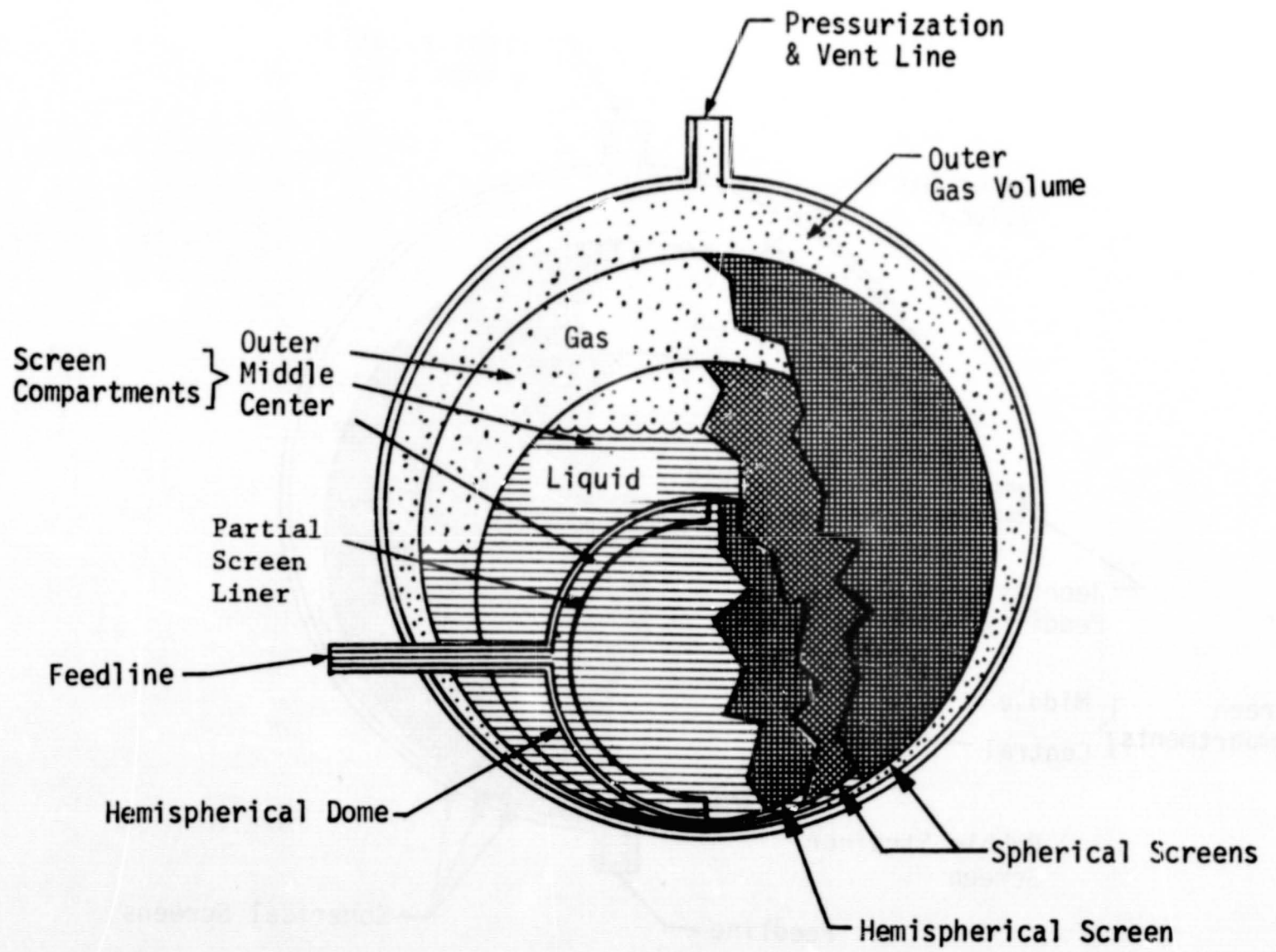


Figure V-4 Modified DSL Single-Feedline Design

middle compartment and then continue through the screen into the central
compartment. The liquid level in the outer screen compartment drops until
the liquid height in the middle screen compartment is greater than the retention
capability of the second screen. At this point, the second screen will break
down and outflow continues with the distance between the two liquid levels equal
to the retention capability of the second screen. Ultimately, the outer screen
will be emptied, and the liquid will then be contained within the second screen
compartment. During the maximum acceleration maneuvers, additional breakdown
of the second screen could result. If this occurs, then the liquid that can not
be retained by the second screen flows into the first screen compartment and is
retained. The breakdown in the second screen volume will continue until a
stable hydrostatic condition is reached, i.e., the distance between the two
liquid levels equals the static head which the screen can retain. The first
screen, therefore, reduces the amount of breakdown of the second screen.

If the outermost compartment contains any liquid, it will always empty
first since the pressure on that liquid during outflow is greater due to pressure
losses across the screens. The spherical screens are offset to minimize the
residuals in each compartment during outflow and retain the liquid at the
opposite end from the vent outlet during low-g coast periods. Venting for this
system is accomplished by expelling gas from the outer controlled gas volumes.

## 2. Analysis

The selection of screen mesh is a function of hydrostatic pressure difference,
static pressure reduction due to velocity and flow loss due to viscosity. Break-
down of a screen occurs when the retention capability of the screen is less than
the sum of these pressure differences. For this preliminary analysis, only the
hydrostatic pressure difference was considered because the other two pressure
differences are generally negligible. Hydrostatic pressure difference is equal
to $\rho ah$, where $\rho$ is liquid density, h is liquid height, and a is the acceleration
g-level. Due to the large diameter $LO_2$ and $LH_2$ tanks and relatively high

lateral acceleration levels, the hydrostatic pressure differences were relatively
large. This means that the retention capability of the screen had to be as large
as possible and Dutch twill screen, 325 x 2300 mesh, woven from stainless steel
wire was selected. This screen has a bubble point of about 26-in. of water
measured in alcohol, as discussed in Chapter IV.E. Inherent defects and possible
degradation due to fabrication were considered by reducing the bubble point to
20 in. of water for these designs. A bubble point with alcohol of 20 in. of
water is equivalent to a retention capability of 0.35 psi with oxygen and 0.06 psi
with hydrogen. For these pressure differences, the supportable hydrostatic heads
for the expected acceleration levels were calculated and are presented in Table
V-2. These data show that $LO_2$ retention is the more difficult case because the
screen can support a hydrogen hydrostatic head that is three times that of oxygen.

Table V-2   Supportable Hydrostatic Head vs Acceleration for 325 x 2300 Stainless
Steel Dutch Twill Screen

| Acceleration (a/g) | Liquid Oxygen Head (ft) | Liquid Hydrogen Head (ft) |
|---|---|---|
| 0.027 | 27.0 | 80.0 |
| 0.141 | 5.2 | 15.2 |
| 0.144 | 5.1 | 14.9 |
| 0.162 | 4.5 | 13.3 |
| 1.75 | 0.4 | 1.2 |
| 2.3 | 0.3 | 0.9 |

The criteria used in determining the diameters of the three screen
compartments for both designs were:

1) The volume enclosed by the outer screen compartment is equal to initial
   liquid volume;

2) The diameter of the middle compartment must be such that any liquid
   loss due to screen breakdown is small and can be retained by the
   outer screen. Also, the diameter must be small enough to keep liquid
   in this compartment always in contact with the central compartment;

3) For the central compartment, the volume must be twice the volume of
   liquid remaining before reentry (for the single feedline design), and
   the compartment diameter must be less than the minimum hydrostatic
   head, excluding reentry.

The compartment diameters were obtained using these criteria, the bubble point
data and the mission duty cycle. Determination of the outer and central
compartment diameters was straightforward. For the $LO_2$ tank, the middle

compartment diameter was based upon minimizing breakdown during the ACPS and
$\Delta V$ maneuvers before docking. The middle compartment diameter in the $LH_2$

tank was based on always keeping liquid in contact with the central compartment.
The calculated compartment diameters are presented in Table V-3.

A weight estimate was made for the complete propellant system including
screen, inner compartment dome (if any), and screen support weights. The
screen weights are based on data obtained from screen suppliers. For 325 x 2300
stainless steel screen, the approximate weight per unit area was given as
0.10 $lb_m/ft^2$. For the single outlet designs, the weight of the thin wall dome

was based on a 0.04-in. wall thickness. The spherical supporting structure
for the screens was assumed to be stainless steel tubing, 1/4-in. diameter
by 0.016-in. wall, which formed longitudinal and lateral ribs. In addition,
it was assumed that 2 ft of tubing was required to support 1 $ft^2$ of screen.
Using these assumptions and a tubing weight of 0.04 $lb_m/ft$, the support

weight was calculated. Total system weights are also presented in Table V-3.

Table V-3  Modified Dual Screen Liner System Sizes and Weights

| Tank | Spherical Screen Diameters (ft) | | | Spherical Screen Weights ($lb_m$) | | | Support Structure Weight ($lb_m$) | Total System Weight ($lb_m$) |
|------|-------|--------|-------|-------|--------|-------|------|------|
| | Outer | Middle | Inner | Outer | Middle | Inner | | |
| $LH_2$ (Single Outlet) | 13.1 | 10.7 | 6.88 | 53.9 | 36.0 | 38.5 | 77.8 | 206.2 |
| $LO_2$ (Single Outlet) | 9.0 | 7.0 | 4.25 | 25.5 | 15.4 | 14.7 * | 35.0 | 90.6 |
| $LO_2$ (Dual Outlet) | 9.0 | 7.0 | 4.0 | 25.5 | 15.4 | 5.5 * | 36.7 | 83.1 |

*Includes the weight of the thin walled stainless steel hemispherical dome.

### 3. Evaluation

Modification of the DSL system offers two designs that are capable of both expelling gas-free liquid and venting liquid-free gas for the baseline mission. Both the single and dual feedline designs are completely passive and have minimum complexity; they are low in weight and completely reusable. The operating characteristics of the two designs are essentially identical. The dual feedline design offers a small weight savings over the single feedline design. The single feedline design, however, does eliminate the complexity of an additional feedline, valve, and controls.

For this system, the control of the ullage and bulk liquid is entirely dependent on the ability of each screen to remain wet. Maintaining wet screens is a function of the wicking and capillary pumping capability of the screens. The type of screen selected for this design does have this capability. However, because the wicking rate of a screen is a function of length, the question that arises is whether the wicking rate for the large diameter is sufficient to keep the screens wet. No data are presently available to provide an answer.

The potential failure mode most evident for this system is the loss of liquid retention capability by drying out the outer screen that could result in venting some liquid. This potential problem is more pronounced with the outer screen because of its location and larger diameter. The central compartment does not present a retention problem because of its smaller size and because it is completely surrounded by liquid during most of the mission.

There are additional ways in which the outer screen could lose its liquid retention capability. If the pressure in the outer gas volume is less than the pressure plus hydrostatic head in the first screen compartment, then liquid will flow into the outer compartment until a new stable condition is reached. Pressure drops that could cause breakdown of the outer screen can occur by rapid venting and rapid cooling of the gases following a hot gas pressurization. The low venting rate anticipated for this duty cycle should not cause breakdown. Using a cold gas pressurant would circumvent both the pressure drop following pressurization and drying out of the screen due to hot gas impingement.

If breakdown of the outer screen should occur, the system is designed so that the liquid is retained at the end opposite the vent outlet. By offsetting the screens, the minimum surface area for the outer compartment is away from the vent outlet. In a low-g environment, liquid will tend to flow and orient itself inside a tank in the minimum liquid/vapor interface area configuration.

### C. MODIFIED TRAP/FEEDER-ARM SYSTEM

### 1. Description and Operating Characteristics

A propellant trap was investigated as a means of providing retention of the propellant within the tanks of the STS orbiter. The operation of a simple propellant trap depends on the settling of propellant over the outlet during outflow and a rather well defined mission profile. For these reasons, a trap by itself would not be adequate; but, by adding feeder arms to the trap, a

Liquid Flow Passage ⟍      Feeder Arm Wall

Gas and/or Liquid Region ⟍      Inner Screen

Standoff ⟍      Outer Screen

|← 8" →|      Tank Wall

Section A-A

Feeder Arms (8)

Manifold/Trap

Feedline
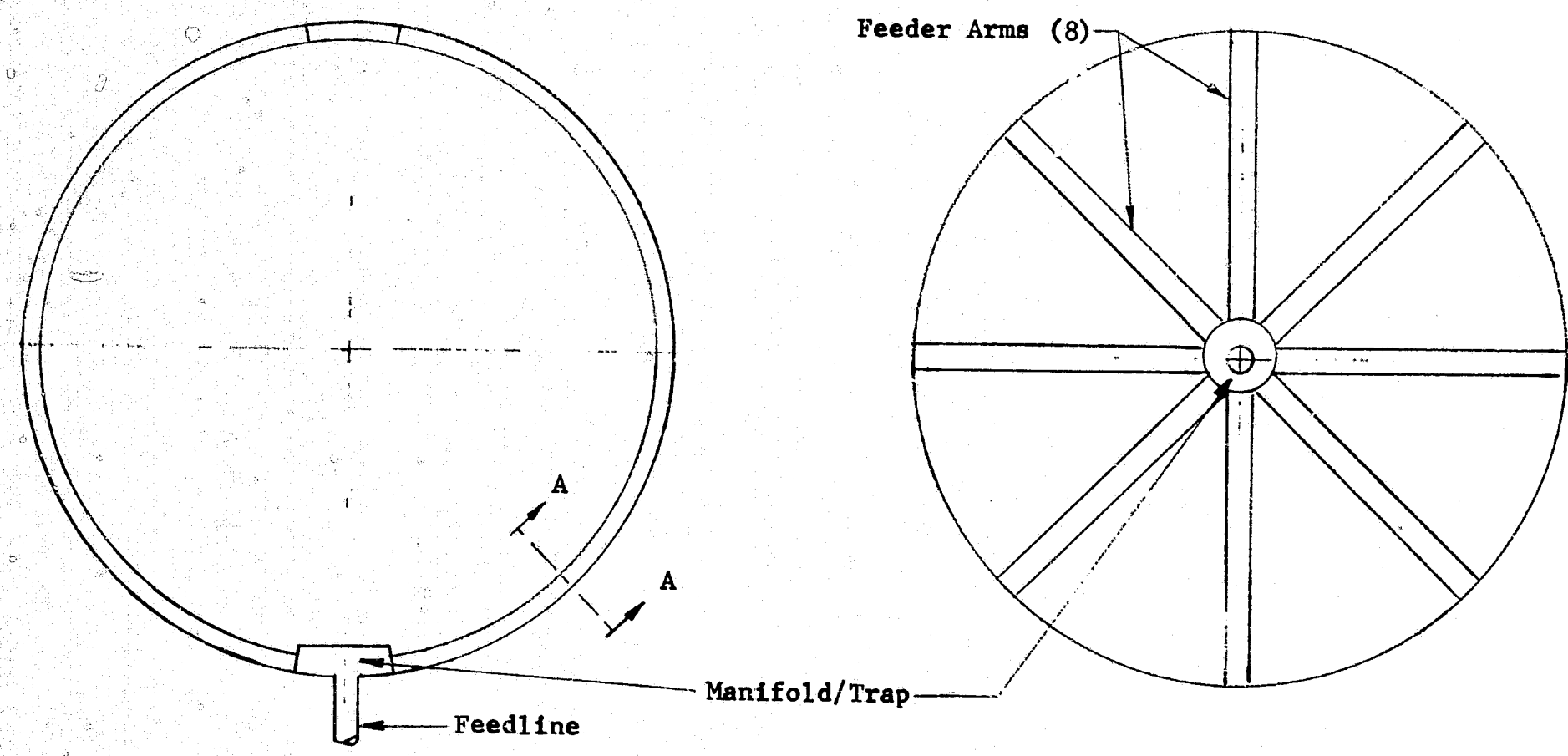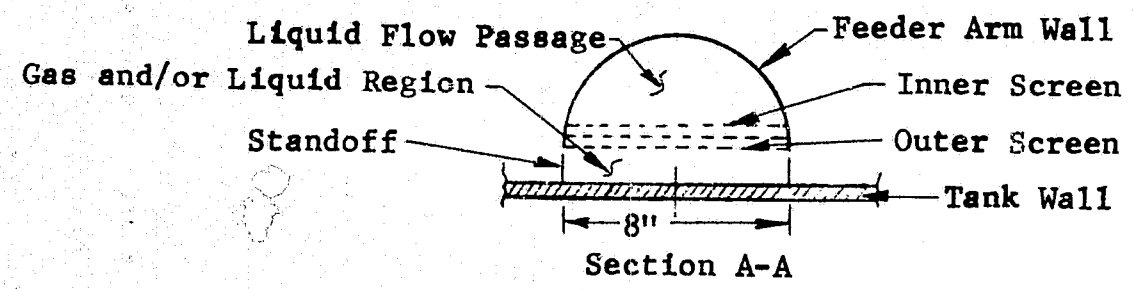
Figure V-5  Modified Trap/Feeder-Arm System

device that could meet the mission requirements is obtained. The configuration of this device is shown in Fig. V-5.

The trap serves as a manifold for the eight feeder arms at the tank outlet. A communication path between the propellant, regardless of its orientation within the tank, and the trap is provided by the feeder arms. By having eight arms, at least one arm will always be in contact with liquid. In addition, a single arm is capable of meeting the propellant demand.

Successful operation of the feeder arms depends on their remaining full of liquid while the orbiter is operating in space. During boost and reentry, the arms will not remain full of liquid. This is not a problem during reentry because the tank is oriented such that the liquid will settle over the outlet. At this point, supply of propellant would not longer depend on the surface tension device.

After the boost phase and before the first propellant expulsion requirement, the feeder arms must refill with liquid. Under low-g conditions, liquid will tend to flow into the arms due to capillary forces, but gas within the arms must be vented. A vent port that would remain open until the arms are completely full of liquid would provide this capability.

During the remainder of the mission, liquid would be retained in the arms by the layers of screen on the underside of each arm. Whenever propellant is required, it flows through the screens into the arms, along the arms into the trap and out the feed line.

Selection of the screen used for the feeder arms depends on the maximum pressure difference that could occur between the liquid in the arm and gas outside the arm, exclusive of boost and reentry as previously discussed. A preliminary analysis indicates that a single screen is not adequate. The pressure retention capability of the finest screen available is less than the maximum pressure difference. It has been shown that the retention capability of foraminous materials placed in parallel is nearly the sum of their individual bubble points (Ref V-1). In this case, two parallel screens are required for the hydrogen tank feeder arms and three parallel screens are required for the arms of the oxygen tank.

Breakdown of the single outer screen exposed to gas can occur, but when this occurs the pressure differential across the remaining layers of screen is reduced by the bubble point of the screen that broke down. By this mechanism, one or more screens can break down until the pressure differential can be supported. The inner screen should not break down, retaining only gas-free liquid in the flow passage of the feeder arms.

### 2. Analysis

A detailed analysis of the pressure losses within the feeder arms is required before the final screen configuration is selected. For the purposes of this study, it was assumed that the hydrostatic head is the primary

contributor to the pressure difference. Other contributions to the pressure difference are inherently small or can be made small through proper design. The flow area per arm is large enough (approximately 0.17 $ft^2$) to minimize pressure losses due to liquid flow along each arm. The screen area per arm is approximately 16.5 $ft^2$; with this area, the loss due to flow through the screen should be small.

A worst-case condition is imposed by the ACPS maneuver that occurs just before reentry. Under this condition, the propellant volume will be a minimum and the screen will be required to support the maximum hydrostatic head. At this time, the pressure differential due to hydrostatic head will be approximately 0.6 psi for the oxygen tank and 0.08 psi for the hydrogen tank. Dutch twill stainless steel screen, 325 x 2300 mesh, was also selected for this system. A comparison of the screen bubble point and the hydrostatic pressure differences establishes the number of layers of screen required for the arms. Three layers are necessary for the oxygen tank, making allowance for other pressure losses in addition to the hydrostatic head, and two layers should be adequate for the hydrogen tank.

The preliminary analysis also included an assessment of total system weight. This weight includes the weights of screens, manifolds, feeder arms, and the vent heat exchanger system. The vent heat exchanger weight must be included to make a realistic comparison between this system and the modified DSL system. The weight of screen was calculated by the previously mentioned approach. For this preliminary design, the arms and manifold were considered to be constructed of stainless steel having a wall thickness of 0.05 in.

A preliminary heat exchanger analysis was conducted to estimate the weight of the tubing mounted in a continuous spiral fashion on the external surface of each tank. Aluminum tubing, 1/4-in. diameter x 0.030-in. wall, having a weight per unit length of 0.025 lb/ft was assumed. The heat flux into each tank was assumed to be 0.5 Btu/$ft^2$ hr. Using the techniques outlined in Ref V-2, the tube spacings were estimated to be 16 and 20 in. for the $LO_2$ and $LH_2$ tanks, respectively. These spacings gave tube lengths of 243 ft for the LOX tank and 532 ft for the $LH_2$ tank. The $LO_2$ and $LH_2$ tank heat exchanger weights were calculated to be 6.1 and 13.3 $lb_m$, respectively. Total system weight for each tank is presented in Table V-4.

Table V-4  Modified Trap/Feeder-Arm System Mass Estimates

|  | $LO_2$ Tank | $LH_2$ Tank |
|---|---|---|
| Trap (Top and Bottom Manifolds) | 17.8 | 17.8 |
| Feeder Arms | 164.7 | 268.0 |
| Screens | 19.0 | 20.4 |
| Heat Exchanger Tubing | 6.1 | 13.3 |
| Total System | 207.6($lb_m$) | 319.5($lb_m$) |

### 3. Evaluation

This surface tension device provides a relatively simple means of providing for the acquisition and expulsion of gas-free liquid propellants. It is relatively lightweight and does not restrict the flexibility of the spacecraft, since it can be designed to function for any flight profile. No modifications to the propulsion system would be required in order to accommodate the device.

The system has some difficiencies that became apparent during this analysis. One of the more complicated design problems is the vent that allows the feeder arms to refill following boost. The vent must be located on the arm so that it is at the point last to fill and it must not significantly degrade the retention capability of the arms. One approach is to keep a small section of screen dry while the arms refill.* When the arms are completely full, the screen would wet and seal the vent. However, the motion of the liquid must be predictable and the dry section of the screen must be isolated from premature wicking and propellant slosh.

Another problem is the ingestion of gas into the spaces between the screen layers. Whenever a single layer of screen breaks down, gas will be drawn into the space between the screens; there is no means of venting the gas from this space. Each time a screen breaks down, more gas will be ingested. If the space should completely fill with gas, liquid will not be able to flow into the arms. An evaluation must be accomplished to determine the maximum amount of gas which could be ingested into these spaces. The analysis should also determine if the gas ingestion will result in a flow restriction such that the flow rate of liquid out of the tank is reduced.

An additional disadvantage of this device is that it does not provide for the direct venting of gas from the tank. There is no point in the tank at which liquid-free gas would be available for venting. Venting would have to be accomplished using a thermodynamic vent (venting liquid through a heat exchanger mounted on the tank wall). This vent heat exchanger must be considered as a contribution to the weight of the device, and its effect on the reliability of the system must be considered.

### D. CONCEPT COMPARISON AND SELECTION

The preliminary analysis and evaluation of both candidate concepts indicates that both are capable of satisfying the mission design requirements. To select the best system, a comparison of the modified trap and feeder arm system with the modified DSL system was made. The comparison considered significant performance and design problems, system failure modes, system complexity, and system weight. Any additional areas for comparison, such as reliability, cost, component availability, etc, were considered to be beyond the scope of this study.

---

* Perforated plate and square weave screen are possible material candidates, based on the non-wicking characteristics discussed in Ref V-1.

The modified trap/feeder arm system has one significant design problem that has to be solved and another potential problem that should be investigated. As described in the last section, this system has the problem of refilling the feeder arms following the gas ingestion during the boost phase. A problem could exist when the outer screen breaks down and the ingested gas is trapped between the outer and inner screens. If the volume of gas between the screens increases, the liquid flow area into the flow passage could be reduced. This could result in a reduction of the outflow rate followed by gas ingestion into the flow passage. Solutions to both problems would require significant detailed analysis and design effort.

The modified DSL system has only one potential problem; this is the possibility of the outer screen losing its liquid retention capability that could result in the venting of some liquid. This is the only apparent failure mode for this syst . because the central compartment is capable of expelling gas-free liquid under all the expected flight conditions.

The modified trap/feeder arm system is more complex than the modified DSL system. It requires a vent heat exchanger system and also additional components, possibly a valve, to refill the arms following boost.

A weight comparison clearly favors the modified DSL over the modified trap/feeder arm system. The $LO_2$ and $LH_2$ modified DSL systems have weights savings of 117 and 113.3 $lb_m$ respectively, over the modified trap/feeder arm systems. This represents 90 and 35% weight reductions for the $LO_2$ and $LH_2$ systems, respectively. Based on these comparisons, the modified DSL system is the better propellant management system.

### E. EFFECT OF MISSION DUTY CYCLE AND DESIGN CRITERIA CHANGES

The selected expulsion system was designed for a specific mission duty cycle and design requirements. Any changes in either duty cycle or design requirements would affect the system design. There is flexibility in the design, and small changes in duty cycle or design requirements may not affect the system performance. In general, however, the specified propellant management system design would require some modifications for any changes to obtain an optimum system.

Because this is a preliminary design effort and the selected orbiter configuration and duty cycle were arbitrary, several mission duty cycle and design parameters are subject to change. The four parameters having the greatest effect on the expulsion system design are acceleration levels, tank volume, propellant load, and propellant outflow schedule. Of these four parameters, the acceleration level is the most important. For the selected orbiter configuration, the acceleration profile could be altered considerably not only by changing thrust and system mass but also by changing location of the propellant tanks. Increasing the acceleration levels (considered unlikely) would have the most adverse effect on the design. This change could possibly result in additional screens for additional retention capability that would

increase the system weight. Decreasing the acceleration levels results in an opposite effect, i.e., less screens are required thereby reducing system weight. Any reduction in the lateral acceleration levels, considered as unduly high, would also reduce the complexity of the system.

An increase or decrease in tank volume would result in a corresponding change in expulsion system size. Changes in the propellant load could occur without change in the tank volume because an initial ullage of 30% was considered in the design; however, changes in the expulsion system could result. These changes cannot be evaluated without also considering change in the outflow schedule to which the design is also sensitive. For example, if the outflow schedule is changed such that the amount of propellant remaining before docking is increased, the outer screen could break down, forcing liquid into the outer volume. The central compartment is sized so that the compartment volume is approximately twice the volume of liquid required for reentry. Any additional liquid remaining at this time would not be retained within the central compartment and might not be expelled.

## VI. FORMULATION OF TEST PROGRAM

One of the tasks under this program was to formulate a plan for testing the DSL to provide verification of the concept in as many test modes as possible. Thus, bench tests, drop tower tests, and KC-135 aircraft tests have been considered to help determine the capillary system capability of the DSL. Note that these tests are aimed at determining and verifying capillary system performance and are not intended as operational tests of a prototype of a real cryogen tank. The actual tests in the various test modes will be dictated by the requirement to show the DSL can indeed:

1) Provide liquid-free vapor venting;

2) Provide vapor-free liquid draining;

3) Provide near-continuous control of the liquid in the bulk region.

All tests will be performed with $LN_2$ at a storage pressure of one atmosphere. The following paragraphs will briefly discuss the three test modes. Details are presented in Martin Marietta Report MCR-71-38 (Ref VI-1) submitted in February 1971 as part of this contractual effort.

### A. ONE-G BENCH TESTS

During this phase of testing, consideration will be given to investigating all the parameters we now feel are important for the operation of the DSL. Simple tests such as vapor-free liquid outflow, vapor venting, and bubble point check will be made to assure the basic concept feasibility. Because of the relatively large hydrostatic heads and heat transfer rates in the 1-g environment, bench tests present certain operational difficulties that have been experienced in an earlier IR&D test program with $LN_2$ in a cylindrical tank (Ref VI-2). For example, liquid trapped in a vent line vaporized and the pressure increase forced liquid out of a capillary controlled region. The need to support a relatively large hydrostatic head (with a safety factor of 2.0) has dictated the sizing of the subscale model, as will be discussed in the following chapter. The bench tests will also give an indication of the extent and sensitivity of the control system necessary to provide near continuous control of the bulk region.

A matrix of test conditions will be simulated to investigate such things as:

1) Outer annulus pressurization;

2) Bulk region pressurization;

3) Liquid outflow to depletion;

4) Sensitivity of vent control;

5) Selective rapid venting (liquid fallout);

6) Large heat input rates (screen breakdown);

7) Operation of communication screen in control of venting;

8) Feasibility of manual and/or automated control functions;

9) Continuous vapor venting from the outer annulus.

## B. DROP TOWER TESTS

It is desirable to make several relatively inexpensive drop tests to assure equipment function during periods of low-g operation. Of particular interest are the control requirements needed to obtain meaningful data during the short low-g test periods. Emphasis will be placed on system checkout for the somewhat longer low-g test times available in the KC-135 aircraft.

## C. KC-135 AIRCRAFT TESTS

The emphasis during this phase of testing will be to demonstrate that the passive DSL can indeed outflow vapor-free liquid, vent liquid-free vapor, and provide propellant control during the low-g test period available. In addition, based on the earlier test data, it may be desirable to investigate such things as selective rapid venting where the vent is positioned to take advantage of a known acceleration vector and the bulk fluid is dropped out of the bulk fluid control region. These phenomena have been investigated for $LH_2$ in drop tests conducted by Martin Marietta under Contract NAS8-11328 (Ref VI-3).

## VII.  TEST ARTICLE DESIGN AND FABRICATION

As discussed in Chapter II, the DSL concept was selected as the basic capillary system design for this program.  To verify the concept, a subscale passive retention/expulsion DSL system was designed and fabricated to accomplish the test program presented in Chapter VI.  The design considerations, design details, and fabrication and assembly methods of the subscale DSL system are presented in this chapter.

### A.  DESIGN CONSIDERATIONS

The primary objective of designing and fabricating the subscale DSL passive retention/expulsion system was to provide system design verification when subjected to 1-g bench, drop tower, and KC-135 aircraft testing, as discussed in Chapter VI.  Weight optimization of the system was not a primary objective. The following considerations and requirements were used in the design.

The cryogenic storage system was to be composed of a low heat-leak storage tank containing the passive retention/expulsion system.  Both gas-free liquid expulsion and liquid-free, nonpropulsive, vapor venting were to be provided. The cryogenic storage system was to be similar to the standard 10-liter $LO_2$ converter used by the Air Force and was to be designed for testing with $LN_2$ at a storage pressure of one atmosphere.  Maximum design operating pressure of the storage tank was to be 100 psia and provisions for rapid pressure buildup were to be included.

The cryogenic storage system and DSL system were to be designed, to withstand the drop tower deceleration loads and the KC-135 aircraft g-loads.  Stable retention of $LN_2$ over the range of accelerations as specified in the test program was to be provided by the DSL system.  As discussed in Chapter VI, the test program acceleration range is from -1 to +1 g. A design safety factor on stability of 2.0 was to be used.  The range of liquid expulsion flow rates was to be consistent with these requirements.

### B.  DSL SUBSCALE DESIGN

Details of the system design are shown in Fig. VII-1 and VII-2.  The 3.82-liter $LN_2$ storage tank is contained by an 18-in.-diameter vacuum jacket sphere.  The DSL passive retention/expulsion system is positioned inside the storage tank, and two 124 ohm electrical heater blankets encompass the storage tank wall barrel section to provide a heating capability up to 200 w with a 110-v power supply.  Each separately controlled heater covers one-half of the tank barrel section.  The storage tank and heaters are insulated with multilayer insulation (MLI) comprised of 20 layers of Mylar aluminized on both sides with each layer separated by nylon netting.  Eight support rods attach and position the storage tank to the vacuum jacket.  A combined vacuum pumpout/pressure relief valve is incorporated in the vacuum jacket wall.  The system is constructed of 300-series stainless steel.
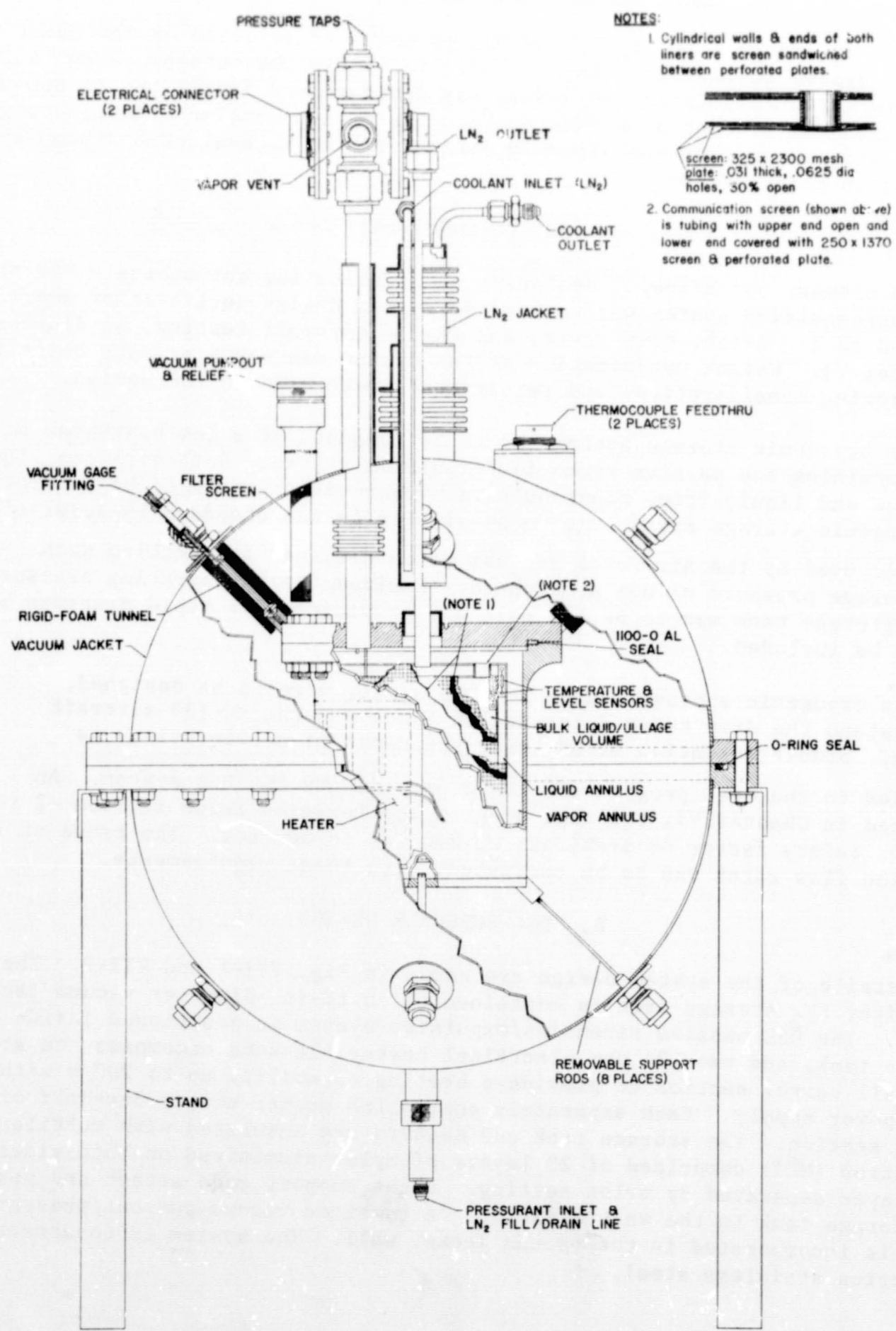
Figure VII-1  Cutaway View of Subscale DSL Passive Retention/Expulsion System

Figure VII-2   Subscale DSL Passive Retention/Expulsion System Detail Design

A 1/4-in. line from the bottom of the $LN_2$ storage tank is provided for evacuation, $LN_2$ fill and drain, pressurization, and as an alternate vapor vent line. The $LN_2$ outflow line and the regular vent line for the vapor are connected to the top of the $LN_2$ storage tank. The 1/2-in. $LN_2$ outflow line is connected to the DSL liquid annulus and has a $LN_2$ jacket starting just

above the top of the storage tank and extending through the vacuum jacket. The 3/4-in. vent line duct connects to the DSL vapor annulus and also extends through the vacuum jacket. This duct contains electrical leads to sensors located within the storage tank and 1/16-in. pressure-tap lines to the vapor annulus and the bulk liquid/vapor region. It also allows gas venting through a 1/4-in. gas vent line which leads from the duct after it passes through the vacuum jacket. This gas vent line can also be employed for pressurization.

## 1. Operational Characteristics

Retention and expulsion of cryogenic liquid in an adverse 1-g environment, coupled with vapor venting, presents a stringent requirement on the design of a capillary retention system. The g-level is from one to five orders of magnitude higher than usually presented by the actual low-g operational environment.

The capillary retention capability of a circular pore is given by

$$\Delta P_c = \frac{2\sigma}{R} \cos\theta, \qquad \text{(VII-1)}$$

where $\Delta P_c$ is the capillary pressure difference across the liquid/gas interface in the pore, $\sigma$ is the liquid/gas surface tension, R is pore radius, and $\theta$ is the liquid-to-solid contact angle. Considering static retention only, the small $\Delta P_c$ must offset the liquid hydrostatic head for stable retention:

$$\Delta P_c \geq \rho ah, \qquad \text{(VII-2)}$$

where $\rho$ is liquid density, a is the acceleration level, and h is the hydrostatic head. Combining Equations (VII-1) and (VII-2) and solving for the supportable hydrostatic head,

$$h \leq \frac{2\sigma \cos\theta}{\rho aR}. \qquad \text{(VII-3)}$$

For a given liquid, it is seen that the supportable hydrostatic head varies inversely with the acceleration level-pore radius product. Under low-g conditions, even relatively large pores will support a considerable hydrostatic head. However, the hydrostatic head supportable in a 1-g environment is limited to relatively low values with pore sizes that are both available and practical. From these considerations, it is seen that 1-g testing places a very stringent requirement on a capillary retention system. This requirement becomes even more severe when the dynamics associated with expulsion are considered, as discussed on page 56.

The design of the subscale DSL was dictated by:

1) The requirement for stable retention of $LN_2$ in a 1-g environment with a safety factor of 2.0 on stability;

2) The pressure retention capability of fine mesh screen;

3) Fabrication considerations;

4) The necessity of providing a reasonable pressure-band for vapor venting.

Fluid properties used in the design were established by the requirement of testing with $LN_2$ at a storage pressure of one atmosphere.

To support the maximum $LN_2$ head in 1-g, and, thereby, provide a storage system of reasonable size, 325 x 2300 Dutch twill stainless steel screen was selected for the DSL prototype. This is the finest mesh screen readily available from screen suppliers in this country. Using a safety factor of 2.0 on the measured bubble point of this screen (Table IV-5) resulted in a design BP of 13 in. of water measured in methanol. This translates into a BP of 5.15 in. of $H_2O$ in $LN_2$, which converts to a supportable $LN_2$ head of 6.4 in. since:

$$( \rho ah)_{LN_2} = ( \rho ah)_{H_2O}. \qquad \text{(VII-4)}$$

Therefore, the maximum height of $LN_2$ to be supported in the axis of Earth's gravity vector was 6.4 in. Physical properties of nitrogen, used in the design, are presented in Table VII-1.

Table VII-1   Properties of Nitrogen at $140^{\circ}R$

| Surface Tension($lb_f$/ft) | $0.615 \times 10^{-3}$ |
|---|---|
| Density ($lb_m$/ft$^3$) | |
| Liquid | 50.4 |
| Vapor | 0.287 |
| Viscosity ($lb_m$/ft-hr) | |
| Liquid | 0.39 |
| Vapor | 0.013 |

In addition, the surface tension of methanol was taken as $1.55 \times 10^{-3}$ $lb_f$/ft and the density of water as 62.4 $lb_m$/ft$^3$.

Because the primary objective in designing and building the subscale system was to provide a test article for verifying the DSL concept, a simple cylindrical geometry was selected. Present technology for forming and fabricating compound curvature screen systems results in a lowering of the screen bubble point; this BP decrease becomes significant for small screen systems on the order of 6 to 12-in. diameter. To circumvent unnecessary fabrication problems that could result in a size reduction from 6.4 in., the more easily fabricated cylindrical screen configuration with flat ends was selected.

To maintain the subscale DSL as large as possible, the liquid annulus width was selected to provide negligible flow losses. This width was increased at the top and bottom of the cylinder to decrease the head support requirement on the communication screen. The resulting dimensions for the DSL are shown in Fig. VII-3. As discussed previously in Chapter II, the communication screen provides a preferential path for gas breakthrough into the bulk storage region rather than into the liquid annulus. With 325 x 2300 Dutch twill screen liners, the next larger pore size screen, 250 x 1370 Dutch twill (Table IV-5), was selected for the 0.5-in. diameter communication port. This selection provides a pressure-band for vapor venting of up to 0.12 psi which is the difference between the 0.18 psi required to support the 6.4-in. $LN_2$ hydrostatic head and the communication screen bubble point of 0.30 psi in $LN_2$. The 0.12-psi pressure band is reasonable to demonstrate liquid-free gas venting since differential pressure sensors are available in this range.

The analysis of vapor annulus pressure decay during venting of the DSL, presented in Chapter IV, was used to size the vapor annulus gap width. Because the system was to be controlled manually, a vent duration of at least 10 sec was selected. The test article heat flux was estimated to be on the order of 2 Btu/hr-ft$^2$. Using these values with the 0.12-psi vent pressure-band resulted in a q$\theta$/$\Delta$P of 167 Btu-sec/hr ft$^2$-psi. The vapor annulus gap size, $\Delta$R, was then selected using the information presented in Fig. II-13. With a K of 1.2, $\Delta$R must be 0.1 in. and the total vent-cycle time would be 22 sec; with a K of 2.0, would be 0.5 in. and vent-cycle time would be 30 sec. A long vent-cycle time was desirable; however, the small-size system, dictated by the 1-g test requirement, resulted in $\Delta$R = 0.5 in. being the largest practical gap width that could be considered. For this reason, a 0.5-in. gap width was selected for the vapor annulus (vent valve open 10 sec and closed 20 sec).

Six-inch diameter, Schedule 10 stainless steel pipe was selected for the $LN_2$ storage tank. This approach led to the system dimensions shown in Fig. VII-3. A summary of the DSL subscale system design is presented in Table VII-2. Maximum $LN_2$ outflow rate for the subscale systems without gas ingestion is approximately 0.1 lb$_m$/sec or 0.9 gpm.

## 2. Computer Simulation of Subscale Design

A computer simulation was made, in conjunction with the capillary design effort for the subscale tank, to estimate the operational characteristics of such a system. Pressurization, outflow, and venting under a 1-g acceleration
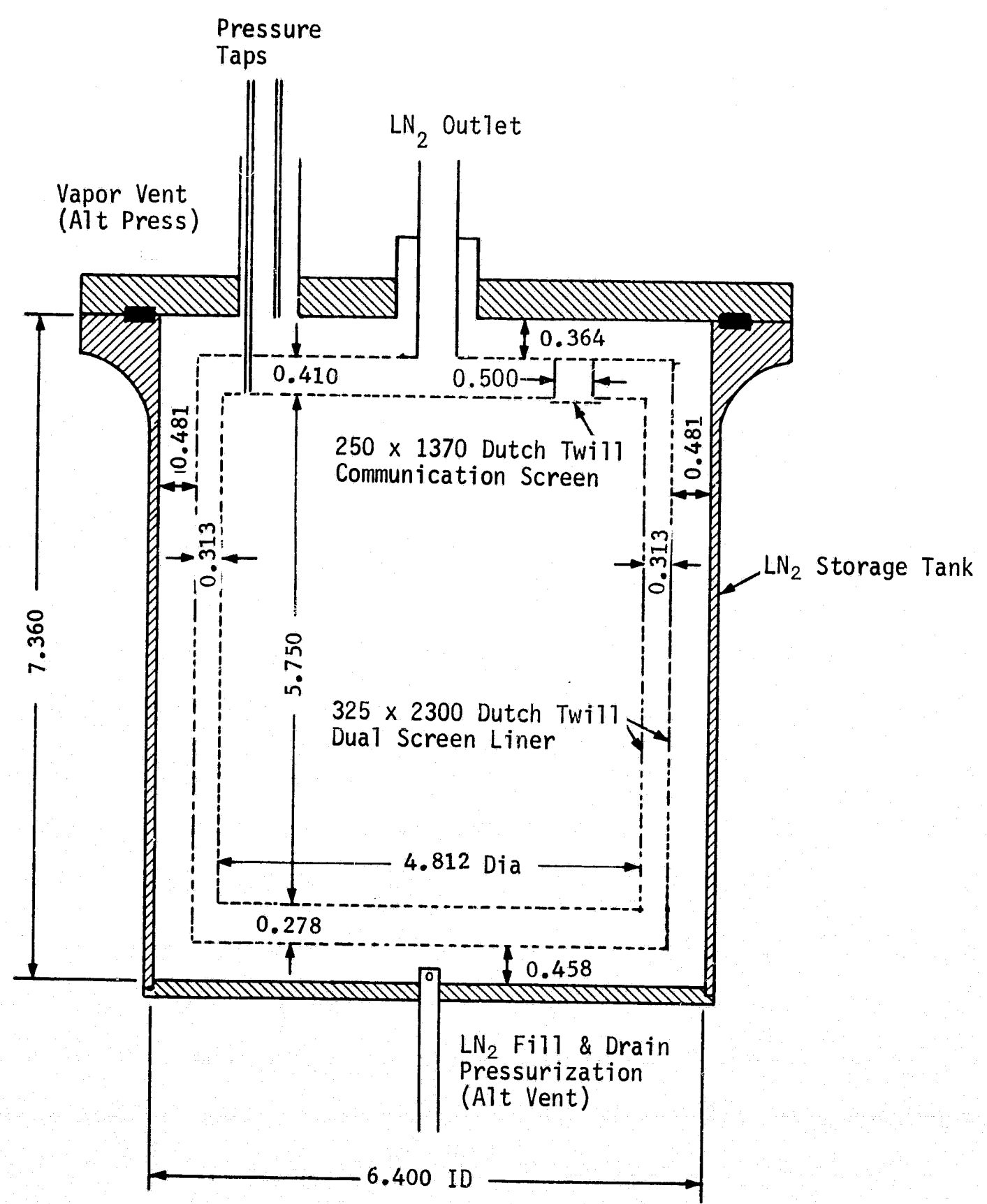
Figure VII-3  Subscale DSL Dimensions

Table VII-2  DSL Subscale System Design Summary*

| | |
|---|---|
| $LN_2$ Storage Tank | |
|     Volume ($ft^3$) | 0.1371 |
|     Internal Dimensions (in.) | |
|       Diameter | 6.400 |
|       Length | 7.360 |
| | |
| Vapor Annulus | |
|     Volume ($ft^3$) | 0.0503 |
|     Attachment Volume ($ft^3$) | 0.0035 |
|     Effective Volume ($ft^3$) | 0.0538 |
|     Effective Gap Width (in.) | 0.507 |
| | |
| Liquid Annulus | |
|     Volume ($ft^3$) | 0.0266 |
|     Effective Gap Width (in.) | 0.330 |
| | |
| Bulk Liquid/Vapor Region | |
|     Volume ($ft^3$) | 0.0602 |
|     Diameter (in.) | 4.812 |
|     Length (in.) | 5.750 |
| | |
| Dual-Screen Liners | |
|     Screen Material | |
|       Mesh | 325 x 2300 |
|       Weave | Dutch Twill |
|     Outer Liner (in.) | |
|       Diameter | 5.438 |
|       Length | 6.438 |
|     Inner Liner (in.) | |
|       Diameter | 4.812 |
|       Length | 5.750 |
| | |
| Communication Screen | |
|     Screen Material | |
|       Mesh | 250 x 1370 |
|       Weave | Dutch Twill |
|     Diameter (in.) | 0.500 |

*Material = 300-Series stainless steel.

were simulated to determine pressure and temperature profiles for each of the fluid regions in the tank. An operational heat flux of 0.75 Btu/hr ft$^2$ was employed. Thus, the pressure rise rate for the 1-g subscale test simulation is greater than for the low-g simulation presented earlier due, in part, to the small tank size, large vapor gap-to-tank diameter ratio, and a greater heat flux.

A 1-g simulation of the subscale cylindrical tank with a complete DSL is shown in Fig. VII-4 for a 1-hr time period. The upper portion of the figure shows the pressure rise rate in both the vapor annulus and the bulk ullage region. This particular venting scheme is similar to the low-g case wherein the vent is opened during each cycle before the communication screen is broken down, thus preventing vapor from moving from the outer annulus to the bulk region. This is but one of several operational vent schemes that will be investigated during the 1-g test program. Temperatures in the various tank regions of the subscale model are also shown in Fig. VII-4. The temperature at the outer screen is assumed to be at saturation corresponding to the partial pressure of the propellant vapor in the outer annulus. The saturation temperature line shown in the figure corresponds to the partial pressure of propellant vapor in the bulk fluid region. As shown in the figure, the bulk liquid temperature has risen approximately 1/4°R in the 1-hr time span, but still exhibits some subcooling.

Tank pressurization followed with propellant outflow by blowdown of tank pressure for the subscale configuration is shown in Fig. VII-5. Pressure increase as a function of time is shown for both the outer annulus and the bulk ullage region, with the pressure in the outer annulus remaining higher than the bulk pressure by the pressure drop through the communication screen. The tank was pressurized to 50 psia with cool helium (400°R) at a rate of 0.2 lb$_m$/hr. After holding at this pressure for a short time, the tank was outflowed to depletion at a rate of 1.5 ft$^3$/hr.

A regulator type pressurization system can also be simulated with the computer program. The bulk ullage pressure is compared to the regulator setting to determine if pressurant should be added. The pressurant enters the vapor annulus and is diffused to prevent direct impingement on the screen. As in the previous case, the communication port limits the pressure differential between the vapor annulus and the bulk ullage to its bubble point. Using this approach, a simulation for the subscale model was made where the tank was pressurized to 30 psia by cool helium and then regulated to maintain that pressure during the remainder of the run. The results are shown in Fig. VII-6. At 0.01 hr after pressurization was initiated, a constant liquid withdrawal of 1.5 ft$^3$/hr was begun. A line representing percentage of liquid remaining from 100% full to tank empty, is shown with the 0% point representing the situation where the bulk region has been depleted but the liquid annulus region is still filled with liquid.

### 3. Structural Design

The subscale system design, presented in Fig. VII-1 and VII-2, provided for the structural loads to be expected from (1) the pressure in the LN$_2$ storage

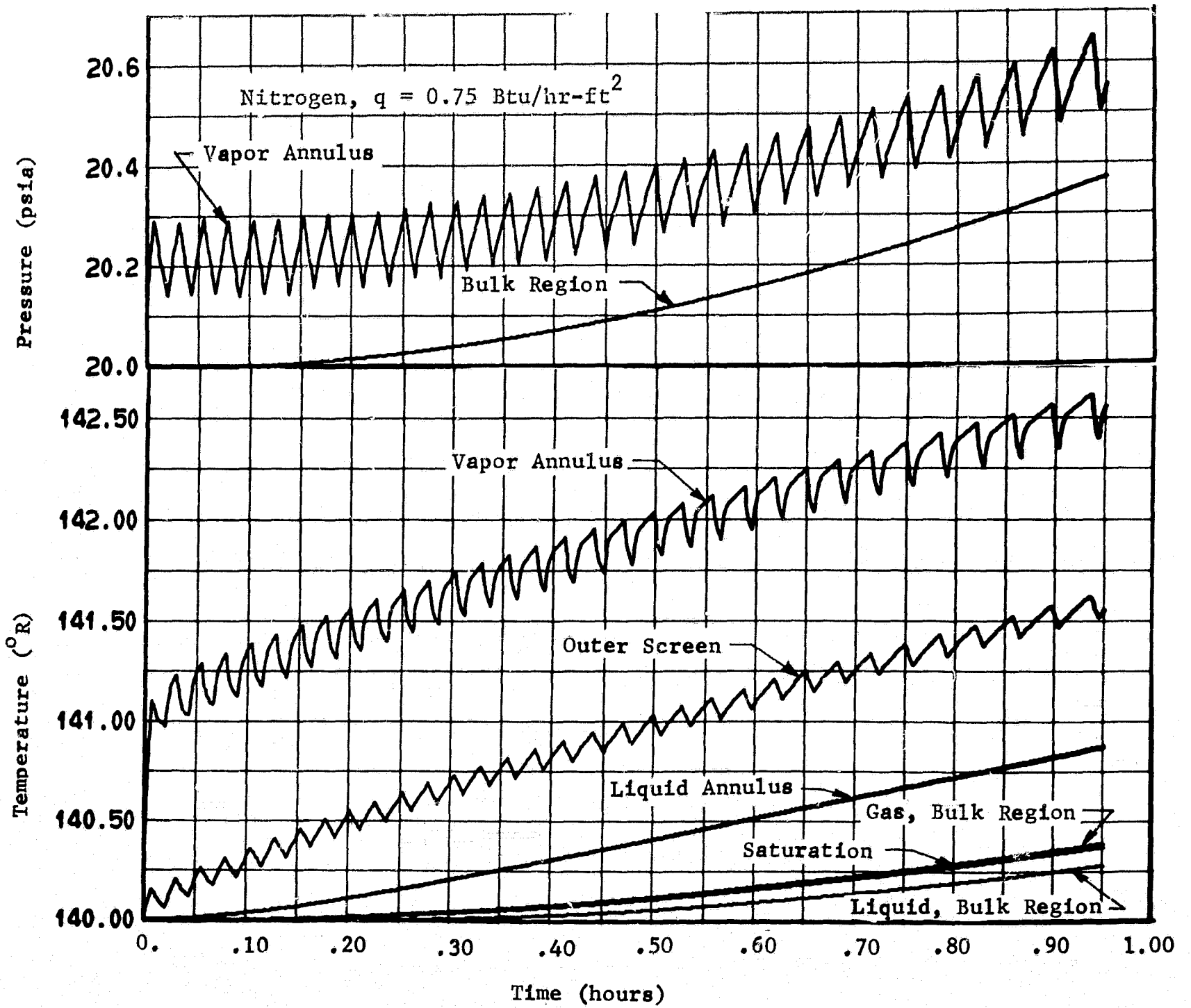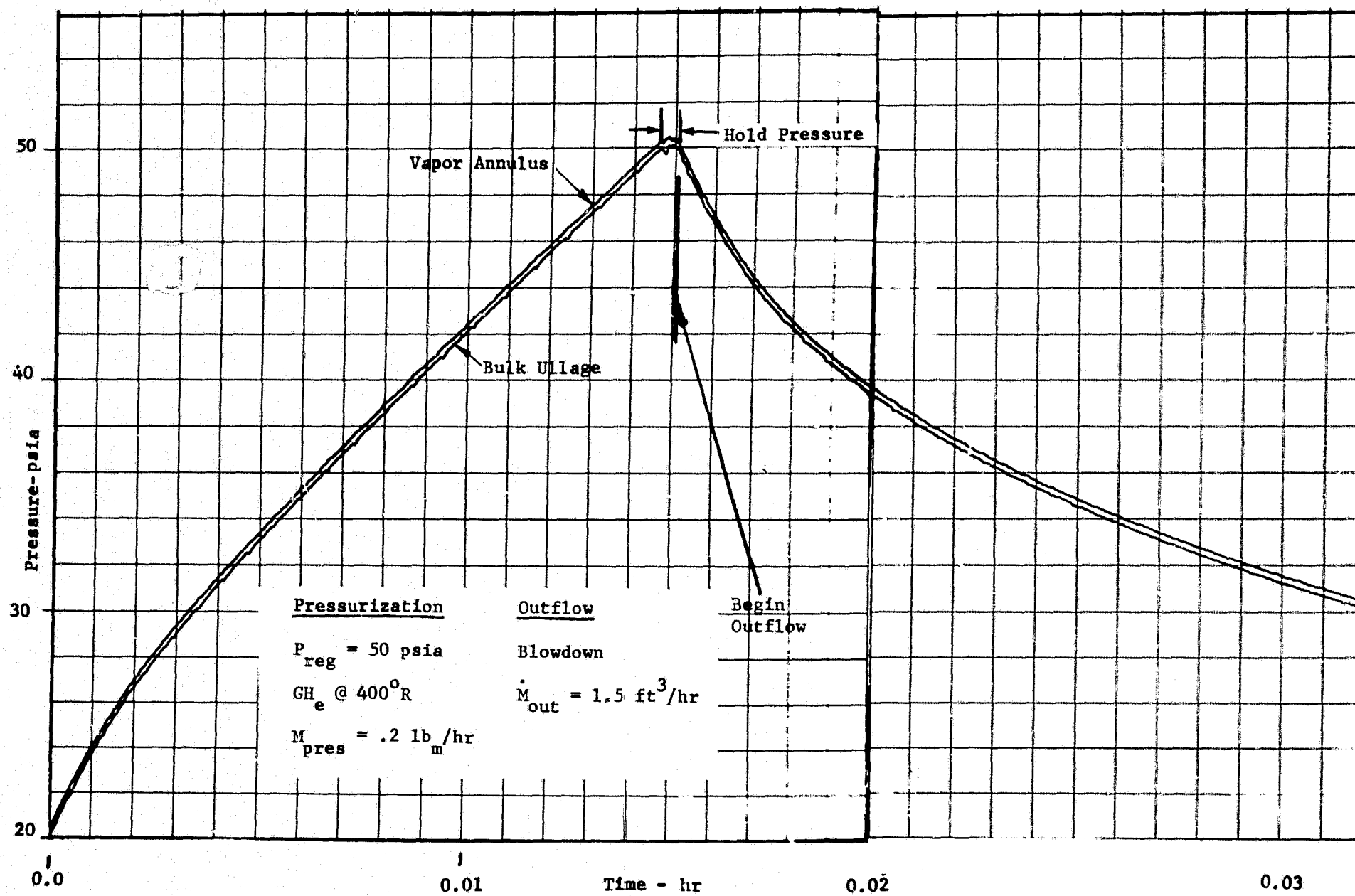Figure VII-4  LN$_2$ 1-g Venting for Subscale DSL System

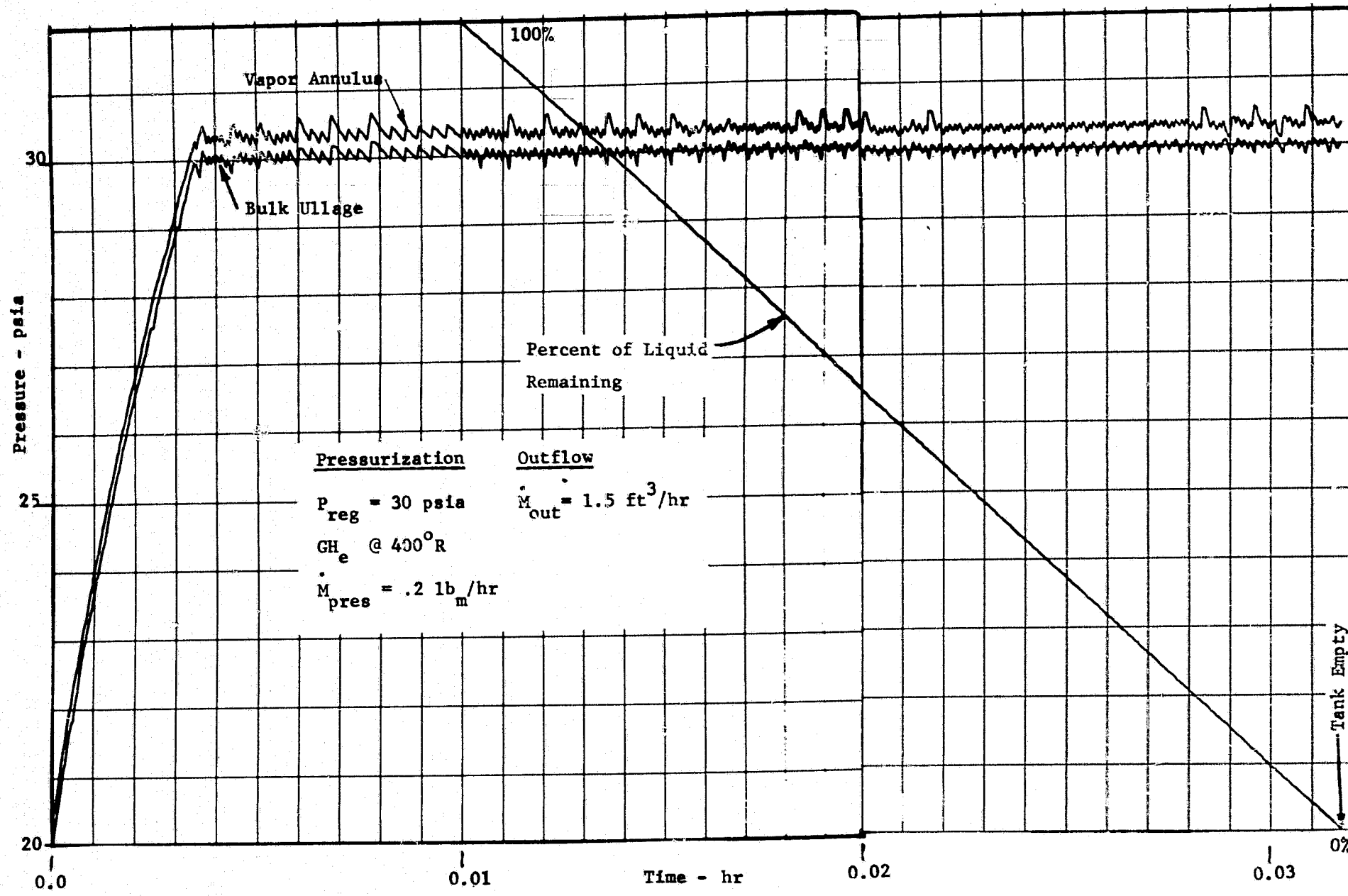Figure VII-5 Predicted Pressurization and Outflow (by Blowdown) of $LN_2$, Subscale DSL System

Figure VII-6 Predicted Pressurization and Outflow of LN₂ with Pressure Regulation, Subscale DSL System

tank, (2) the vacuum in the outer sphere, and (3) g-loading during testing. Virtually all of the metal components are stainless steel because of strength, formability, and cryogenic compatibility.

The LN$_2$ storage tank was designed to contain a pressure of 100 psia while within a vacuum environment. Consistent with the geometry of the screen liner, the vessel configuration is cylindrical with flat ends. A section of 6-in. diameter, schedule 10 pipe, was used for the cylindrical wall and this was closed at the lower end by welding to a 0.312-in.-thick disc. A bolted-flange assembly, using material of nominal 0.75-in. thickness, was used to enclose the upper end and to provide access. A soft metal gasket (1100-0 aluminum) is compressed between the flanges by means of 24, 3/8-in. cap screws to provide a leak-proof seal. Structurally, the design is conservative in all respects, exceeding a safety factor of 4 on ultimate strength.

The spherical shell of the vacuum jacket was constructed from two 18-in.-diameter hemispheres having a wall thickness of 0.070-in. Each hemisphere was welded to a 3/4-in.-thick bolted flange, one of which was provided with an O-ring groove. A vacuum seal is formed by the O-ring when the two flanges are bolted together with the 24, 3/8-in. cap screws. Our experience is that an 18-in.-diameter sphere having a shell thickness of 0.070 in. has more than adequate strength to withstand a collapse pressure differential of one atmosphere.

From a structural standpoint, the most critical design loads were those imposed by zero-g or low-g testing. High g-loading is experienced during drop tests due to the terminal deceleration, while flight tests involve substantial g-loads as a result of maneuvering. Aside from the fact the drop-test loads are much greater than those of flight tests, the axis through which these forces will act is fixed. The structure for accommodating the drop-test loads can be essentially a one axis suspension system. Flight test loads, however, may be imposed in any direction, so the mechanical restraint system was designed with this in mind.

The g-load criteria used in the design were:

1) Flight test (KC-135 aircraft) (Ref VII-1 and VII-2),
   a) Forward, 16 g,
   b) Down, 8 g,
   c) Up and laterally, 4 g,
   d) Aft, 15 g;

2) Drop test,
   a) MMC facility, 25 g (Ref VII-3),
   b) NASA-LeRC, 32 g (Ref VII-4).

The storage tank was estimated to weigh 45 lb, which would present flight-test loads of up to 720 lb and drop-test loads of 1125 and 1440 lb in the Martin Marietta and NASA-LeRC drop towers, respectively. To withstand

these g-loads, removable support rods were placed around the top and bottom
of the vessel at $90^\circ$ intervals, each making a $45^\circ$ angle with the vertical axis.
The rods were sized to correspond with the loads using a safety factor of 1.4.
Each of the rods can be removed individually, without separating the sphere,
by the vacuum-tight AN caps on the outside of the vessel.

A complete set of support rods consists of four rods having a 0.0085-in.$^2$
cross-sectional area and eight rods of 0.0066-in.$^2$ each. This approach allows
selection of a support configuration that is adequate for the expected loads
and that, in addition, will minimize the heat leak. For example, drop tests
at NASA-LeRC would use the four larger rods around the top of the inner vessel
with no rods around the bottom. The flight-test program would use the smaller
rods in all eight positions. For 1-g tests where no additional loads are expected,
all rods could be removed so that the vessel is supported by the tubing penetra-
tions. The rigid, styrofoam tunnel at each rod position allows the rod to be
inserted or withdrawn without interference.

A 3.15-in.$^2$ bearing area was provided on the shell of the vacuum sphere
at each of the eight support rod fittings. This was accomplished by adding a
2-in.-diameter by 1/8-in.-thick coupler between the shell and the shoulder
of the fitting. This bearing area will accommodate the load transmitted to
the shell by the four support rods during a 32-g deceleration drop test.

The cylindrical shape of the DSL resulted in substantial areas of flat
or simply-curved screen that required supplementary support for the aircraft
and drop tower g-loads. Primarily, this support was provided by sandwiching
the screen liners between two perforated plates. The perforated plate
material is 0.031-in. thick with 0.0625-in.-diameter holes on 0.109-in.
centers (30% open area). Thin metal clips, $120^\circ$ apart at the top and bottom,
support the inner liner within the outer liner and the outer liner within the
$LN_2$ storage tank.

### 4. Instrumentation

Platinum sensors are used to measure the temperature and to sense the
presence of liquid inside the $LN_2$ storage tank. Three of these sensors are
located at the bottom, mid-point, and top of the bulk liquid/vapor region just
inside of the inner screen liner. Two more sensors are located at the top and
bottom of the liquid annulus between the screen layers. The four remaining
sensors are positioned at the liquid fill/drain inlet, at the bottom of the
vapor annulus outside the outer screen liner, at the liquid outlet, and at
the vapor vent port. All nine of these sensors are located inside of the
pressure vessel and their lead wires pass through the vapor vent tube to
two electrical connectors that branch out from this tube. Wire passage through
the screen/perforated plate bulkheads was provided by discs welded to the
screen and drilled through with an appropriate size and number of holes to
accommodate the wires.

Two pressure taps are provided; these 1/16-in. tubes also pass through the vapor vent. One tap ends in the vapor annulus (between the vessel cover and the outer screen liner) and the other ends in the bulk liquid/vapor region (inside the inner screen liner). Vacuum level in the sphere is measured by installing an appropriate gage tube in one of the support-rod fittings that is specially equipped for this purpose.

Additional temperature measurements are made with chromel-constantan thermocouples attached to the outside of the inner vessel and to the plumbing in the evacuated interspace. These thermocouple wires are connected to two feedthroughs in the spherical vacuum jacket wall.

## C. FABRICATION AND ASSEMBLY DETAILS

### 1. Fabrication

In addition to the structural support members described in the foregoing section, there are three additional connections between the cryogen container and the vacuum jacket. These are (1) the pressurant inlet, liquid fill and drain line at the bottom of the vessel, (2) the liquid outlet line at the top, and (3) the vapor vent line at the top. Vacuum jacketing, $LN_2$ jacketing, and bellows sections were used to minimize the heat leak through these connections and to provide for expansion and contraction. With the exception of the flange joints and a small amount of brazing in the screen liners, all joints are welded. Periodic leak testing of subassemblies assured that the final assembly was leaktight.

Fabrication of the screen liners commanded the greatest degree of attention due to the sensitivity of this material to forming and welding. The edges of the end pieces were turned up to form a flat-bottomed cup. This cup was inserted into the screen cylinder and the exposed edges were fused together. The essential ingredients of a satisfactory welding setup for this screen material includes close contact of the individual pieces and an adequate, close-coupled heat sink. In cases where the edge of the screen couldn't be satisfactorily welded to heavier material (such as the communication screen), a brazing process was used. While this process does not tend to burn away unprotected screen, the braze material will wet the screen thus filling its pores. If the use of brazing is not discretely limited, essential wicking action can be lost and the performance of the screen liner will be degraded.

### 2. Assembly

The major subassembly consists of (1) upper hemisphere, (2) support-rod fittings, (3) vacuum port, (4) thermocouple-feedthrough ports, (5) vapor vent tube, (6) jacketed liquid outlet, (7) cover of inner vessel, and (8) the DSL attached to the liquid outlet tube. This subassembly also includes the platinum temperature/level sensors with their wires threaded up through the vapor vent tube. The pressure vessel itself, with thermocouples, heaters, and fill/drain line attached, was slipped over the screen liner and bolted to the cover with the jacket in place. At this point, the inner vessel was somewhat mobile due to the flexing of the bellows joints. The assembly was rigidized by installing the four support rods and adjusting them so that the vessel was properly positioned in the hemisphere. The foam tunnels were then positioned.

After installing the multilayer insulation, the lower hemisphere with a compression-gland fitting on the bottom and O-ring in place, was slipped up over the fill/drain line. The vacuum-jacket hemispheres were then bolted together and installed on the support stand. The four lower support rods were installed and closure of the vacuum jacket was completed by tightening the bottom compression gland, installing caps and metal seals on seven of the support-rod fittings, and installing the vacuum-gage fitting and seal on the remaining support-rod fitting.

### 3. Checkout

A check on screen integrity was performed during each stage in the fabrication of the DSL. This was accomplished by measuring and comparing bubble points of the screen before and after fabricating each part. The bubble point was also measured after fabrication of both the inner and outer liners. In addition, helium leak tests and electrical checks were performed during fabrication.

Checkout of the assembled test article included electrical checks (thermocouples, sensors, heaters) plus determination of the pressure integrity of the $LN_2$ storage tank, and vacuum integrity of the sphere. The electrical checkout was performed first because any discrepancy could have required some degree of disassembly.

Ohmmeter checks of all circuits were made to assure continuity and proper connections. The vessel heaters were energized and thermocouples on the storage tank wall were monitored. Operation of the remaining thermocouples, as well as the platinum sensors, was verified by flowing warm gaseous nitrogen through the vessel.

Pressure and vacuum checks were made at the same time because they are, to some extent, interdependent. Helium was used for pressurization and a leak detector with pressure monitoring was used to verify system integrity.

## VIII.   CONCLUSIONS AND RECOMMENDATIONS

The results of this program have shown that the DSL passive retention/ expulsion concept is attractive for a wide range of cryogenic storage applications, including the Space Shuttle orbiter.  It is not limited by tank shape or size and is a completely passive device (no moving parts within the storage tank). It is the only passive concept that, by itself, tends to assure: (1) gas-free liquid expulsion on demand, (2) liquid-free gas venting, and (3) a near-continuous propellant control.  The dual-screen pressure relief method compares favorably to other techniques (such as liquid vent systems) with regard to minimizing the vented mass during orbital storage in the pressure range (one-to-four atmospheres) of the Shuttle orbiter.

The DSL appears to be relatively flexible in certain respects.  For example, the basic operational concept is for the total liner to orient the bulk propellant away from the tank wall.  Venting of gas directly from this vapor annulus and out the tank can be continuous or intermittent.  Continuous venting from an oxygen and nitrogen tank can be used directly for life support. If intermittent venting is used (desired from a control standpoint) the desired vent rate and frequency are dictated by a relatively sensitive pressure deadband (less than 0.3 psi) or the bulk liquid control is lost.  The latter may be advantageous in the case where a sudden and significant pressure relief of the tank is required.  If the low-g acceleration vector positions the bulk liquid (lost from the central region) away from the vent port, the bulk ullage will be relieved through the passive communication system between the bulk ullage and gas annulus.  The bulk liquid entering the gas annulus will be forced back into the central region by subsequent vapor pressure increase in the gas annulus and the system is restored to its desired condition.  A second example of the dual-screen concept's flexibility is with regard to its ability to restore itself.  Liquid entering the gas annulus, as described in the rapid pressure relief sequence or by a screen breakdown (weeping of liquid), will eventually be forced back into the lower pressure central region.

The passive communication screen, mentioned in the previous paragraph, provides a margin on the vent pressure difference while also reducing the vent frequency.  It affords a path of least resistance (in comparison to the liquid annulus screen) so there can be communication between the gas annulus and bulk propellant region without vapor ingestion into the liquid annulus.

The dual-screen concept is attractive for the Shuttle orbiter, based on these study results.  No insurmountable problems were uncovered, however, more development of the concept is recommended.  Its operational characteristics and performance must be determined experimentally before its practicability can be measured.  It is, therefore, strongly recommended that the test plan formulated during the program be implemented using the subscale dual-screen model with nitrogen as the test fluid.  It is doubtful that a single series of bench, drop tower, and aircraft tests, as proposed in the test plan will resolve all the questions with regard to the concept's operational mannerisms; however, they should lend sufficient information to support or question the practicality of the concept.  The tests may point up modifications needed.

The 1-g bench tests are needed to develop an operational feel for the concept before proceeding with the more sophisticated low-g tests. The latter will require different instrumentation and, in the case of drop tower and aircraft tests, the need for remote controls. The drop tower, though limited in the low-g test duration, is recommended for developing the instrumentation technique and control methods before conducting tie-down KC-135 aircraft tests that will provide low-g durations of 28 to 30 sec. The latter is sufficient to obtain data for gas venting, liquid draining and bulk liquid control.

The tests described in the test plan should be a precursor to orbital testing of the dual-screen system that is needed to provide long-term low-g durations (days). The orbital test, if pursued in the near future, would provide qualification of the dual-screen acquisition/expulsion device for the Shuttle cryogenic storage system. Such tests are required to qualify the dual-screen device for cryogenic service.

In addition to this vital experimental program, additional analytical work is recommended with regard to integrating the dual-screen concept into the complete storage system, i.e., including the propellant feedline and pump (NPSP) concerns. This can best be done by considering a specific design, such as the Shuttle orbiter, rather than attempting to design a universal system.

No structural analyses were made for the dual-screen device during this program, except for the subscale model. This is critical for determining an accurate system weight and to assure system integrity under the operational loads. This is viewed as a significant task.

Finally, it is recommended that fine mesh screen fabrication of devices (at least 3 ft in size) be started. Presently, prototype tankage is built to demonstrate the fabrication capability; screen devices are equally justifiable. As mentioned in the report, the largest fine-mesh device of compound curvature built to date is on the order of 1 ft. In addition to the fabrication and assembly effort, specifications must be compiled for the reusable Shuttle orbiter on (1) inspecting, (2) cleaning, (3) handling, (4) loading, and (5) maintenance procedures with regard to passive devices.

# IX. REFERENCES

I-1     H. L. Paynter et al.: Investigation of Space Storable Propellant Acquisition Devices. Final Report. Volume I - Evaluation. MCR-70-171. Martin Marietta Corporation, Denver, Colorado, October 1970 (Contract NAS7-754).

I-2     D. L. Balzer et al.: Advanced Propellant Management System for Spacecraft Propulsion Systems. Phase I - Survey Study and Evaluation. MCR-69-87, Martin Marietta Corporation, Denver, Colorado, February 1969 (Contract NAS9-8939).

I-3     T. E. Bowman and H. L. Paynter: "Weightless Liquids." Science Journal, Vol 2, No. 9, London, England, September 1966.

I-4     S. C. DeBrock et al: "A Survey of Current Developments in Surface Tension Devices for Propellant Acquisition." Journal of Spacecraft and Rockets. Vol 8, No. 2, February 1971, pp. 83-98.

I-5     M. H. Blatt et al.: Low-Gravity Propellant Control Using Capillary Devices in Large Scale Cryogenic Vehicles. Final Report. Phase I. GDC-DDB70-007. Convair Division of General Dynamics, San Diego, August 1970 (Contract NAS8-21465).

I-6     M. H. Blatt et al.: Low-Gravity Propellant Control Using Capillary Devices in Large-Scale Cryogenic Vehicles. Final Report. Phase II. GDC-DDB70-008. Convair Division of General Dynamics, San Diego, August 1970 (Contract NAS8-21465).

I-7     J. A. Start et al.: Study of Low-Gravity Propellant Transfer. First Quarterly Progress Report. GDC-584-4-549. Convair Division of General Dynamics, San Diego, September 1970 (Contract NAS8-26236).

I-8     Advanced Maneuvering Propulsion Technology Program, Fourth Quarterly Report (U). AFRPL-TR-68-221. Rocketdyne Division, North American Rockwell Corporation, Canoga Park, California, December 1968 (Confidential).

I-9     L. Morgan et al.: Orbital Refueling and Checkout Study. Final Report. Volume III - Evaluation of Fluid Transfer Modes. T1-51-67-21. Lockheed Missiles and Space Company, Sunnyvale, California, February 1968 (Contract NAS10-4606).

I-10    H. L. Paynter et al.: Experimental Investigation of Capillary Propellant Control Devices for Low-Gravity Environments. Volume I - Summary Report. MCR-69-585. Martin Marietta Corporation, Denver, Colorado. June 1970 (Contract NAS8-21259).

I-11    H. L. Paynter et al.: Experimental Investigation of Capillary Propellant Control Devices for Low-Gravity Environments. Volume II - Final Report. MCR-69-585. Martin Marietta Corporation. Denver, Colorado, June 1970 (NAS8-21259).

I-12    R. E. Hise: <u>Passive Retention/Expulsion Methods for Subcritical Storage</u> <u>of Cryogens.  Test Plan - Subscale Dual-Screen-Liner Retention/Expulsion</u> <u>System</u>.  MCR-71-38.  Martin Marietta Corporation.  Denver, Colorado, July 1971 (Contract NAS9-10480).

II-1    H. L. Paynter <u>et al</u>.: <u>Final Design Report: Development of a Capillary</u> <u>System for Liquid Propellant Orientation during Low-g</u>.  TM-0444-66-3. Martin Marietta Corporation, Denver, Colorado, December 1965.

II-2    H. L. Paynter <u>et al</u>.: <u>Experimental Investigation of Capillary Propellant</u> <u>Control Devices for Low-Gravity Environments, Volume II - Final Report</u>. MCR-69-585.  Martin Marietta Corporation, Denver, Colorado, June 1970. (Contract NAS8-21259).

II-3    G. D. Bizzell, M. P. Hollister, and R. K. Grove: <u>Low-Gravity Orientation</u> <u>of Cryogenic Propellant (U), Phase I, Technical Report</u>.  AFRPL-TR-70-149. Lockheed Missiles and Space Company, December 1970 (Confidential).

II-4    G. R. Page, D. W. Murphy, and J. P. Gille: <u>Vent-Free Fluorine Feed System</u> <u>(U)</u>.  AFRPL-TR-67-323 (Vol I).  Martin Marietta Corporation, Denver, Colorado, March 1968 (Contract F04611-67-C-0044) (Confidential).

II-5    D. W. Murphy and L. J. Rose: <u>Vent-Free Fluorine Feed System</u>.  AFRPL-TR-67-323 (Vol II).  Martin Marietta Corporation, Denver, Colorado, June 1968 (Contract F04611-67-C-0044).

II-6    G. R. Page and J. R. Tegart: <u>Vent-Free Fluorine Feed System Analysis</u>. AFRPL-TR-69-200.  Martin Marietta Corporation, Denver, Colorado, September 1969 (Contract F04611-69-C-0033).

II-7    R. E. Tatro: "Cryogenic Propellant Acquisition and Transfer."  Paper presented at Space Transportation System Technology Symposium.  NASA Lewis Research Center, Cleveland, Ohio, July 15-17, 1970 (NASA TMX-52876, Vol V, pp. 167-188).

II-8    J. A. Stark and M. H. Blatt: <u>Analysis of Zero-Gravity Receiver Tank Vent</u> <u>Systems, Phase III Final Report</u>.  GDC-DDB69-001.  General Dynamics/Convair, San Diego, California, July 1969 (Contract NAS8-20146).

II-9    H. L. Jensen, T. C. Nast, and A. P. M. Glassford: <u>Investigation of</u> <u>External Refrigeration Systems for Long Term Cryogenic Storage</u>.  LMSC/ A903162.  Lockheed Missiles and Space Company, Sunnyvale, California, May 1970 (Contract NAS9-10412).

II-10  <u>Advanced Maneuvering Propulsion System (Convair Propellant Feed System</u> <u>Design) Volume III - Optimization Studies (U)</u>.  AFRPL-TR-70-103. Rocketdyne, Canoga Park, California, September 1970 (Confidential).

II-11  <u>Advanced Maneuvering Propulsion-System (Lockheed Propellant Feed System</u> <u>Design) Volume III Screening and Optimization Analyses (U)</u>.  AFRPL-TR-70-104.  Rocketdyne, Canoga Park, California, September 1970 (Confidential).

II-12  J. C. Howell et al.: Main-Tank Injection for Packaged Liquid Missiles, Phase I Report. AFRPL-TR-66-115. Martin Marietta Corporation, Denver, Colorado, March 1967.

II-13  H. L. Paynter et al.: Progress Report - Research Authorization Task - 631. SR1660-68-14. Martin Marietta Corporation, Denver, Colorado, October 1968.

II-14  J. L. McGrew and B. K. Larkin: Cryogen Liquid Experiments in Orbit. Volume II: Bubble Mechanics, Boiling Heat Transfer, and Propellant Tank Venting in a Zero-Gravity Environment. NASA CR-652. Martin Marietta Corporation, Denver, Colorado, December 1962 (Contract NAS8-11328).

III-1  G. R. Page and J. R. Tegart: Vent-Free Fluorine Feed System Analysis, Computer Program Report. MCR-69-465. Martin Marietta Corporation, Denver, Colorado, September 1969 (Contract F04611-69-C-0033).

III-2  E. R. G. Eckert and Robert M. Drake, Jr.: Heat and Mass Transfer, McGraw-Hill Book Company, New York, New York, 1959, pp. 322-331.

III-3  Frank Kreith: Principles of Heat Transfer, International Textbook Co. Scranton, Pennsylvania, 1960, pp. 305-306.

IV-1  H. L. Paynter et al.: Experimental Investigation of Capillary Propellant Control Devices for Low-Gravity Environments, Volume II-Final Report. MCR-69-585 (Vol II). Martin Marietta Corporation, Denver, Colorado, June 1970.

IV-2  James C. Armour and Joseph N. Cannon: "Fluid Flow Through Woven Screen." AIChE Journal, Vol 14, No. 3, May 1968, pp. 415-420.

IV-3  D. L. Balzer et al.: Advanced Propellant Management System for Spacecraft Propulsion Systems. Phase II - Detail Design. MCR-69-436. Martin Marietta Corporation, Denver, Colorado, September 1969 (Contract NAS9-8939).

IV-4  H. L. Paynter et al.: Progress Report - Research Authorization Task - 631. SR1660-68-14. Martin Marietta Corporation, Denver, Colorado, October 1968.

IV-5  L. J. DiPeri: "A Resume of the Management of Liquid/Gas Interface Using Surface Tension Technology." Joint AIAA/Aerospace Corporation Symposium on Low Gravity Propellant Orientation and Expulsion. Technical Session Proceedings. Los Angeles, California, May 1968, p. 81.

IV-6  S. C. DeBrock et al.: "A Survey of Current Developments in Surface Tension Devices for Propellant Acquisition." J. of Spacecraft and Rockets. Vol 8, No. 2, February 1971, p. 84.

IV-7  Capillary Screen Device Technology. M-70-18. Martin Marietta Corporation. Denver, Colorado, July 1970.

IV-8  D. A. Fester and P. E. Bingham: Evaluation of Fine Mesh Screen Device in Liquid Fluorine. R-70-48631-010. Martin Marietta Corporation, Denver, Colorado, June 1970.

128

V-1     H. L. Paynter et al.:  Experimental Investigation of Capillary Propellant
        Control Devices for Low-Gravity Environments, Volume II - Final Report.
        MCR-69-585 (Vol II), Martin Marietta Corporation, Denver, Colorado,
        June 1970 (Contract NAS8-21259).

V-2     R. P. Warren and J. W. Anderson: "A System for Venting a Propellant
        Tank in the Absence of Gravity." Advances in Cryogenic Engineering,
        Vol 12, Plenum Press, New York, New York, 1967.

VI-1    R. E. Hise: Passive Retention/Expulsion Methods for Subcritical Storage
        of Cryogens.  Test Plan - Subscale Dual-Screen-Liner Retention/Expulsion
        System.  MCR-71-38.  Martin Marietta Corporation, Denver, Colorado,
        July 1971 (Contract NAS9-10480).

VI-2    L. E. Greenberg: Cryogenic Tests of a Dual-Screen Liner Breadboard
        Configuration in the Minus One-g Outflow Mode.  R-70-48631-007.
        Martin Marietta Corporation, Denver, Colorado, May 1970.

VI-3    J. L. McGrew and B. K. Larkin: Cryogen Liquid Experiments in Orbit.
        Volume II: Bubble Mechanics, Boiling Heat Transfer, and Propellant
        Tank Venting in a Zero-Gravity Environment.  NASA CR-652.  Martin
        Marietta Corporation, Denver, Colorado, December 1966, Contract
        NAS8-11328.

VII-1   Unofficial Syllabus for Zero G Test Programs.  Zero-g Test Office, Wright-
        Patterson Air Force Base, Ohio.

VII-2   MIL Spec MIL-S-5705.

VII-3   H. L. Paynter: Martin Marietta Corporation's Low-g Experimental Facility.
        M-65-67, Martin Marietta Corporation, Denver, Colorado, August 1965.

VII-4   E. P. Symons: Zero-Gravity Equilibrium Configuration of Liquid/Vapor
        Interface in Toroidal Tanks.  NASA TN D-6076 NASA Lewis Research Center,
        Cleveland, Ohio, November 1970.